UNIVERSIDAD DE INGENIERÍA Y TECNOLOGÍA

CARRERA DE INGENIERÍA DE LA ENERGÍA

DEVELOPMENT OF TECHNICAL-ECONOMIC SCENARIOS FOR THE INCORPORATION OF AN SPT-TES + PV HYBRID POWER PLANT IN THE SOUTH OF PERU

THESIS

To obtain the college degree in Energy Engineering

AUTHOR

Andrea Yolanda Álvarez Vera (CÓDIGO: 201410008)

ADVISOR

Eunice Villicaña Ortiz (ORCID: 0000-0001-7495-2395)

Lima – Peru

May 2021

Dedication:

This research is dedicated to my friends Thomas and Pompom,
for their support and confidence.

Acknowledgments:

This thesis, although it has required effort and a lot of dedication by the author, achieving the results in every aspect of the project was influenced by the disinterested cooperation of each and every one of the people that I will quote below:

I want to thank my advisor and professor at UTEC Eunice Villicaña, who with their knowledge and support guided me in developing this project to achieve the results sought.

To all my colleagues in the ENGIE project area, I would like to thank them for their unselfish and unconditional help, who from the beginning have welcomed me very well as one of the team.

I especially thank Cesar Cornejo, my boss at ENGIE and former teacher at UTEC, for providing me with all the resources and tools necessary to carry out this project. Thank you, César for every detail and your time, for the clarity and accuracy with which you taught me, and for motivating me throughout the final stage of my professional training.

Finally, thank my sister Lucero for reinforcing my energies with the best playlists and dance sessions.

CONTENT

LIST OF TABLES

LIST OF FIGURES

Page

RESUMEN

El desarrollo de las centrales de concentración solar podría desempeñar un papel esencial en la transición energética y el desarrollo sostenible del Perú, uno de los países de América Latina con el mayor potencial solar. En este sentido, además de analizar la factibilidad técnica y los costos de generación de electricidad, también es importante evaluar en qué escenarios es factible su incorporación, identificando las barreras y los impulsores más relevantes para su implementación en un horizonte 2030, así como las estrategias que se requieren para impulsar su desarrollo, todo ello basado en una revisión exhaustiva de la literatura, análisis de data y el desarrollo de modelos técnico-económicos.

PALABRAS CLAVE:

LCOE, escenarios técnico-económicos, factibilidad.

INTRODUCTION

In the last few years, the change in global energy models has been aimed at accelerating the transition to clean energy to meet the objectives[1] of the Paris Agreement and to achieve the seventh[2] Sustainable Development Goal related to "Ensuring access to affordable, reliable, sustainable and modern energy for all." The new energy models are geared toward the development of long-term solutions that provide benefits such as lower renewable power costs, an increase in energy access, emissions and air pollution reduction, improvement in people's welfare, and growth of society [1].

Because of this, renewables continue to gain ground globally. Their progress is uneven across sectors and regions [2], but Latin America has undergone a great transformation in the last two decades, driven by new energy policies, with a more favorable environment for new investments and efforts to reduce greenhouse gasses emissions and fossil fuel dependency. In this context, several countries have chosen to diversify their generation matrices with renewable energy, including Peru.

Peru has initiated its energy transition since 2010, with the approval of the Energy Policy 2010–2040[3] law and Legislative Decree No. 1002[4] for the promotion of investment in renewable energy sources (RESs) generation. Both proposals were accompanied by the

---

[1] The Agreement seeks to keep the rise in average global temperatures below 2°C and ideally to limit warming to 1.5°C in the present century, compared to pre-industrial levels [113].

[2] The seventh Sustainable Development Goal is "to ensure access to affordable, reliable, sustainable and modern energy for all." The main targets are to ensure universal access to affordable, reliable, and modern energy services; increase substantially the share of renewable energy in the global energy mix; and double the global rate of improvement in energy efficiency [114].

[3] It proposes an energy system that satisfies energy demand in a reliable, regular, continuous, and efficient manner; and it has as one of its objectives a diversified energy matrix, with emphasis on renewable sources and energy efficiency.

[4] Legislative Decree N° 1002, of September 13, 2010, of Promotion of the Investment for the Generation of Electricity with the Use of Renewable Energies, Article 2, Section 2.2: The MINEM will establish every five (5) years an objective percentage in which the electricity generated from RESs must participate in the national electricity consumption, not considering hydroelectric plants in this objective percentage. Such target percentage will be up to five percent (5%) in each first five-year period.

NUMES Plan,[5] which proposed guidelines for a new energy matrix with a 20% RES participation by 2040. Later on, the National Energy Plan 2014–2025[6] was approved, which sets generation goals every two years to reach a 5% RES participation in the matrix before 2025.

Currently, RES participation in the generation has reached 5%, and therefore, the new objective of the Ministry of Energy and Mines (MINEM) presents two proposals. The first one, according to Prosemer[7], is to achieve 15% of RES participation by 2030 [3], while the study of the Multisectoral Working Group[8] proposes to achieve 6.8% RES participation and to reach 88% of rural electricity coverage by 2030 [4].

Under the policies and regulations mentioned above, Peru has included renewable technologies in its energy matrix, and recently, there has been an increase in the penetration of solar and wind power technologies with more competitive prices [5]. However, market conditions could be hindering the deployment of new power plants due to the uncertainty and lack of updates in the regulation of RES plants, related to assigning some level of firm capacity to these kinds of technologies, which could allow them to sign power purchase agreements.

On the other hand, a new panorama of mining investments in the south of Peru with projects such as RelavesB2 San Rafael, Quecher Main, Toromocho Extension, Ariana, Mina Justa, and Quellaveco [6] proposes to boost the country's economy. However, the infrastructure created for the exploitation of Camisea gas remains stalled due to the delay in the construction of the former Peruvian south gas pipeline. The operation of the plants planned for the years 2023–2025 is uncertain, requiring the generation of at least 100 MW extra by the year 2023 in a medium-term scenario of mining development [7] [8]. This

---

[5] Diversification of the supply of energy generation by 2040. Objectives: hydroelectricity with 40%, gas (thermal) with 40% and alternative renewable resources (RER) with 20%.

[6] Achieve a contribution of RES with: Mini hydro 391 MW, Solar 96 MW, Wind turbines 232 MW and other 27 MW.

[7] Programa para la Gestión Eficiente y Sostenible de los Recursos Energéticos del Perú

[8] Grupo de Trabajo Multisectorial de naturaleza temporal encargado de generar información técnica para orientar la implementación de las Contribuciones Nacionalmente Determinadas

situation leads to a deficit of efficient power generation, which will eventually demand the use of thermal power plants run by diesel, increasing both electricity market costs by 80–120 USD/MWh and simultaneously the country's greenhouses gas emissions.

Given the energy context by 2023, new electric generation technologies are attractive for a market that demands energy throughout the day. The technology of concentrating solar power (CSP) is an energy solution that meets the requirements of firm capacity and the dispatch of clean energy (free of emissions), taking advantage of direct irradiation in the southern part of the country; a high production of energy is predicted with this type of technology. However, due to the lack of information on costs, resource optimization, and possible energy configurations, this type of technology has been discarded because of the economic factor that considers it costly compared to baseload solutions such as natural gas and hydroelectric power plants [9].

However, CSP plants with storage have emerged as a viable competitor to fossil fuel thermal power plants. The critical progress in the research and development of CSP has led to a reduction of the levelized cost of electricity (LCOE) because technological improvements have been found in the design of heliostats (resulting in more efficient and economical units). As proof of this, in Chile, the prices of the last auction with CSP reached values between 65–60 USD/MWh [8].

Therefore, the present thesis proposes the development of technical-economic scenarios that allow the incorporation of CSP in the south of Peru starting with the energetic design of a solar tower power (STP) plant, its economic analysis (including the calculation of the LCOE), and its environmental evaluation. Essential factors that have been taken into consideration are direct normal irradiation (DNI), land use, water availability, proximity to the network, transmission lines, demand points (final consumers), dispatched energy, job creation, CO_2 emissions, CAPEX, and OPEX.

Scope

This investigation includes a technical and economic analysis for the implementation of a solar power tower with thermal energy storage and photovoltaic (SPT-TES + PV) hybrid power plant in the region of Arequipa and the elaboration of scenarios for its incorporation in the National Grid System.

The technical analysis includes the study of the bankable data provided by SolarGis for the period 1999–2015, the selection of the location of the plant, and the energy design with an optimal configuration of the STP-TES at a conceptual level. The design and detailed sizing of the parts of the proposed plant have not been considered.

The economic analysis covers the development of a preliminary economic model and calculation of the LCOE. The sensitivity analysis has not been included.

The scope of the scenarios to be developed includes the preparation of projections up to 2028 in terms of the evolution of technology costs, the behavior of energy demand and supply, and the economic growth of the southern zone of Peru.

Background

The growth of energy demand worldwide in the last two years has been 2.3%, considered the fastest growth of the last decade [10], d ue to a robust global economy and the increase in the heating and cooling needs of some regions.

The general demand for fossil fuels for electricity generation worldwide increased by 70% from 2017 to 2018, including the use of coal. This situation generated an increase in CO_2 emissions of 33 gigatons for that period [10].

On the other hand, the share of renewable energy in the new global generation capacity of electric power has increased by around 7.5% from 2017 to 2018, mostly due to an increase in installed capacity, the reduction of technology costs, more favorable energy policies, and environmental commitments [2–5].

In Peru, solar energy has had a share in electricity generation through photovoltaic power plants [13]. There have been four auctions of renewable energy nationwide, and so far seven solar power plants have been awarded with an installed capacity of 285 MW [8], which are located in the regions of Moquegua, Arequipa, and Tacna.

Solar thermal energy is used through solar collectors [14] to produce domestic hot water for residential, hotel, and industrial purposes. Currently, there are about 30 companies dedicated to the installation, manufacture, and maintenance of commercial solar thermal panels [15], and its presence is generally observed in the southern zone and the central highlands of Peru [14–18].

Concentrating plant technology has not yet been developed in Peru. However, the neighboring country of Chile has the Cerro Dominador project, a 100 MW CSP-PV with thermal storage (TES), which will start operating in 2020 [21]. In addition, Chile has five CSP projects in its portfolio,[9] and in the last auction, this type of technology reached the price of 60–65 USD/MWh, a highly competitive price compared to the prices of natural gas and hydroelectric power plants in that country.

Regarding research on CSP in Peru, two postgraduate theses have been found that develop in detail the techno-economic feasibility of this technology:

- In "Viabilidad técnica y económica para la construcción de una central termosolar en la región Puno," the author Terrazos analyzed the radiation data provided by a weather station of Senamhi in Puno and estimated the hourly radiation through the GEOSOL V.2.0 software for the Chuquibambilla area to design a 50 MW parabolic trough collector (PTC) type concentrated solar plant. He used the SAM software for economic analysis, showing a value of 225 USD/MWh as the LCOE. The study showed that the environmental impact is low, after the semi-detailed analysis of the environmental impact of

---

[9] CSP with approved environmental permit: Likana Solar 450 MW (SolarReserve Chile), Tamarugal Solar 450 MW (SolarReserve Chile), Copiapó Solar 240 MW (SolarReserve Chile), Camarones 105 MW (Elecnor Chile), and CEME 1 70 MW (Ceme 1 SpA) [115].

this type of technology. Additionally, it included a comparison of the results obtained with the Andasol 3 and Extresol 3 plants in Spain, noting that the plant proposed in the study achieved lower investment costs and higher generation of electric power with similar technical characteristics [22].

- In "Concentrating solar power potential in Peru," the author Pliego evaluated the development potential of solar concentration technology through the application of geographical information systems based on multicriteria decision making, analyzing the DNI map provided by SolarGis. Based on the criteria of high direct radiation, proximity to water sources, infrastructure, and demand, the results determined as hotspots the regions of Tacna, Ayacucho, Arequipa, Puno, and Moquegua. Likewise, the study evaluated the conceptual design of a 50 MW solar power tower (SPT) plant with TES of 14 hours in Arequipa, obtaining an LCOE of 84.74 USD/MWh [23].

In scientific and academic terms, there is a variety of documents that perform a technical-economic analysis of CSP and its configurations to determine its feasibility in various scenarios:

- In "Socioeconomic, Environmental, and Social Impacts of a Concentrated Solar Power Energy Project in Northern Chile," the authors Rodríguez, Caldés, Garrido, et al. used an input-output methodology based on plant cost data and estimated the direct and indirect socioeconomic and environmental effects of the Concentrated Solar Power Energy project. In terms of economic activity, the plant would amount to 3.124 billion USD, which is related to the creation of jobs because the project would generate new jobs during construction, but these would be reduced when the plant starts operating. It would produce 64.36 g CO_2/kWh [24].

- In "Is Concentrated Solar Power (CSP) a feasible option for Sub-Saharan Africa? Investigating the techno-economic feasibility of CSP in Tanzania,"

the authors Aly, Bernardos, Fernandez-Peruchena, et al. used the SAM software to model a STP and PTC plant, to determine their technical-economic feasibility. The results yielded LCOE values of 116–125 USD/MWh for the STP and 130–144 USD/MWh for the PTC plant, considering that both are projects directed by the government with an interest rate of 7%; in the case of leading investors with a rate of 18%, the price increased up to 250 USD/MWh. The study concluded that it is necessary to implement political mechanisms that allow investment in CSP projects with lower interest rates to guarantee their competitiveness [25].

- In "Technical feasibility of a sustainable Concentrated Solar Power in Morocco through an energy analysis," the authors Bouhal, Agrouaz, Kousksou, et al. developed a methodology for calculating and analyzing the economic feasibility of a PTC plant in six climatic regions of Morocco. The study concluded that the choice of thermal heat transfer fluid is crucial for increasing CSP efficiency and cost effectiveness. Likewise, characteristics such as water availability, site characteristics, connection infrastructure, installation costs, market, and political environment must be considered to improve and optimize the performance of the CSP-PTC in different climatic conditions [26].

- In "The impact of concentrated solar power in electric power systems: A Chilean case study," the authors Mena, Escobar, Lorca, et al. constructed six scenarios to evaluate the impact of long-term STP and PTC-type CSP in the Chilean national grid with or without the CSP and a carbon tax of 5–26 USD/tCO$_2$. The results of the study show a trend toward the use of the STP as the optimal system for the expansion plan of this technology, due to superior efficiency and TES capacity with a configuration of 150 MW and 13 hours of TES. It also mentions that, in scenarios close to the central system load, the investment costs increase due to the requirement of new systems for

transmission and expansion of existing ones. Finally, the study mentions the synergy between photovoltaic systems and CSP, recommending a joint operation, allocating the CSP for storage during the day and production at night, while the PV operates vice versa, highlighting the flexibility provided by the CSP plants to the system under a context of a high share of variable renewable energy [27].

In contrast to the research mentioned above, the present study seeks to evaluate the development potential of CSP technology in Peru, analyzing bankable data to identify the most favorable location. Then a CSP STP-type plant is designed with TES + PV by choosing the most suitable configuration according to market conditions, and it is then optimized economically. The results are expected to show a competitive LCOE compared to the dominant solutions. Subsequently, technical-economic scenarios are developed which will allow its incorporation into the Peruvian generation matrix and its use to meet the growing demands in southern Peru.

Justification and motivation

The economic growth and the projection of new mining projects in a medium-term scenario in the south of Peru will lead to an increase in energy demand, congestion in the central-south grid connection, and a deficit of efficient generation by 2022 [8]. This context would boost the operation of the southern energy node with diesel to meet growing demand, thus increasing the marginal cost of energy up to 80–120 USD/MWh and the amount of greenhouse gas emissions into the environment until the uncertain arrival of the gas pipeline in 2026 [7]. Therefore, there is a need for an efficient generation of 100 MW by 2024 and 200 MW by 2025 that can be supplied by different types of generation technologies, including solar power [7].

A study by the Operations Committee of the National Interconnected System (COES) states that to cover the energy demand in the south by clean and competitive generation, projects should be developed that rely mainly on solar, wind, and water (mini-hydro) to avoid

developing a dependency on thermal power plants that use the gas pipeline, which, due to the uncertainty surrounding the arrival of natural gas, would operate at high prices because of diesel consumption [7].

In addition, southern Peru has high-quality solar irradiance from 2,191 to 2,629 kWh/m^2 yearly and is one of the regions in South America with the highest values after Chile, which allows for the development of technologies that optimally take advantage of this solar resource.

In recent years, the use of photovoltaic power plants for the generation of electricity has been deployed, and currently, there are seven solar plants in operation, with 285 MW of installed power. However, due to the type of load required by the new mining portfolio, the system requires new technologies that can offer clean energy throughout the day and that, in turn, provide flexibility.

In this context, it is favorable to bet on new technologies such as CSP, because, unlike conventional renewable power plants, this type of power plant is capable of storing energy through TES and using it in times of low radiation (cloudy days) or no solar radiation (overnight) to generate electricity, offering dispatch all during the day. Likewise, this type of technology can be hybridized with PV systems and provide firm capacity, required in markets with high demand.

Moreover, the development of technology that takes advantage of the resources of southern Peru would not only reinforce the southern energy node but also strengthen the on-site transmission system, relieving the congestion of the central-south grid connection.

In addition, introducing more renewable energy into the SEIN helps meet the country's greenhouse gas emissions mitigation commitments under the Paris Agreement, from which the introduction of renewable energy in the energy matrix represents 4.24% of the amount of emissions reduction expected by 2030, which is equivalent to 3.793 MtCO$_2$eq [4].

Currently, in Peru, there are not many research studies related to CSP, so this thesis can help to lay the foundation for the development of future research to take advantage of

solar resources. Moreover, this thesis shows the technical-economic scenarios that allow the incorporation of CSP in the south, giving way to the economic development of that area of Peru.

General objective

- Develop technical-economic scenarios for the incorporation of a solar power tower with thermal energy storage and photovoltaic (SPT-TES + PV) hybrid power plant in the south of Peru.

Specific objectives

- Analyze the solar resources and meteorological data of the Arequipa region.
- Develop the conceptual design of a solar power tower with thermal energy storage and photovoltaic (SPT-TES + PV) hybrid power plant.
- Calculate the LCOE for the SPT-TES + PV hybrid power plant.
- Elaborate scenarios for the incorporation of a SPT-TES + PV hybrid power plant into the Peruvian national grid.

CHAPTER I

THEORETICAL FRAMEWORK

1.1 Electric generation in Peru

Peru has a diversified power capacity (**Figure 1.1**), which shows a predominance of thermoelectric power in installed capacity with 55%, followed by hydroelectric power with 40%, and finally by the most relevant RESs such as wind with 3% and solar with 2% [13].
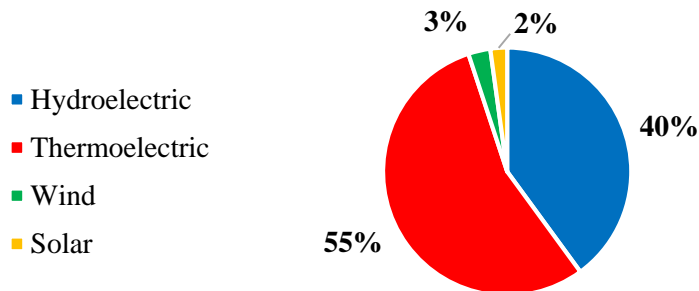
Figure 1.1 Installed power by type of generation – SEIN 2020
Source: COES-SINAC. Estadistica anual del SEIN 2020 [13]

On the other hand, generation by type of technology (**Figure 1.2**) shows an energy matrix with a predominance of hydroelectric power generation with 60% of the total share, followed by thermoelectric power generation with 35%, and finally by the RESs with 5% (wind – 3% and solar – 2%) [13].
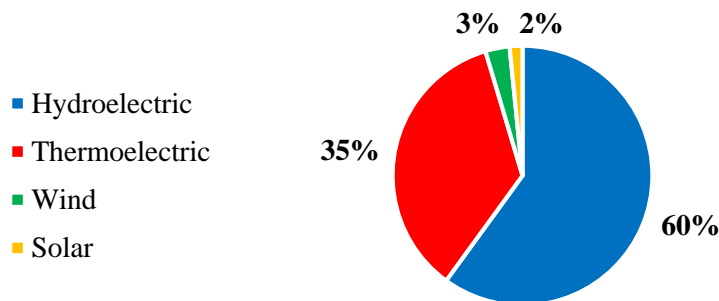
Figure 1.2 Energy production by type of technology – SEIN 2020
Source: COES-SINAC. Estadistica anual del SEIN 2020 [13]

1.1.1 Hydroelectric power generation

Hydroelectric power generation has an installed capacity of 4,995 MW (the main plants are listed in **Table 1.1**) and is responsible for 58% of electricity generation in Peru, reaching its maximum production during the wet season [13]. On the other hand, Peru's hydroelectric potential, with the development of small- and medium-sized plants, is 70,000 MW [28]; likewise, this type of generation provides flexibility for the system.

Company	Name	Power (MW)	Region
Electroperú	C. H. Mantaro I	798	Huancavelica
Kallpa Generación	C. H. Cerro del Águila	513.9	Huancavelica
Eghuallaga	C. H. Chaglla	450.7	Huánuco
Enel Generación Perú	C. H. Huinco	258.4	Lima
Celepsa	C. H. Platanal	220	Lima

Table 1.1 Main hydroelectric power plants
Source: Osinergmin. Proyectos Generación [29]

1.1.2 Thermoelectric power generation

Thermoelectric power generation represents approximately 38% of the country's generation and has 7,396 MW of installed capacity [13] (the main plants are listed in **Table 1.2**). This generation has been mainly encouraged by the production of the Camisea reserves. In addition, this type of generation provides security and reliability for the system.

Company	Name	Power (MW)	Region
Kallpa Generación	C.T. Kallpa	874	Lima
Engie Energía Perú	C.T. Chilca 1	862	Lima
Fenix Power Peru	C.T. Chilca	535	Lima
Enel Generación Perú	C.T. Ventanilla	485	Lima
Termochilca	C.T. Santo Domingo de los Olleros	198	Lima

Table 1.2 Main thermoelectric power plants
Source: Osinergmin. Centrales de generación eléctrica - En operación [30]

1.1.2.1 Consumption of natural gas from Camisea

The consumption of natural gas for power generation has been evaluated for thermal power plants in the area of Lima and Ica, because gas transportation does not represent a

restriction. **Table 1.3** shows the projected natural gas consumption for the period 2019–2020 of the thermal power plants in the Lima and Ica area, showing an increase in both scenarios.

MMPCD	2019	2020
Maximum	431	477
Minimum	241	311
Average	341	398

Table 1.3 Average annual Camisea gas dispatch in MMPCD
Source: COES. Informe de Diagnóstico de las Condiciones Operativas del SEIN, Período 2021–2030 [8]

On the other hand, **Figure 1.3** shows the monthly consumption of natural gas in power plants, showing that in the months of the dry season gas consumption is higher than in the months of the wet season.
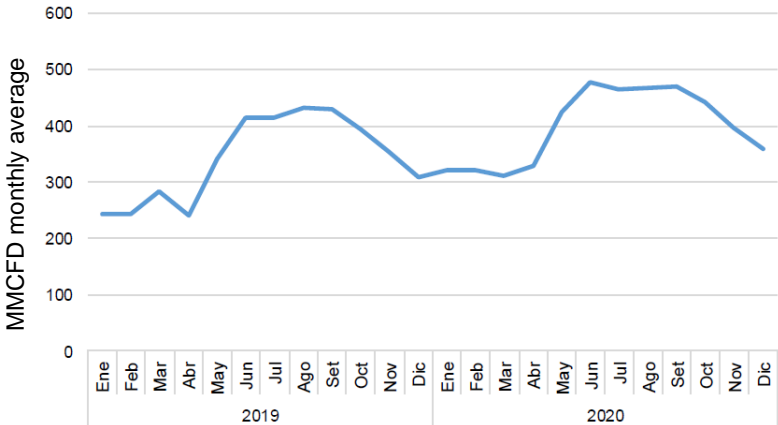
Figure 1.3 Monthly consumption of Camisea natural gas for power plants (Lima and Ica)
Source: COES. Informe de Diagnóstico de las Condiciones Operativas del SEIN, Período 2021–2030 [8]

1.1.3 Renewable energy source generation (solar and wind)

The RES share in electricity generation represents 4%, considering photovoltaic solar and wind power generation [13]. The contribution of technology and potential of the resources are detailed below.

1.1.3.1 Solar photovoltaic power generation

Figure 1.4 Photovoltaic power potential
Source: World Bank Group, SolarGis, and
ESMAP. Solar resource maps of Peru [31]

Solar photovoltaic power generation represents about 1% of the country's generation. In recent years, seven projects have been awarded, which have a total installed capacity of 285 MW [13]. The plants are listed in **Table 1.4**).

In addition, new studies are under development due to the high photovoltaic potential of the country that has values of 5.0–6.2 kWh/m^2 [31] on the coast and the highlands of southern Peru (see **Figure 1.4**).

Company	Name	Power (MW)	Region
Engie Energía Perú	C.S. Intipampa	44.5	Moquegua
GTS Majes	C.S. Majes Solar 20T	20	Arequipa
Moquegua FV	C.S. Moquegua FV	16	Moquegua
Panamericana Solar	C.S. Panamericana Solar 20 TS	20	Moquegua
GTS Repartición	C.S. Repartición Solar 20T	20	Arequipa
Enel Green Power Peru	C.S. Rubi	144.48	Moquegua
Tacna Solar	C.S. Tacna Solar 20TS	20	Tacna

Table 1.4 Main solar photovoltaic power plants
Source: Osinergmin. Centrales de generación eléctrica – En operación [30]

1.1.3.2 Wind power generation
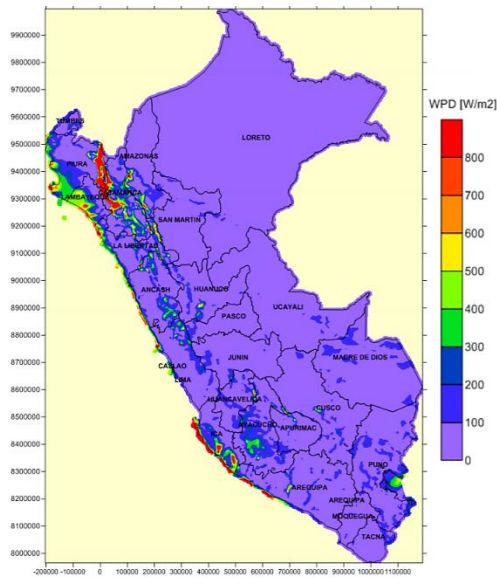
Figure 1.5 Average annual wind power density at 100 m
Source: MINEM, Vortex, and Barlovento.
Atlas Eólico del Perú [32]

Wind power generation represents about 3% of the country's generation. In recent years, five projects have been awarded, which have a total installed capacity of 375 MW [13] The plants are listed in **Table 1.5**. Currently, two new projects are about to go into operation and would add 36 MW to the system.

Moreover, the usable wind potential is 20,493 MW, and there are high annual power density values[10] of 400–800 W/m^2 (see **Figure 1.5**) on the north and south coast of Peru [32].

Company	Name	Power (MW)	Region
Energía Eólica	C.E. Cupisnique	80.15	La Libertad
Parque Eólico Marcona	C.E. Parque Eólico Marcona	32	Ica
Energía Eólica	C.E. Talara	30.86	Piura
Parque Eólico Tres Hermanas	C.E. Tres Hermanas	97.15	Ica
Enel Green Power Peru	C.E. Wayra I	132	Ica

Table 1.5 Main wind power plants
Source: Osinergmin. Centrales de generación eléctrica – En operación [30]

Additionally, the north has hydro biological resources such as cane, rice husks, and bagasse waste (dry forests), which drive the development of biomass projects.

---

[10] Average annual wind power density at 100 m.

1.2 Regulatory framework

The most relevant regulatory framework for RES generation is described below.

1.2.1 Decree Law N°. 25844, Electric Concessions Law and Supreme Decree N°. 009-93-EM, Regulation of the Electric Concessions Law

This law regulates and controls the provision of power generation, power distribution, and transmission services; provides for the general provisions of electricity tariffs; offers guidelines for concessions and authorization; and describes the guarantees for the promotion of investment in the electricity sector.

1.2.1.1 Temporary concessions

This type of concession is for developing feasibility studies. The maximum term for these concessions is two years, and they can be renewed for an additional year, only once, at the request of the interested party. This concession has no contract, since the title is granted by the Ministerial Resolution, and its term of validity is counted from the date of publication of the Resolution of granting.

On the other hand, the temporary concession is not exclusive. Consequently, the MINEM may grant a temporary concession for studies of generation plants, substations, and transmission lines within the same areas to more than one petitioner at a time.

1.2.1.2 Definitive concessions

This type of concession is granted if one wishes to carry out an electricity generation activity that exceeds 0.50 MW. The final concession is approved by a Supreme Resolution and is paired with a concession contract. Likewise, this type of concession provides exclusivity to the interested party for the agreed period of years.

1.2.2 Legislative Decree N°. 1002, Promotion of Investment for Electricity Generation with the Use of Renewable Energies

The following articles of the decree pertain to RES

- Article 2: Declares of national interest and public necessity the development of new electricity generation through the use of RES.

- Article 5: The RES generation has priority in the daily cargo dispatch.

- Article 7: The allocation of premiums to each project will be auctioned.

1.2.2.1 Renewable energy source auctions

The development of RES generation plants through auctions has resulted in 64 projects (1,257 MW). **Figure 1.6** shows the average price obtained in the auctions already carried out, differentiating them by the type of technology auctioned.
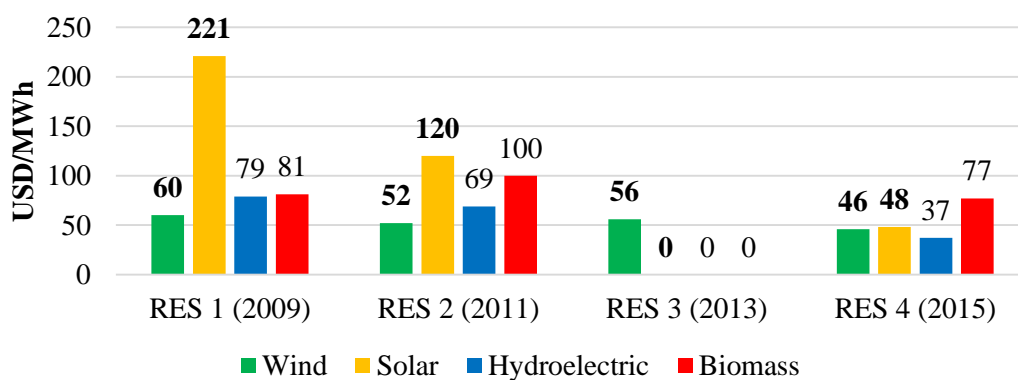
Figure 1.6 Average price of energy by type of technology – RES auctions
Source: Equilibrium. Análisis del Sector Eléctrico Peruano: Generación [5]

1.2.3 Resolution of the board of directors' supervisory body for investment in energy and mining, Osinergmin N°. 144-2019-OS/CD

This resolution describes the modification of number 8.6.3. of the Technical Procedure of the COES Nº 26 "Calculation of the Firm capacity" (approved by R.M. N°.

344-2004-MEM/DM). The modification of the procedure provides a new calculation of firm capacity for RES power plants, allowing them to access power income.

The firm capacity of RES power plant that use wind, solar, or tidal technology will be determined by considering the energy production at peak hours of the system as defined by the MINEM with the following equation:

$$PF_i = \frac{\sum_1^h EG}{h}$$

PF_i Firm capacity of the central RES power plant

EG Production of active energy of the RES power plant during the system's peak hours of the last 36 months (period of evaluation)[11]

h Total number of peak hours of the system corresponding to the evaluation period of the EG

1.3 Mining sector

1.3.1 Mining contributions

One of the most important economic activities in Peru is mining, because it generates added value, contributes 10% to the gross domestic product [33], and represents 60% of national exports [34]. The metals with the greatest participation are copper and gold.

---

[11] If this series is not available, it will be necessary to consider the period from the date of commercial operation start-up of the RES plant until the month of evaluation of the PF_i.
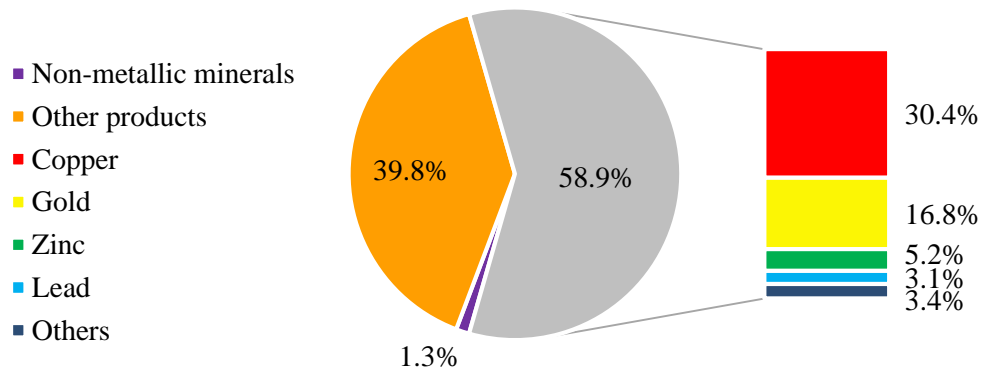
Figure 1.7 Structure of Peru exports, 2018
Source: [34], [35]

1.3.2 Mining reserves

Peru is a country with polymetallic resources, with important products such as copper (the second largest producer in the world), gold (the sixth largest producer in the world), silver (the second largest producer in the world), iron (the fourth largest producer in Latin America), zinc (the second largest producer in the world), molybdenum (the fourth largest producer in the world), and lead (the third largest producer in the world) [36]. The value of mineral reserves is approximately 1.2 billion USD, which is equivalent to six times the country's gross domestic product (0.2 billion USD, 2017). The largest amount of mineral reserves is in the south of Peru (54%), as can be seen in **Figure 1.8**.
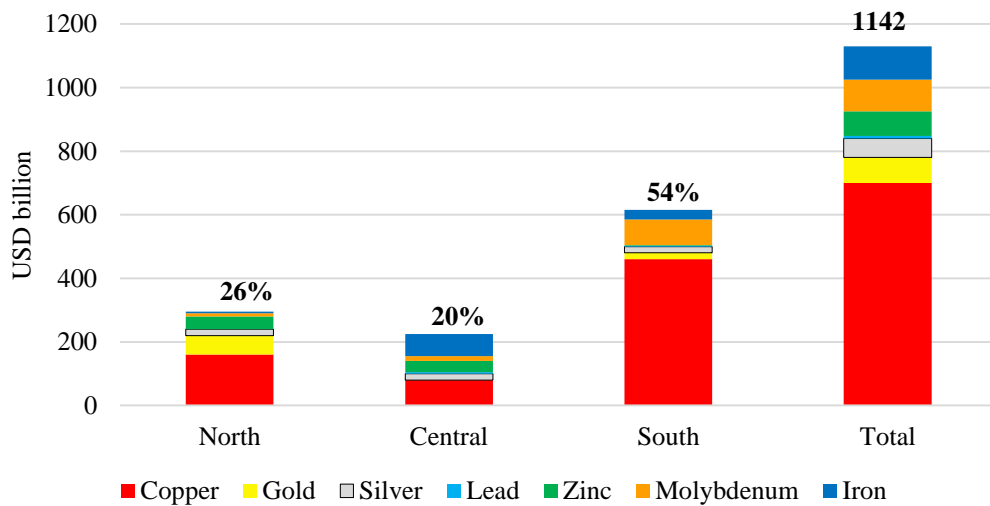
Figure 1.8 Value of metal reserves in Peru
Source: [37], [38]

1.3.3 Energy consumption

The mix of energy consumption by type of source shows that diesel has the largest share with 35%, followed by electricity representing 26% of consumption, and finally by natural gas with 13% (see **Figure 1.9**). However, 40% of electricity is produced by thermoelectric generation with natural gas [39].

On the other hand, energy consumption by productive sector shows that the main sector is vehicular transport with 51% participation, while mining comprises 10% of national consumption, covering its demand mainly with electricity (89%) [40].
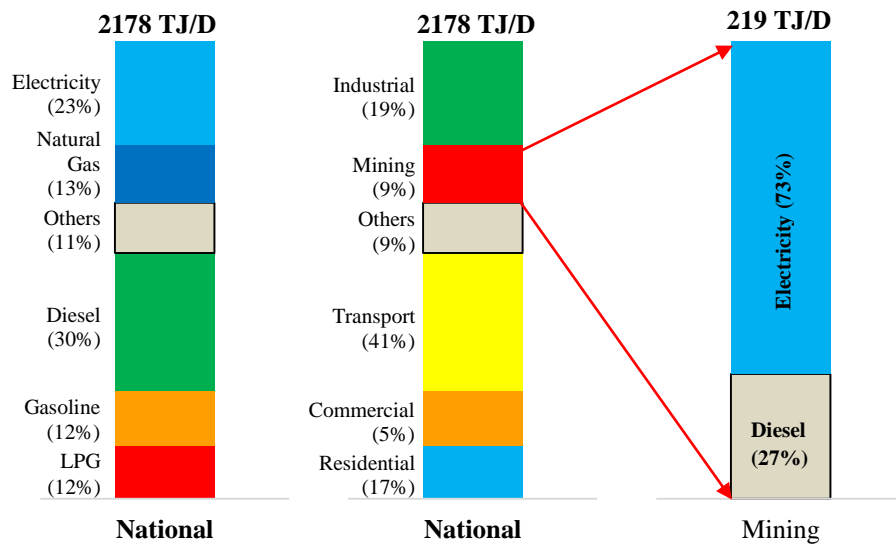
Figure 1.9 Daily energy consumption, 2019
Source: [38], [40]

1.4 Natural gas in the south

1.4.1.1 Southern energy node

Aiming to provide generation service reliability and to ensure 70% of the demand for natural gas that will come from the Peruvian Southern Gas Pipeline (PSGP), the Southern Energy Node was developed. The Southern Energy Node is comprised of two thermal power plants: Puerto Bravo (Mollendo – Arequipa) and Ilo 4 (Ilo – Moquegua), both having an installed power of 1500 MW [23].

In the first stage, plants will work with diesel until a second stage that includes the arrival of natural gas from the PSGP and the operation of power plants with natural gas. However, with the delay of the PSGP and the transition of the thermal power plants of the Southern Energy Node to natural gas is restricted.

1.4.1.2 Integrated gas transport system

The integrated gas transportation system project (SIT GAS) continues (before the Southern Peruvian Gas Pipeline) with the proposal to bring natural gas to the south. The SIT GAS is managed by the firm Mott MacDonald [41].

The MINEM estimates that it will bid this project in 2020. The project is granted for 2022, and the commercial operation date (COD) is planned for July 2025. For evaluation of the scenarios described below, it has been considered that the SIT GAS would reach the south of Peru in 2026 [42].

1.5   Projection of the demand – SEIN

The projection of the SEIN demand at the generation level for the 2018–2021 period estimates a growth in energy and power at an annual rate of 5.6% and 4.2%, respectively (details in **Table 1.6**).

Year	Energy		Power	
	MW	**%**	**MW**	**%**
2019	54,640	6.3	7,330	4.4
2020	57,910	6.0	7,783	6.2
2021	61,871	6.8	8,313	6.8
2022	66,871	7.8	8,866	6.7
2023	70,887	6.2	9,327	5.2
2024	74,764	5.5	9,816	5.2

Average 2019–2024	6.4%	5.7%

Table 1.6 Global demand for the SEIN, 2019–2021
Source: COES-SINAC. Informe de Diagnóstico de las Condiciones Operativas del SEIN, Período 2021-2030
[8]

Projection of the power and energy requirements of the main projects in the mining sector for a medium-term scenario, according to the area, is shown in **Table 1.7**. Here it is noted an expected increase in demand by the commissioning of large mining projects from 2018–2021. Concerning their geographical distribution, the mining projects are concentrated in the south and center of the country.

Main demand projects	2018		2019		2020		2021	
	MW	GWh	MW	GWh	MW	GWh	MW	GWh
Proyecto Tía María								
Ampliación Concentradora Cuajone	21	87	21	174	67	554	67	554
Ampliación Concentradora Toquepala	26	220	53	439	53	439	53	439
Ampliación Cerro Verde	14	104	14	170	24	248	24	248
El Brocal (Colquijiroa)	11	69	9	171	9	171	9	171
Ampliación Shougang Hierros Perú	30	47	60	514	60	514	60	514
Ampliación Antamina	22	209	29	261	65	533	65	529
Ampliación de Aceros Arequipa			2	86	22	458	22	472
Ampliación Toromocho	4	23	6	44	66	228	66	342
Cemento Pacasmayo-Fosfatos Bayovar								
Cemento Pacasmayo-Cementos Piura							5	17
Ampliación UNACEM – Condorcocha					9	51	10	105
Las Bambas				17	7	96	14	155
Coroccohuayco – Antapaccay			5	9	25	142	30	226
Quechua								
Quellaveco – Angloamerican					10	13	48	107
Chucapaca	2	7	2	11	16	21	18	126
Hilanon								
Pukaqaqa								
Pampas de Pongo			2	35	121	562	121	1090
Los Calatos								
Michiquillay – Angloamerican								
Haquira								
Mina Justa			15	53	79	276	80	598
Rio Blanco							46	330
Ampliación Refinería Talara	2	10	33	111	84	554	84	66
Corani							33	219
Ollachea (Kuri Kullu)			7	58	10	80	10	80
Salmueras Sudamericanas					2	17	2	18
Magistral (Milpo)								
Zafranal (AQM Copper)								
Tambomayo (Buenaventura)		31	3	31	3	31	3	33
Ampliación-re Comp Met La Oroya								

Main demand projects	2018		2019		2020		2021	
	MW	GWh	MW	GWh	MW	GWh	MW	GWh
Shouxin	2	91	2	91	2	91	2	91
Terminal Portuario SJ Marcona (JMP)					37	184	37	368
Total Projects – North Zone	8	51	41	173	94	627	146	1088
Total Projects – Central Zone	69	439	126	1255	470	3068	173	4280
Total Projects – South Zone	63	448	104	909	214	1623	299	2186
TOTAL PROJECTS	140	938	271	2337	779	5318	918	7553

Table 1.7 Demand of power (MW) and energy (GWH) of major mining projects
Source: COES. Informe de Diagnóstico de las Condiciones Operativas del SEIN, Período 2021-2030 [8]

Considering a scenario with a medium level of development of mining projects in the south, the projection of the demand up to 2028 is shown in **Figure 1.10**. This projection considers the income of the following projects: Extensions SPCC (155 MW), Cerro Verde (24 MW), Las Bambas (70 MW), Quellaveco (180 MW), San Gabriel (60 MW), Ollachea (11 MW), Coroccohuayco (40 MW), Corani (38 MW), the Chankas (90 MW), Haquira (103 MW), and Zafranal (80 MW) [7].
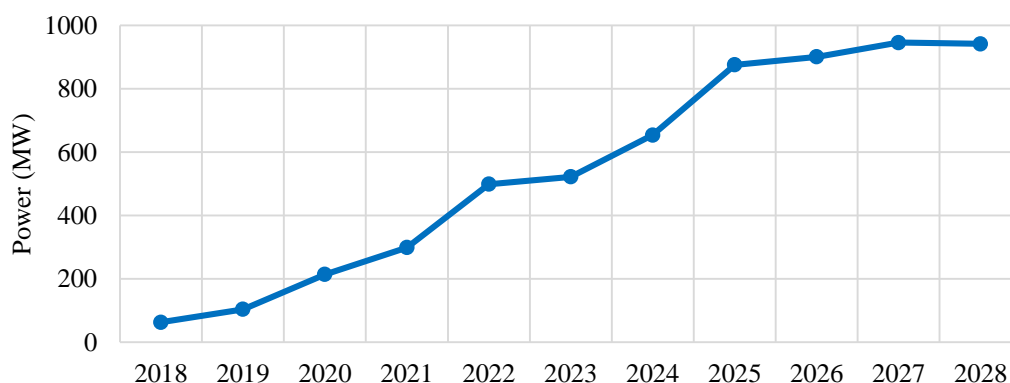
Figure 1.10 Projection of demand for mining projects in the southern area for 2019–2028 (medium-term scenario)
Source: COES. Evaluación de la necesidad de generación eficiente en el SEIN y prospectiva del suministro eléctrico del sur en el corto, mediano y largo plazo [7]

1.5.1   Generation works program

For the period 2018–2021, the installation of 995 MW is planned, which represents an increase of 8% over the effective power of the SEIN with respect to 2017. Likewise, 23% of the works will be installed in the north, 51 % in the center, and 26% in the south [8].

Year	Project	Technology	Company	MW
2018	CS Rubi	Solar	Enel Green Power Perú	144.5
	CH RenovAndes H1	Hydro-RES	Empresa De Generación Santa Ana	20
	CH Angel III	Hydro-RES	Generadora De Energía Del Perú	20
	CH Angel III	Hydro-RES	Generadora De Energía Del Perú	20
	CH La Virgen	Hydro-RES	La Virgen	84
	CS Intipampa	Solar	Engie	40
	CB Doña Catalina (Huaycoloro II)	Biomass	Empresa Concesionaria Energía Limpia	2.4
	CE Wayra I (Parque Nazca)	Wind	Enel Green Power Perú	126
	CH Angel I	Hydro-RES	Generadora De Energía Del Perú	20
	CH Her 1	Hydro-RES	Edegel	0.7
	CT Santo Domingo de los Olleros - TV	Combined cycle	Termochilca	100
	CH Centauro – Etapa I	Hydro	Corporación Minera Del Perú S.A. – Cormipesa	12.5
	CH Carhuac	Hydro-RES	Andean Power	20
2019	CH 8 de Agosto	Hydro-RES	Generación Andina	19.8
	CH El Carmen	Hydro-RES	Generación Andina	8.6
	CB Callao	Biomass	Empresa Concesionaria Energía Limpia	2.4
	CH Zaña 1	Hydro-RES	Electro Zaña	13.2
	CE Huambos	Wind	Gr Paino	18.4
	CE Duna	Wind	Gr Taruca	18.4
	CH Ayanunga	Hydro-RES	Energetica Monzon	20
	CH Santa Lorenza I	Hydro-RES	Empresa De Generación Santa Lorenza	18.7
	CH Karpa	Hydro-RES	Hidroeléctrica Karpa	20
	CH Huatziroki I	Hydro-RES	Empresa De Generación Hidraúlica Selva	11.1
	CH Hydrika 6	Hydro-RES	Hydkra 6 S.A.C.	8.9
	CH Manta	Hydro-RES	Peruana De Inversiones En Energías Renovables	19.8
2020	CH Centauro – Etapa II	Hydro	Corporación Minera Del Perú S.A. – Cormipesa	12.5
	CH Laguna Azul	Hydro-RES	Chimamacocha S.R.L.	20
	CT Refinería Talara	Thermal	Petroperu	100
2021	CH Colca	Hydro-RES	Empresa De Generación Eléctrica Colca	12.1
	CH Shima	Hydro-RES	Energía Hidro S.A.C.	9
	CH Kusa	Hydro-RES	Consorcio Hidroeléctrico Sur Medio	15.6
	CH Alli	Hydro-RES	Consorcio Hidroeléctrico Sur Medio	14.5
	CH Hydrika 5	Hydro-RES	Hydkra 5 S.A.C.	10
	CH Hydrika 2	Hydro-RES	Hydkra 2 S.A.C.	4
	CH Hydrika 4	Hydro-RES	Hydkra 4 S.A.C.	8

Table 1.8 Generation works program for 2018–2021
Source: COES. Informe de Diagnóstico de las Condiciones Operativas del SEIN, Período 2021-2030 [8]

1.5.2 Supply offer

With consideration of the information of the COES in the Diagnostic Report of the operational conditions of the SEIN for the period 2021–2030, in a scenario of average growth, the system would only have an excess to efficient generation until 2022. Then it would require new generation projects to meet the demand for the period 2023–2025, until the arrival of gas to the south in 2026 (details in **Figure 1.11**).
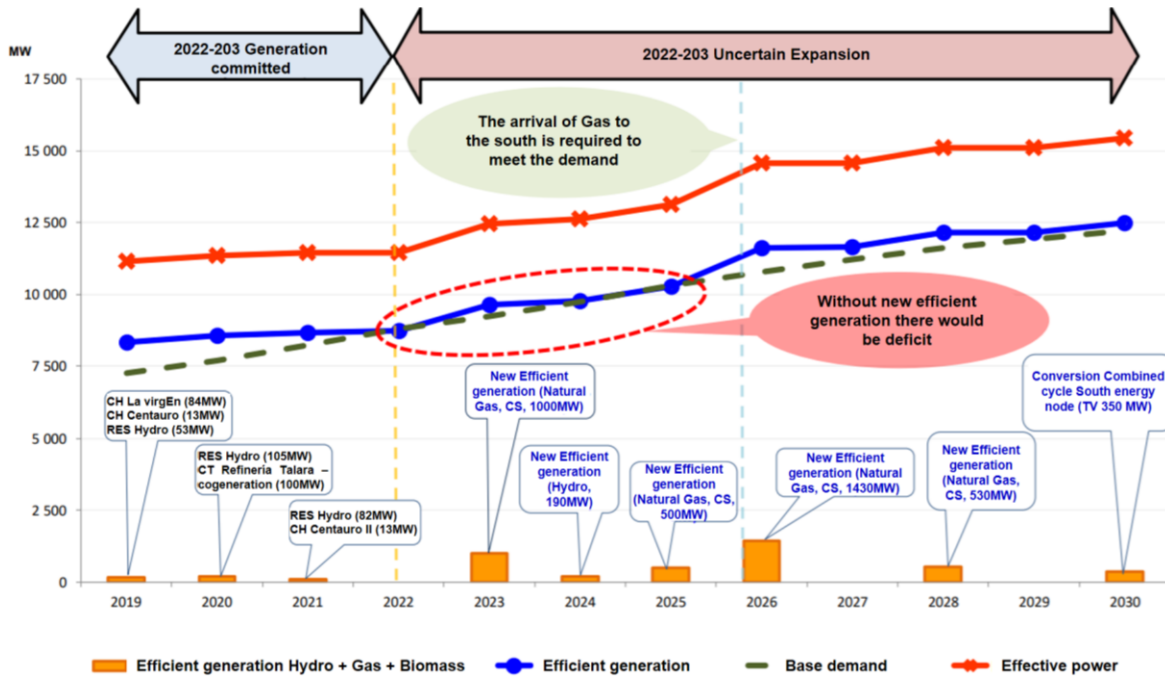
Figure 1.11 Efficient generation in the SEIN – medium demand scenario
Source: COES. Informe de Diagnóstico de las Condiciones Operativas del SEIN, Período 2021-2030 [8]

Figure 1.11 shows that for the projects to be developed in the period 2023–2025, the system demand is covered with a tight balance until 2025. Then, it necessarily requires the operation of the energy node in the south [8].

On the other hand, in a case without efficient generation (no new projects), the deficit to cover the demand would be observed by 2022. This would drive the operation of diesel thermal power plants, thus increasing energy prices progressively from 80 USD/MWh to 120 USD/MWh, until the arrival of the gas pipeline in 2026 [7]. However, in a scenario that

considers delays in the construction of the gas pipeline, energy prices would reach values between 150 USD/MWh and 200 USD/MWh for the period 2026–2028 [7].

1.5.3   Need for efficient generation

In the scenario of average demand of the SEIN and without the entry of efficient new generation in the period 2022–2028, there would be a continuous increase in diesel-based generation by 2022, which evidences the need for new efficient generation in the SEIN to avoid increasing the operating costs of the system, as can be seen in **Figure 1.12**.
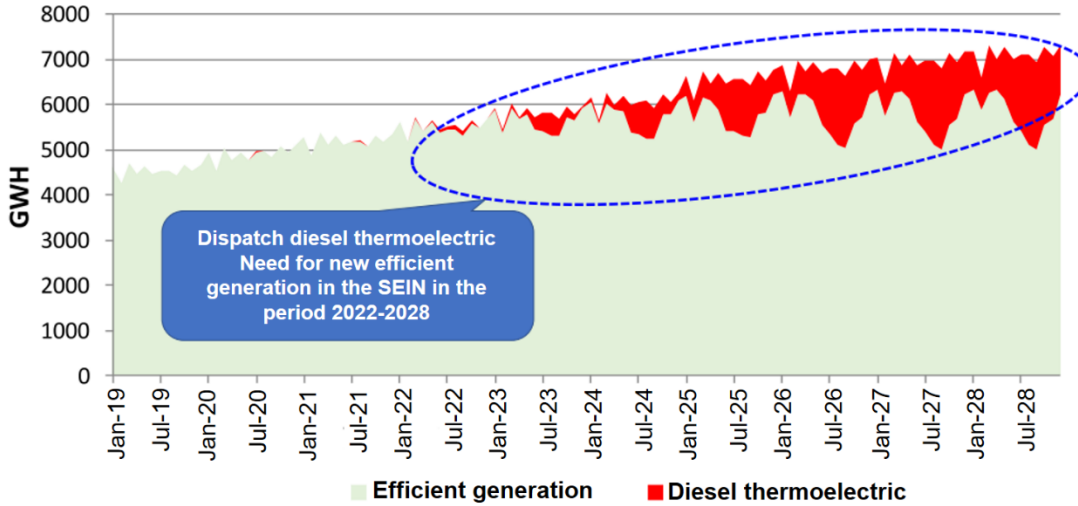
Figure 1.12 Energy dispatch in the SEIN in the medium-term scenario
Source: COES. Evaluación de la necesidad de generación eficiente en el SEIN y prospectiva del suministro eléctrico del sur en el corto, mediano y largo plazo [7]

Given the medium-term mining development scenario in the south, the generation required in the south to avoid congestion on the central-south grid is 100 MW in 2024 and 200 MW in 2025 (see **Figure 1.13**).
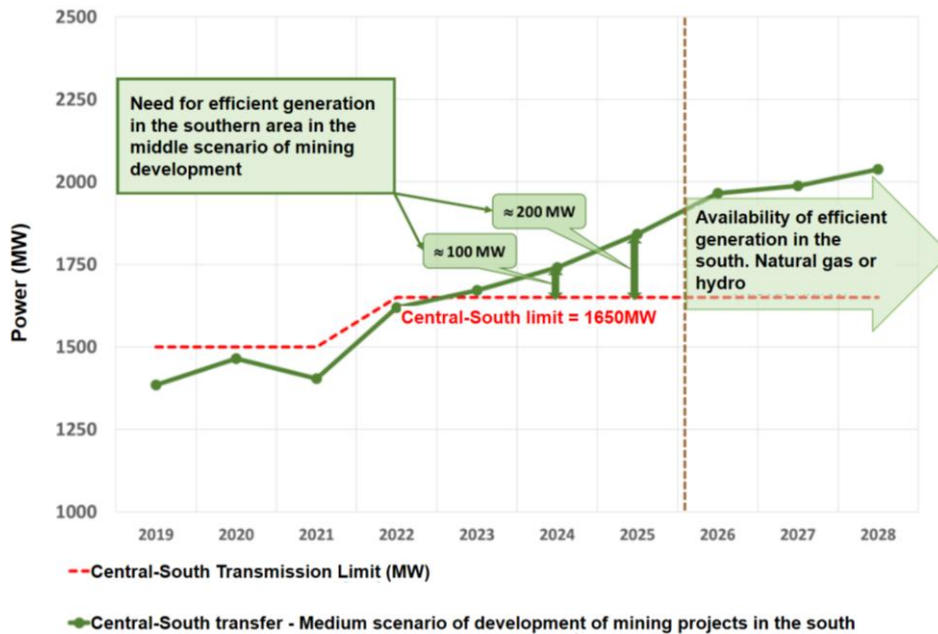
Figure 1.13 Efficient generation required estimated in the south area so as not to exceed the central-south limit in the medium-term scenario of development of mining projects in the south
Source: COES. Evaluación de la necesidad de generación eficiente en el SEIN y prospectiva del suministro eléctrico del sur en el corto, mediano y largo plazo [7]

Moreover, the central-south grid would be congested by 2024. In 2025, the congestion would occur in all the demand blocks, but by 2026, with the commissioning of the SIT GAS, congestion would be eliminated (see **Figure 1.14**).
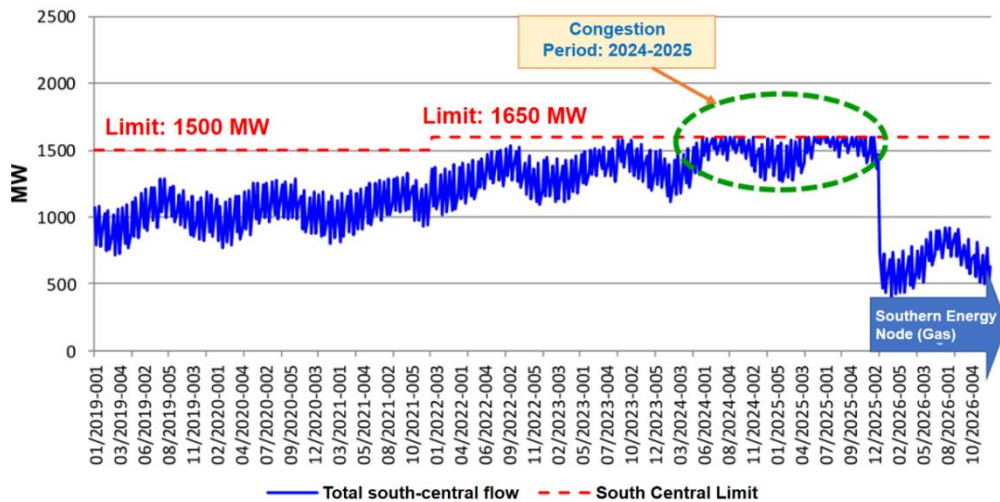
Figure 1.14 Central-south transfer in the medium-term scenario of mining development in the south and without new efficient generation in the south until 2025
Source: COES. Evaluación de la necesidad de generación eficiente en el SEIN y prospectiva del suministro eléctrico del sur en el corto, mediano y largo plazo [7]

1.6   Solar resources

Depending on the solar power plant to be developed, different measurements are required either PV or CSP, due to the components of solar irradiation.[12]

Component	Measurement	Application
GHI* (global horizontal irradiation)	Pyranometer, reference cell	PV and CSP
GTI (global tilted irradiation)	Pyranometer (tilted), reference cell (tilted)	PV
DHI (diffuse horizontal irradiation)	Rotating Shadowband Irradiometer, pyranometer with shadow ring or ball	PV
DNI* (direct normal irradiation)	Pyrheliometer installed on Sun Tracker, rotating Shadowband Irradiometer	CSP and large PV power plants

Table 1.9 Components of solar irradiation
Source: Ammonit. Solar Measurement for Solar site assessment [43]

1.6.1   Direct normal irradiance

Direct normal irradiance (DNI) is the amount of solar radiation received by a unit area that is perpendicular (i.e., normal) to the incoming sun rays [44]. Studies suggest that DNI should be at least 2000 kWh/m^2 per year to provide a viable energy yield [45], [46].

The DNI is strongly affected by the composition of the atmosphere and the weather corresponding to a specific location [46], [47] (**Figure 1.15**). Moreover, it is necessary to consider auxiliary meteorological parameters (such as ambient air temperature, humidity, wind conditions, and atmospheric pressure), because they will affect the value of the measurement.

---

[12] The term irradiation is used to consider the amount of solar energy falling on a unit area over a stated time interval such as a day or a year. The term irradiance is used to describe the solar power (instantaneous energy flux) falling on a unit area per unit time, that is, in W/m^2 [46].
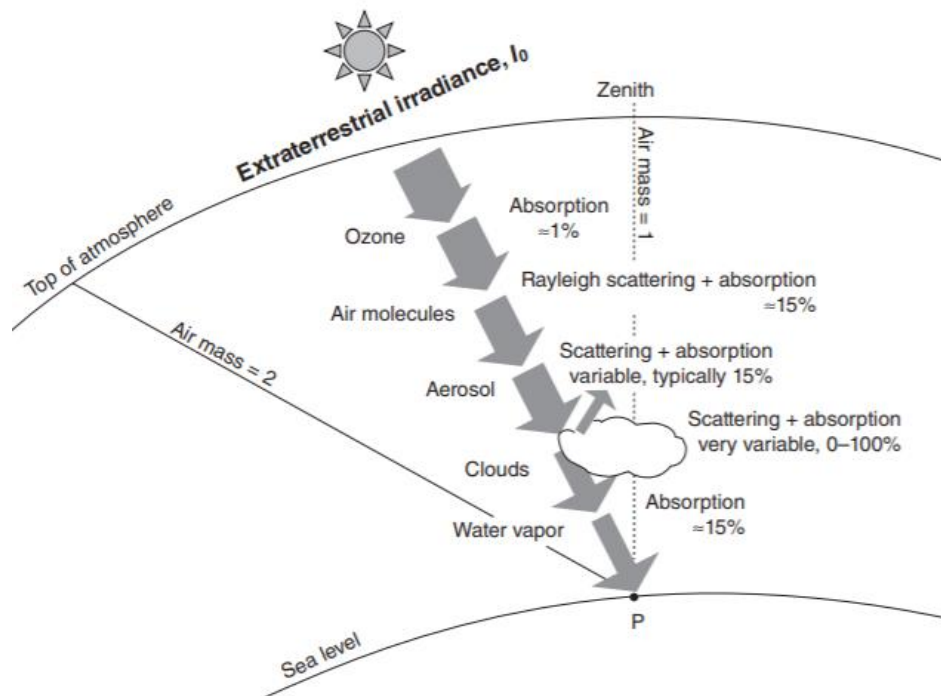
Figure 1.15 The main processes influencing solar radiation in the atmosphere, split into the major three components (global, direct, and diffuse)
Source: K. Lovegrove and W. Stein. Concentrating Solar Power Technology : Principles, Developments and Applications [46]

1.6.1.1 Solar resource assessment – direct normal irradiance

Sun irradiation differs from site to site. Thus, it is important to measure the local irradiation to design profitable solar power plants [44]. The main methods and technologies to measure the irradiation are the following:

A. LT Satellite-derived data

- Suppliers for irradiance: SolarGis (ex-GeoModel Solar), TIER3/Vaisala, Meteonorm 7, NASA-SSE, DLR-ISIS, HelioClim-3, and IrSOLaV.

- Advantages: Long-term data (up to 21+ years), good for inter-annual variability, continuous geographical coverage, spatial and temporal consistency, and calibration stability.

- Disadvantages: Lower accuracy for the point estimate (compared to ground measurements) [47].

B. Ground measurements

- Instruments: Rotating Shadowband Irradiometer and Pyrheliometer.

  - o Rotating Shadowband Irradiometer: It measures global horizontal irradiation (GHI)* and DHI* from which the DNI can be calculated, for a given site, and sun position.

  - o Pyrheliometer: It is for high precision DNI* measurements, and it requires regular (sometimes daily) maintenance and calibration [43]. Any small error in the tracking system and the instrument may give unreliable readings. Normally, new stations will have Pyranometers or Rotating Shadowband Irradiometers. Once the site is established and the plant is operational, Pyrheliometers are installed.

- Advantages: High frequency of measurements (seconds to minutes), high accuracy if properly maintained.

- Disadvantages: Limited time availability, limited geographical representation, costs for acquisition and operation, regular maintenance and calibration, and data quality control (continuous).

C. Typical meteorological year

The value of typical meteorological year (TMY; P50) is built such that it represents the long-term average value of DNI. It is constructed by a selection of the most representative months from the available time series which are finally concatenated into one artificial and representative single year [47]: "Real" data, hourly (pre-feasibility phase); 1 to 10-minute interval (engineering).

1.7 Concentrating solar power

The CSP plants consist primarily of three parts (**Figure 1.16**): (A) solar field, (B) power block, and (C) TES. The solar field is composed of solar concentrators which reflect and

focus the DNI onto the receiver where the heat transfer fluid (HTF) is heated. The energy received by the HTF in transferred through a heat exchanger to the power block, where it is converted into electricity by turbines and generators [48]. In addition, to increase the global efficiency of the plant and help to assure continuous power generation on overcast days and during the night, a TES is integrated into the system [49].

(A) Solar field	**(B) Power block**
Mirrors, receivers, support structures, collector systems, HTF, heat exchanger, HTF pumps, tracking, piping	Turbine, condenser, super-heater, pump, optional boiler, generator, heat exchangers, cooling tower or air coolers, balance of the systems

(C) TES unit
Storage media, encapsulation methodology, HTF, storage tank, heat exchanger, tank insulation

Figure 1.16 Main parts of a CSP plant and their components
Source: S. Kuravi, J. Trahan, D. Y. Goswami, M. M. Rahman, and E. K. Stefanakos. Thermal energy storage technologies and systems for concentrating solar power plants [49]

1.7.1 Concentrating solar power types

There are currently four existing CSP technologies classified as line focusing systems, which focus sunlight to a line of receivers typically oriented in the north-south direction, and point focusing systems, which focus sunlight to a point where the receiver is located [50] (**Table 1.10** and **Figure 1.17**).

Line focusing systems	Point focusing systems
Parabolic trough collector (PTC)	Solar power tower (SPT)
Linear Fresnel reflector (LFR)	Parabolic dish systems (PDS)

Table 1.10 Classification of concentrating solar power technologies
Source: F. Trieb and H. Müller-Steinhagen. Concentrating solar power [51]
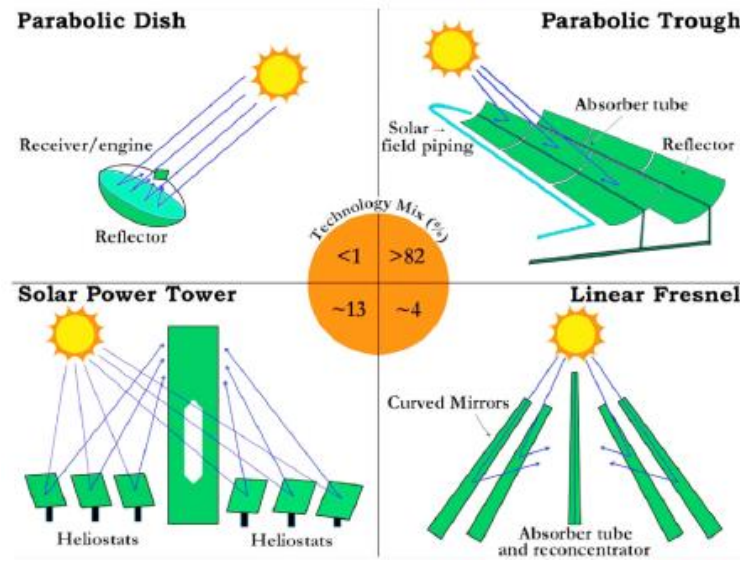
Figure 1.17 Various concentrating solar power technologies along with their installed ratios
Source: X. Xu, K. Vignarooban, B. Xu, K. Hsu, and A. M. Kannan. Prospects and problems of concentrating
solar power technologies for power generation in the desert regions [50]

Around 82% of plants in the world are PTC, followed by 13% that are SPT, 4% that are LFR, and finally 1% that are PDS. Moreover, the current CSP status (**Table 1.11**) shows that there is a greater number of projects under development and construction of PTC and STP technologies [52].

Type of CSP plants	Operational	Under construction	Under development
PTC	77	10	10
SPT	13	6	10
PDS	1	0	0
LFR	7	2	4
Total	98	18	24

Table 1.11 Status of concentrating solar power technologies
Source: NREL. Concentrating Solar Power Projects [52]

1.7.1.1 Parabolic trough collector

For the PTC, U-shaped tubes with mirrors are used, which concentrate the solar energy on hundreds of channels placed in parallel rows and aligned on a north-south axis so that they track the sun in different positions (east to west) throughout the day [53].
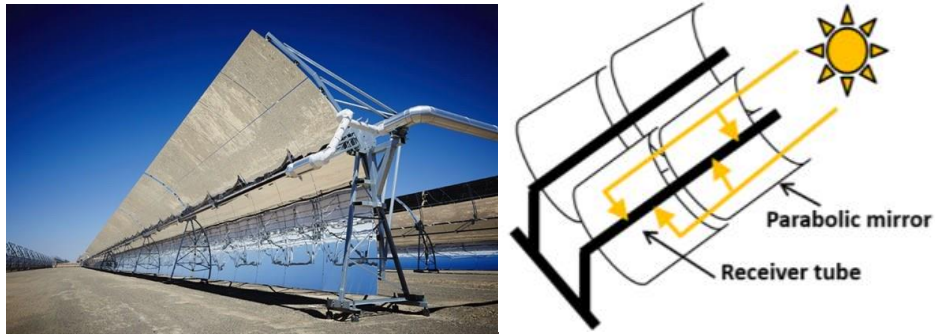
Figure 1.18 KaXu Solar One plant 100 MW, Northern Cape, South Africa (left), Parabolic Trough Collector plant schematics (right)
Source: W. Johwa. SA's KaXu Solar One plant wins UN climate change award [54]

Generally, the heat transfer that flows through the tube has a temperature that reaches 293°C to 393°C. To generate energy, it is necessary to use some liquid like synthetic oil, water, or steam, which uses the thermal energy in a generator of conventional steam [51]. In addition, for efficient fluid heating to be achieved, it is essential that the tube is correctly located in the channel and has a high absorption coefficient, so it is painted in such a way that maximum radiation absorption and a minimum loss of heat are achieved. One of the great benefits of this system is that the hot fluid can be stored for later use when sunlight is absent [55].

1.7.1.2 Linear Fresnel reflector

The LFR system consists of strips of linear mirrors that serve as reflectors that are usually aligned north-south to reflect sunlight toward the upper tube, where a cylindrical receiver contains water tubes, which are heated by high solar radiation and evaporate. Then, under pressure, the vapor enters a steam turbine, causing the generator to turn and produce electricity [55]. For this type of thermal system, the fixed receiver reduces thermal convection losses because its cavity is permanently downward oriented [53]. To itself, the Fresnel reflectors are used in differing quantities and different inclinations to point to different reflectors, allowing a greater optical efficiency and minimizing the use of the ground [46].
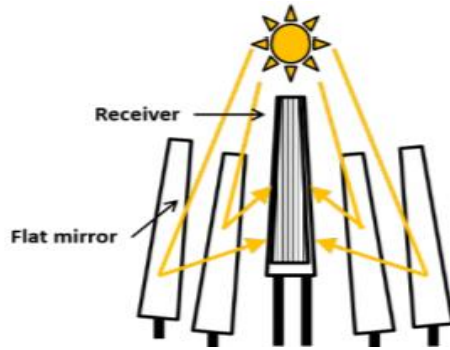
Figure 1.19 Reliance Areva plant 100 MW, Rajasthan, India (left); linear Fresnel reflector plant schematics (right)
Source: A. Kumarankandath. Reliance commissions 100 MW solar power plant in Rajasthan [56]

1.7.1.3 Parabolic dish systems

This system is based on a large satellite dish composed of small flat mirrors (made of silver or aluminum and covered with glass or plastic) that concentrate solar radiation at a focal point [57]. The structure of this dish is designed with a tracking system of two axes to follow the sun, concentrating sunlight on a thermal receiver, which absorbs and collects heat by transferring it to the engine generator (generally the Stirling and Brayton engines are used, which favor the conversion of energy). The fluid heated by the receiver of this system creates mechanical power used to operate a generator or produce energy [58]. Usually this type of system has the capacity to generate energy that ranges from 0.01 to 1.5 MW [53].
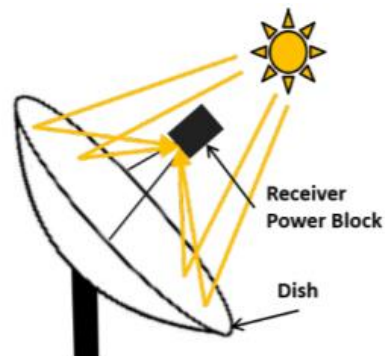
Figure 1.20 Maricopa Dish-Stirling plant 1.5 MW, Arizona, USA (left); parabolic dish system plant schematics (right)
Source: United Sun Systems International Ltd. Maricopa Dish-Stirling plant [59]

1.7.1.4 Solar power tower

The central receiver system uses tracking mirrors (heliostats) to focus concentrating sunlight on a solar receiver at the top of the tower. A transfer fluid is heated to approximately 600°C, and when steam is generated, a conventional turbine generator is used to produce electricity [58].
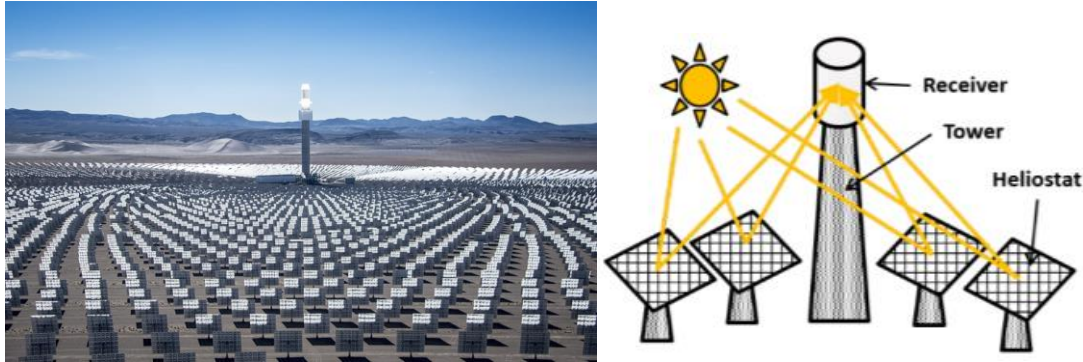
Figure 1.21 The Crescent Dunes Solar Energy Project 110 MW, Nevada, USA (left); solar power tower plant schematics (right)
Source: T. Overton. Crescent Dunes: 24 Hours on the Sun [60]

Some towers use water or steam as their usual HTF; others experiment with salts like molten nitrate for their large energy storage. On the other hand, the system's TES capacity allows it to continue dispatching energy even if it is night or the weather is cloudy [57]. The materials used in the receiver are ceramics or metals stable at elevated temperatures. The average solar flux in the receiver varies from 200 kW/m^2 to 1000 kW/m^2, which allows it to reach a high temperature. At the receiver, the temperature of the fluid becomes high enough to produce steam, which rotates a conventional turbine to generate electricity [53].

For more information about and details of the characteristics of each of the CSP technologies, see **Table 1.12.**

Characteristics	PTC	LFR	SPT	SPD
Capacity (MWe)	10–200	10–200	10–150	0.01–1.5
Concentration ratio	25–100	70–80	300–1000	1000–3000
Solar efficiency max.	20% (expected)	21% (demonstrated)	20% (demonstrated) 35% (expected)	29% (demonstrated)
Annual solar-to-electric efficiency	15%	8–10%	20–35% (concepts)	20–35%
Optical efficiency	Medium	Low	Medium	High
Collector concentration	70-80 suns	>60 suns (depends on secondary reflector)	>1000 suns	>1300 suns
Receiver/absorber	Absorber attached to collector, moves with collector, complex design	Fixed absorber, no evacuation, secondary reflector	External surface or cavity receiver, fixed	Absorber attached to collector, moves with collector
Area requirement (m²/MWh)	4–6*	6–8*	8–12*	30–40
Thermal efficiency (%)	30–40	-	30–40	30–40
Plant peak efficiency (%)	14–20	~18	23–35	~30
Capital cost (US$/kW)	3972	-	4000+, 3850-9000, 3295-5000	12578
	3770 Solar field<$75/m²; receiver and HTF(HTF)<150 USD/kW; power block<1200 USD/kW; thermal energy storage (TES)<$15/kWh		Solar Field 36%, Power Block 24%, Indirect cost 17%, Receiver 15%, Tower 3%, Storage 3%, Land 2%	Solar Field 38%, Power Block 37%, Indirect cost 17%, Receiver 7%, Land 1%
Capital cost (USD/m²)	424	234	476	-
O&M cost (USD/kWh)	0.012–0.02	Low	0.034	0.21
Basic plant cost (USD/W)	3.22	-	3.62	2.65
LCOE (USD/kWh)	0.26–0.37 (no TES) and 0.22–0.34 (with TES)	0.17–0.37 (6h TES)	0.2–0.29 (6–7.5 h TES) and 0.17–0.24 (12–15 h TES)	-
	0.06	0.252-0.168	0.098-0.18 (with TES), 0.06 (4 h TES-Brayton), 0.06-0.065 (8-15 h TES)	

Characteristics	PTC	LFR	SPT	SPD
Land use (m^2/MWh/year)	6–8*	4–6*	8–12*	8–12*
Specific power (W/m^2)	300	-	300	200
Site solar radiation required	Generally sites with annual sum of DNI larger than 1800-2000 kWh/m^2			
Land requirement	Large	Medium	Medium	Small
Typical shape of solar plant	Rectangular	Rectangular	Sector of a circle/rectangular	Rectangular
Water requirement (m^3/MWh)	3 (wet cooling), 0.3 (dry cooling) and 0.4–1.7 (hybrid)	3 (wet cooling) and 0.2 (dry cooling)	2–3 (wet cooling), 0.25 (dry cooling) and 0.3–1 (hybrid)	0.05–0.1 (mirror washing)
Water cooling (L/MWh)	3000 or dry	3000 or dry	2000 or dry	-
Suitability for air cooling	Low to good	Low	Good	Best
Storage with molten salt	Commercially available	Possible, but not proven	Commercially available	Possible, but not proven
Operating temperature of solar field (°C)	290–550	250–390, possible up to 560	250–650	800
Annual CF (%)	25–28 (no TES), 29–43 (7 h TES)	22–24	55 (10h TES), 43–52 (with TES)	25-28
Grid stability	Medium to high (TES or hybridization)	Medium (backup firing possible)	High (large TES)	Low
Power block cycle and fluid conditions	Superheated steam Rankine, steam @380°C/100 bar	Saturated steam Rankine (steam @ 270°C/55 bar), superheated steam Rankine (steam @ 380°C/50 bar)	Superheated steam Rankine (steam @540°C/100–160 bar), Brayton (CO$_2$ @800°C/250 bar)	Stirling/Brayton
Possible backup/hybrid mode	Supercritical steam Rankine, supercritical CO$_2$ Brayton cycle (600°C/200 bar), air Brayton cycle		Yes	Yes, but in limited cases
Storage possibility	Yes	Yes	Depends on plant configuration (3–15 h)	Depends on plant configuration

Characteristics	PTC	LFR	SPT	SPD
Storage system	Yes, but not yet with direct steam generation (DSG) indirect 2-tank molten salt at 380°C (ΔT=100°C) or D\direct 2-tank molten salt at 550°C (ΔT=300°C)	Yes, but not yet DSG short-term pressurized steam storage (< 10 min)	Direct 2-tank molten salt at 550 °C (ΔT=300°C), high-energy density thermochemical (high temperature metal hydride (TMH), H_2, Glycol and Low TMH – 10k cycles)	No storage, chemical storage under development
Heat transfer fluid	Synthetic oil, water/steam (DSG), molten salt with lower melting points, air, steam, supercritical CO_2	Water/steam	Water/steam, molten salt, air (demonstration)	Air, hydrogen, helium
Steam conditions (°C/bar)	380 to 540/100	260/50	540/100 to 160	Not applicable
Development status	Most proven	Demonstration	Mature	Demonstration
Technology development risk	Low	Medium	Medium	Medium
Technology providers	Sener, Solar Millennium, Abengoa, ACS-Cobra, Acciona, Solel, SolarReserve	Austra, MAN Ferrostaal	Abengoa, eSolar, Sener, BrightSource, Torresol, SolarReserve, Brayton Energy	Brayton Energy, Infinia Corporation
Solar fuels	No	No	Yes	Yes
Outlook for improvement	Limited	Significant	Very significant	Through mass production

Table 1.12 Characteristics of concentrating solar power technologies
Adapted from Ref.[53] and updated*
*[2],[50], [27], [33], [34], [40], [43–74]

1.7.2 Solar tower power plant

The current state of this type of technology shows that there are only 34 STP plants worldwide (**Table 1.13**), of which five above 20 MW are operational. The number of existing STP plants of significant size is very limited, but nevertheless, in recent years the participation of this type of technology has grown [2], and there have been developments of plants of greater power.

Project	MW	Status	Year start
Tamarugal Solar Energy Project	450	Development	
Likana Solar Energy Project	390	Development	
Ivanpah Solar Electric Generating System (ISEGS)	377	Operational	2014
Copiapó	260	Development	
Golmud	200	Construction	
Aurora Solar Energy Project	135	Development	
Huanghe Qinghai Delingha DSG Tower CSP Project	135	Development	
NOOR III	134	Construction	
Ashalim Plot B (Megalim)	121	Construction	
Atacama-1	110	Construction	
Crescent Dunes Solar Energy Project (Tonopah)	110	Operational	2015
Golden Tower Molten Salt project	100	Development	
Redstone Solar Thermal Power Plant	100	Development	
SunCan Dunhuang Phase II	100	Construction	
Yumen Molten Salt Tower CSP project	100	Development	
MINOS	52	Development	
Hami CSP Project	50	Development	
Khi Solar One	50	Operational	2016
Qinghai Gonghe CSP Plant	50	Development	
Shangyi DSG Tower CSP project	50	Development	
Supcon Solar Project	50	Construction	
Yumen 50MW Molten Salt Tower CSP project	50	Construction	
Planta Solar 20 (PS20)	20	Operational	2009
Gemasolar Thermosolar Plant (Gemasolar)	19.9	Operational	2011
Planta Solar 10 (PS10)	11	Operational	2007
SunCan Dunhuang Phase I	10	Operational	2016
Sierra SunTower (Sierra)	5	Operational	1009
Lake Cargelligo	3	Operational	2011
ACME Solar Tower	2.5	Operational	2011
Jülich Solar Tower	1.5	Operational	2008
Sundrop CSP Project	1.5	Operational	2016
Jemalong Solar Thermal Station	1.1	Operational	2016
Dahan Power Plant	1	Operational	2012
Greenway CSP Mersin Tower Plant	1	Operational	2012

Table 1.13 Status and characteristics of solar tower power around the world
Source: NREL. Concentrating Solar Power Projects [52]

The development of new STP plants demands the evaluation of the technical aspects, related to the design of the plant, the analysis of the technical parameters of the equipment, and the economic aspects, based on an economic and financial model of the plant to optimize the costs and achieve a competitive LCOE. A standard STP plant consists of three parts: solar field, TES, and power block, which are described below.
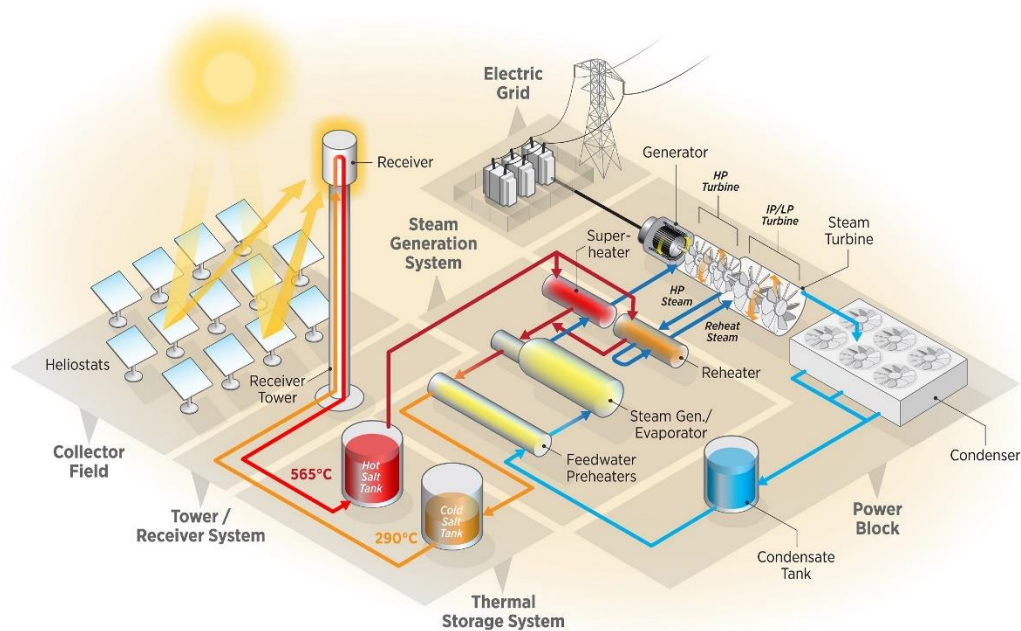
Figure 1.22 Parts of a solar tower power plant (layout)
Source: NREL. Concentrating Solar Power Basics [57]

1.7.2.1 Solar field

A. Heliostats

The solar field is the largest capital investment of a STP plant, and the largest cost components are the heliostats [93], the same ones that require a complex and efficient arrangement to optimize the solar field [94]. The heliostats consist of mounted mirrors that track the sun on two axes and reflect accurately onto the receiver (concentrating the irradiance) [93]. There are a number of factors that affect the arrangement of CSP heliostats, including the tower height, land area, dimensions of the heliostats, and their losses, as seen in **Table 1.14**.

Optical Losses	Abbreviation	Ratio
Cosine effect	η_{cos}	0.85–0.95
Shadow effect	η_{sh}	0.95
Blocking effect	η_{bl}	0.95–0.97
Atmospheric attenuation	η_{aa}	0.9–0.92
Edging factor	η_{edg}	0.86

Table 1.14 Optical losses in heliostats
Source: K. Lovegrove and W. Stein. Concentrating Solar Power Technology : Principles, Developments and Applications [46]

B. Receiver

The solar receiver is located on top of the tower and represents the device to which the incoming radiation from the solar field is directed and concentrated. Then the heat is transferred from the concentrated heat flux to the HTF [93]. It is important to consider the characteristics and properties of the HTF, the speed and pressure of the fluid, the critical temperature ranges, and a correct selection of the receiver type, with the aim of reducing the losses by radiation and convection and achieving better efficiency [94], [46].

1.7.2.2 Thermal energy storage

The most commercial used fluid for TES are the molten salts, because it permits TES in hot and cold reservoirs to decouple electricity production from the availability of sunlight [95], [96].

Designing an optimal TES requires high energy density in the storage material; good heat transfer between the HTF and the storage medium; mechanical and chemical stability of the storage material; chemical compatibility between HTF, heat exchanger, and storage medium; complete reversibility for a large number of charging/discharging cycles; and low thermal losses [49].

Molten salt	NaNO$_3$-KNO$_3$	LiF-NaF-KF	Li$_2$CO$_3$-Na$_2$CO$_3$-K$_2$CO$_3$	NaCl-KCl-ZnCl$_2$
Composition by wt.%	60–40	29.3–11.7–59.0	32.1–33.4–34.5	8.1–31.3–60.6
Melting point (∘C)	220	454	400	229
Thermal stability (∘C)	600	850	715	850
Density (kg m^{-3})	1708.4–1950.1	1851.6–2116.5	1959.7–2069.4	1946.2–2275.5
Heat capacity (kJ/kg.K)	1.48–1.55	1.28–1.82	1.61	0.9–0.92
Viscosity (mPa s)	0.99–5.78	1.64–12.38	6.11–45.09	3.48–29.63
Thermal conductivity (W/m.K)	0.33–0.40	0.05–0.27	0.45–0.49	0.30–0.38
Salt price (USD/kg)	0.8	2.4	2.2	0.7
TES cost (USD/kWht)	22.64	45.98	71.14	16.21

Table 1.15 Properties and costs of different molten salt mixtures (heat transfer fluid-thermal energy storage)
Adapted from Ref.[97] and updated [77], [78], [80–83].

1.7.2.3 Power block

The power block consists of a Rankine cycle usually found in conventional thermal power plants based on fossil fuels, but in this case the fuels are replaced by the transfer of heat provided by the HTF to the cycle fluid water-steam cycle or organic fluids [46]. Therefore, the power block must be optimized to meet daily transient cycles and improve efficiencies during part-load operation (**Figure 1.23**) [93].
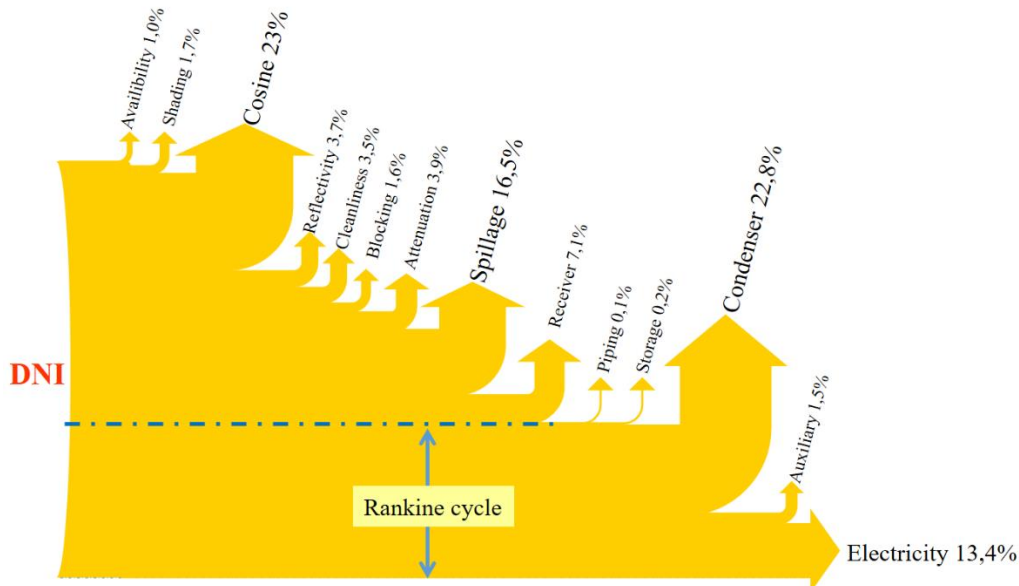
Figure 1.23 Solar power tower loss factors
Source: Private information

1.7.3 Concentrating Solar Power-Photovoltaic hybrid

Concentrating solar power-photovoltaic hybrids offer a way of producing more intermediate, peaking, and baseload power generation for specific markets than CSP or PV would each produce alone. A simplified CSP-PV plant configuration is shown in **Figure 1.24**. The basic concept is that PV, with option of storage, operates during the day at low cost, since PV generally has a lower LCOE than does CSP [93], [102].

Table 1.16 describes the main advantages and disadvantages of a CSP versus PV plant.

Technology	CSP	PV
Advantages	Dispatchable	Low complexity for power plant design and implementation
	Large storage capacities at competitive price	Highly competitive
	Fairly competitive	Easily scalable
Disadvantages	High complexity for power plant design and implementation	Little flexibility in local adaptation
	Strongly dependent on economies of scale	Volatile generation profile
		Storage solutions not competitive

Table 1.16 Comparison of concentrating solar power and photovoltaic plants
Source: [102], [64]
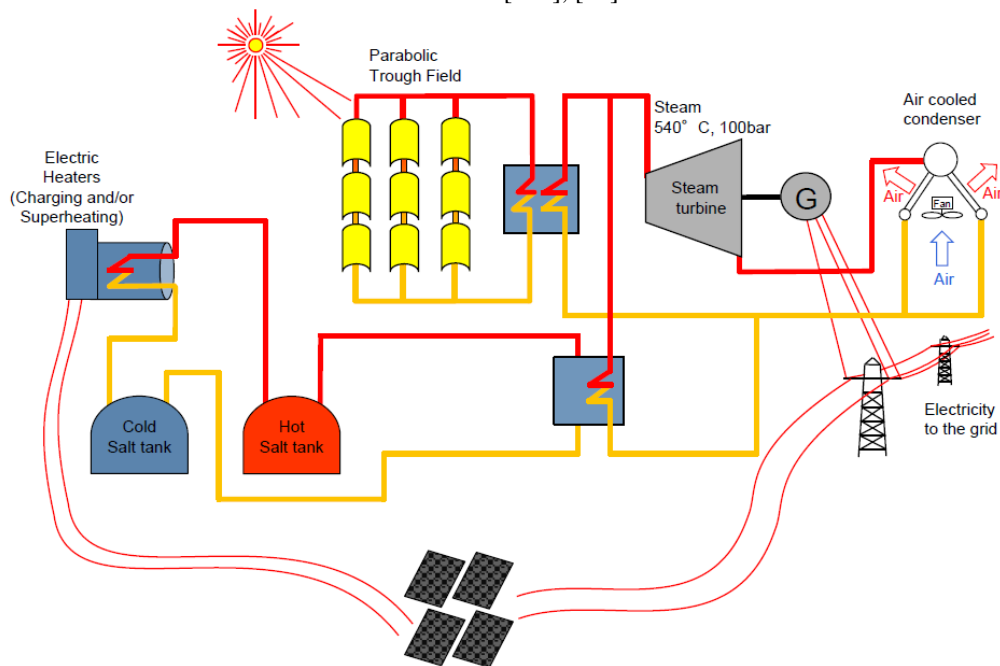
Figure 1.24 concentrating solar power-photovoltaic hybrid system
Source: TSK-Flagsol. Developing a 24-hour Renewable Energy System, CSP-PV-Hybrid Power Plant [103]

1.7.3.1 Operation of a concentrating solar power with thermal energy storage and photovoltaic hybrid power plant on a day with optimal irradiation

The operation of a CSP-TES + PV hybrid power plant on a day with optimal irradiation and connected to the network is shown in **Figure 1.25**.

Hybrid demand	Blue area =	Electrical energy demand for the hybrid plant over one full day
Dumped PV	Red area =	PV electrical energy neither sent to grid, nor used in TES
PV to storage	Green area =	PV electrical energy transformed into thermal energy and stored in the TES
PV to grid	Orange area =	PV electrical energy directly sent to grid
CSP to grid	Purple area =	Difference of blue and orange areas: electrical energy form CSP and TES to grid
Stored PV to grid	Brown area =	Electrical energy generated from the heat stored by transforming PV electrical energy to thermal energy

Figure 1.25 Hybrid plant demand curve: concentrating solar power and photovoltaic contributions
Source: TSK-Flagsol. Developing a 24-hour Renewable Energy System, CSP-PV-Hybrid Power Plant [103]

The demand curve is supplied for periods by the CSP technology and the storage of the CSP and the PV plant, managing to cover around 90% of the real curve, validating the flexibility and reliability of the hybrid system.

1.8   Concentrating solar power costs

To assess the viability of a project, it is necessary to develop an economic and financial model to evaluate the indicators shown in Table 1.17 as part of feasibility studies [93]. The most important part is the optimization of CAPEX to reduce costs and reach a competitive LCOE that can compete in the electricity market better than to other technologies [61], [102].

Indicator	Description
CAPEX	The CAPEX is generally split into direct costs, related to the purchase and installation of plant equipment, and indirect costs, which include the spectrum of costs that are not encompassed in the previous category (land, taxes, and engineering costs).
Lifetime production	Annual plant production multiplied by project lifetime, taking into account an annual degradation factor (%).
Annual OPEX	Includes all operating expenditures: O&M, insurance, land rental, gas consumption, water consumption, and miscellaneous OPEX.
Lifetime revenue	Lifetime production multiplied by the real feed-in tariff.
Discounted cash Flow	Future cash flows are calculated to include an annual power purchase agreement escalation factor and are then discounted to reach a present value.
Internal rate of return (IRR)	It is used to measure the relative profitability of the plant. Its value descends from the net present value (NPV), which can be defined as the difference between the present value of cash inflows and the present value of cash outflows.
LCOE	Is the minimum price of electricity which, over the entire lifetime of the power plant, generates enough revenues to pay back the CAPEX, cover the OPEX, and generate enough cash for plant decommissioning.

Table 1.17 Economic and financial indicator to evaluate concentrating solar power feasibility
Source: [93],[61]

The chapter provides a detailed analysis of the CSP options available in the market and emphasizes their advantages to determine the most efficient option.

From the evaluation of 4 types of CSP technology and based on 39 parameters, it was determined that the best option for the development of the project would be SPT because: it has greater efficiency + 30% vs PTC, greater storage capacity (12h- 15h), offers flexibility in the operation adjusting to the demand and allows punctual maintenance and a lower cost - 15% vs PTC, as well as lower energy consumption for pumping fluids.

In addition, a hybrid arrangement with CSP and PV would offer firm power to the market and provide flexibility to the electrical system.

CHAPTER II:

METHODOLOGY

The following chapter presents the methods that have been used to achieve the objectives of the study. A variety of methods have been considered, including a literature study, analysis of methodologies to develop a complex project, and simulation tools such as SAM and Excel to run the model and construct the scenarios.

2.1   Literature study

The initial phase of the project is based on an exhaustive literature study for global research that concerns a specific approach in Peru. The types of literature studied are listed below:

- Energy statistics portals: IEA, World Bank Group, IRENA, REN 21, and INEI (Peruvian Institute for Statistics).

- Institutional reports: OSINERGMIN, COES, and MINEM.

- Specialized scientific articles about CSP technologies.

2.2   Methodology for the development of hydroelectric power plants

The methodology results from the interaction between the House of Project Complexity,[13] the Vee[14] model, and multidisciplinary system design optimization,[15] which in addition to providing an analysis through the house of project complexity, allows for early

---

[13] House of project complexity is a combined structural and process-based theoretical framework for understanding contributors to complexity [116].

[14] The Vee model highlights the need to (i) define verification plans during all lifecycles of a project, (ii) continuously validate with stakeholders, (iii) have an early prototype the project architecture, and (iv) perform continuous risk and opportunity assessments [117].

[15] Multidisciplinary system design optimization is an engineering field whose objective is to find a system design that will minimize some objective functions [104].

prototyping and optimization (or a trade space search) before the implementation commitment [104]. Thus, the framework shown in **Figure 2.1** is proposed for the development process.
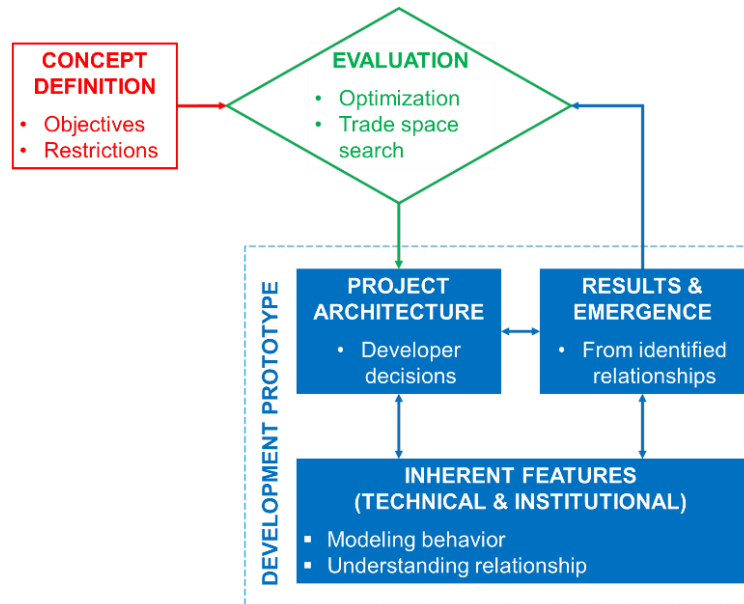
Figure 2.1 Development framework
Source: C. Cornejo Gómez. Methodology for the development of hydroelectric power plants [104]

The development framework consists of the concept definition, development prototype, and evaluation, which are described as follows:

- **Concept definition**

  This consists of analyzing the need for the project by society or stakeholders. Understanding the needs and the context would allow one to define the problem and propose a solution that would later be translated into objectives and restrictions.

- **Development prototype**

  This intends to build a prototype of the system (defined by its inherent characteristics and interactions), with which one can test the project

architecture and evaluate the (emergence) results so that these coincide with the objectives.

Construction of the prototype must integrate the main aspects of the project development to improve the understanding of the system; in this sense, the development prototype framework is divided into the following components:

  o Inherent features[16]: These define the system according to (i) technical features such as resource availability, location features, environment status, and facilities availability and (ii) institutional features such as authorities, local organizations, project members, laws and regulations, and the market.

  o Project architecture: This defines the nature of the project and the way it will be executed. It includes design and technology, construction, organizational set-up, permitting strategy, financing strategy, and the social management plan.

  o Results[17]: These are the output of the development prototype (models and results) and arise from the interaction between architectural choices and inherent features.

- **Evaluation**

This is the evaluation of the results and analysis of the possibilities of optimization or trade space search. This phase allows for the maturing of the project architecture, a better understanding of the inherent features, an accurate comparison between results and objectives or restrictions, and also the prediction of emergence.

---

[16] Understanding the inherent features of the existing system and its behavior is the key element to allowing for the design of an early prototype of the project [104].

[17] In a complex project, there are interactions between results, project architecture, and inherent features. Therefore, all these entities are coupled, and several internal loops must be performed [104].

This methodology can be applied to a CSP plant due to its similarities with a hydropower plant; both have storage for flexible operation, demand complex analysis of resources and location, and require an adequate selection of technology and design. In this sense, the CSP development framework is proposed (see **Figure 2.2**), which is developed in detail below.
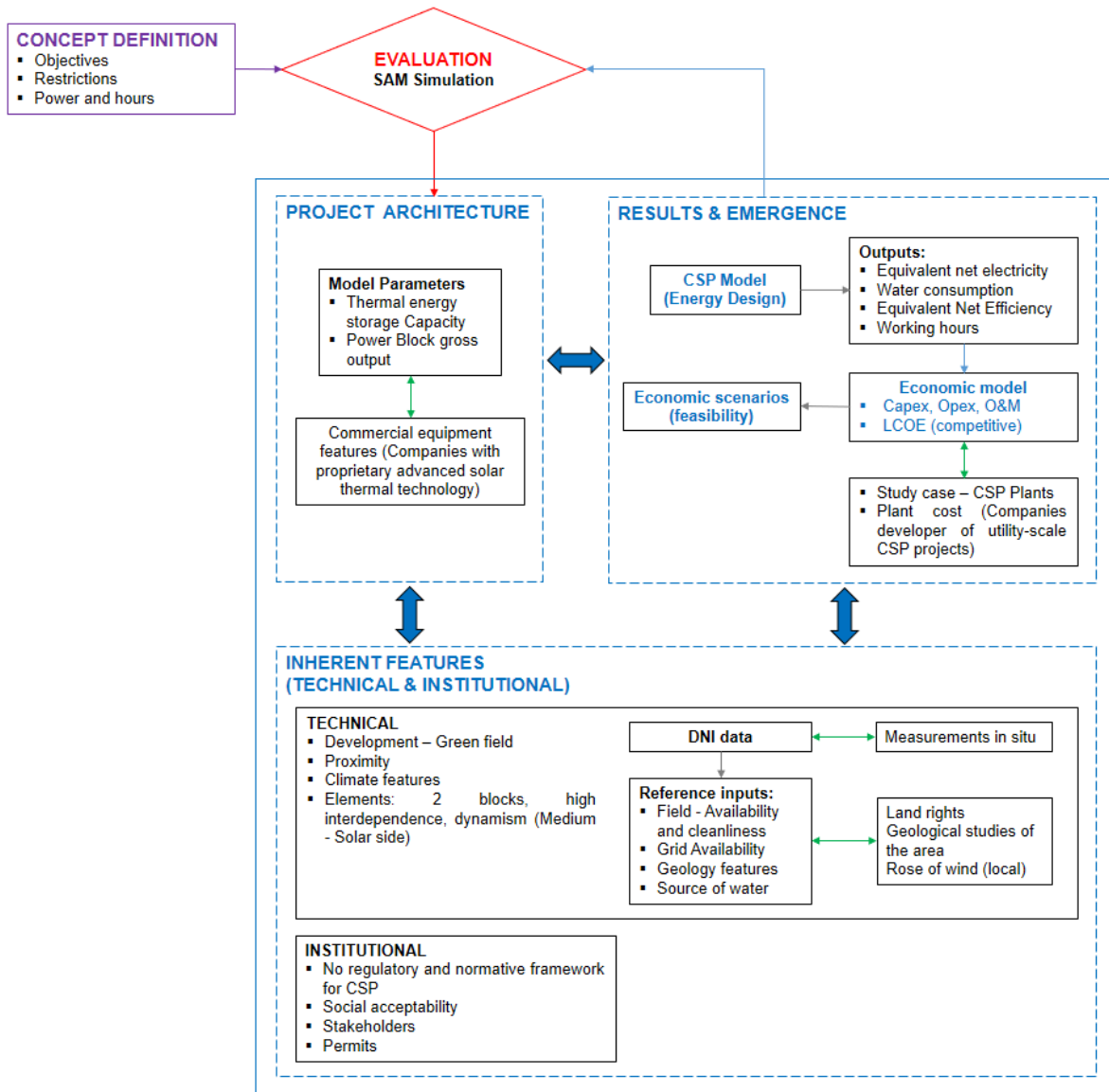
Figure 2.2 Concentrating solar power development framework
Source: Based on [104]

2.2.1 Concept definition

The growing energy demand in the south by the mining sector (for expansion or new projects) in a medium-term scenario that shows deficit scenarios for 2023–2025 and congestion of the central-south connection, leaving around 100–200 MW free in a context that does not contemplate the development of new efficient generation projects until 2028. Moreover, according to the 2021–2030 transmission plan, no new projects have been contemplated to improve the central-south connection, in addition to the possible increase of the limit to 1,650 MW in 2022. On the other hand, there is uncertainty regarding the arrival of gas to the south through the SIT GAS project, which would relieve congestion by 2026.

In this context, the possibility of a new energy auction to address deficit scenarios arising from current market conditions is raised. In this sense, the development of a hybrid power plant (CSP + PV) is proposed, as an alternative for clean, flexible, and competitive generation.

To achieve this goal, the main objectives that have to be met are the following:

- 150 MW generation power plant with Storage capacity

- CAPEX reduction

- Competitive energy prices
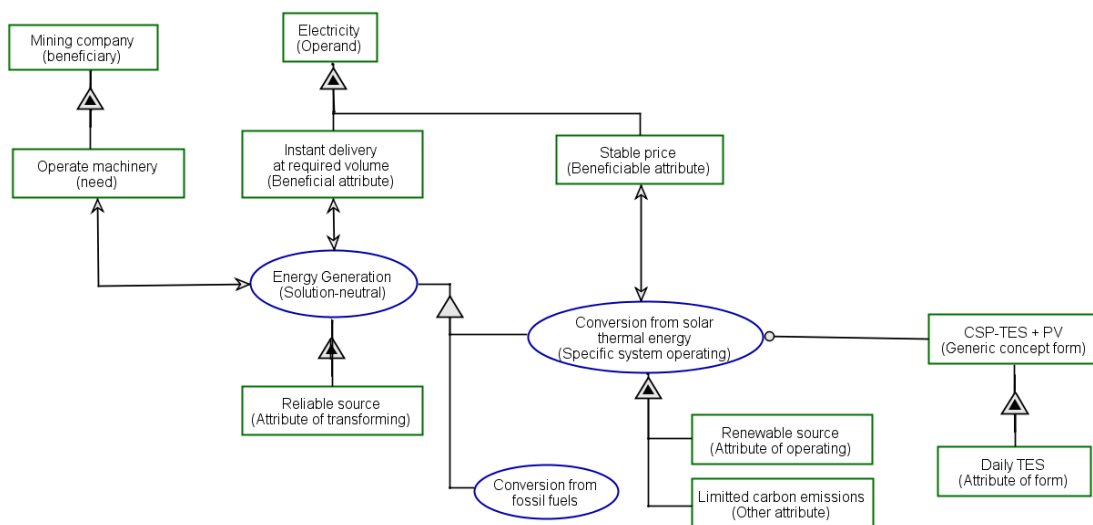
Figure 2.3 Concept definition flow
Source: Based on [104]

51

2.2.2 Development prototype

For the development of a CSP power plant that meets the needs and objectives defined above, it has been proposed to locate the project in La Joya – Arequipa, following an analysis of the hot spots of the SolarGis DNI map and an evaluation of the DNI data provided by a private company. Once the place is defined, it is necessary to analyze the inherent technical and institutional features, define the project architecture, set the system model, and optimize the results. The development prototype framework is described below.

2.2.2.1 Inherent technical features

2.2.2.1.1 Resource availability

The project will use solar radiation to generate electricity as a renewable resource. The chosen site has high DNI values which reach values between 830–917 W/m^2 at noon. In addition, Table 2.1 shows the annual hourly distribution of average DNI for 1999–2015.

Hour	Jan	Feb	Mar	Apr	May	Jun	Jul	Aug	Sept	Oct	Nov	Dic
5 - 6	47									111	169	123
6 - 7	317	202	205	199	165	129	115	159	368	485	534	434
7 - 8	497	395	441	484	541	497	469	530	610	675	705	615
8 - 9	641	552	603	639	681	654	632	676	737	784	811	747
9 - 10	748	664	707	737	766	746	721	762	815	854	879	828
10 - 11	807	705	773	796	815	797	775	817	854	887	908	865
11 - 12	827	701	788	817	832	819	801	837	871	900	917	873
12 - 13	784	674	775	805	819	806	793	837	863	888	902	849
13 - 14	694	596	699	759	784	772	761	803	827	842	858	787
14 - 15	579	475	577	678	722	707	697	739	756	770	780	686
15 - 16	468	357	445	564	615	595	596	639	650	653	668	550
16 - 17	357	254	325	396	401	374	399	459	482	487	511	406
17 - 18	236	156	135	96	23	19	46	111	131	146	211	236
18 - 19	13	8										11
Sum	**7015**	**5739**	**6473**	**6970**	**7164**	**6915**	**6805**	**7369**	**7964**	**8482**	**8853**	**8010**

Table 2.1 Annual direct normal irradiance W/m^2 (typical meteorological year)
Source: Bankable Data SolarGis – Private information

2.2.2.1.2 Location features

The project will be developed in the district of La Joya, in the province of Arequipa (Arequipa Department), and will occupy an area of 650 hectares. The polygon and its coordinates are shown in the **Figure 2.4** and **Table 2.2**.
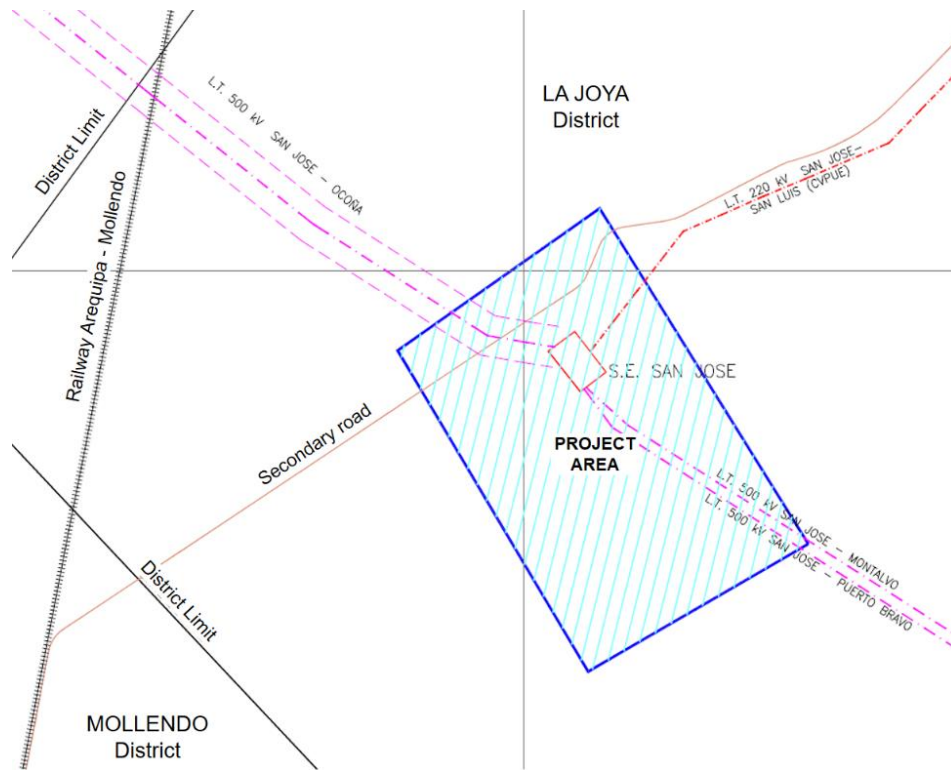
Figure 2.4 Project polygon
Source: Private information

UTM WGS84 coordinates – Zone 19		
Vertex	**East**	**North**
1	178,791.7354	8,154,232.5629
2	200,727.1319	8,155,595.2630
3	202,725.7774	8,152,378.6286
4	200,616.6885	8,151,115.6906

Table 2.2 Location of the vertices of project polygon
Source: Private information

Concerning the legal situation of the property, it is known that it belongs to the Peruvian state, and it will be necessary to request a temporary concession and easements to conduct detailed studies. On the other hand, it has been determined that no concessions of

the generation or distribution of electric power overlap in the area of interest until 2019[18].
Likewise, according to the information provided by the INEI, there is no overlap of
communities within the area. Still, at an approximate distance of 6.25 km (see **Figure 2.5**),
there is the La Joya community.
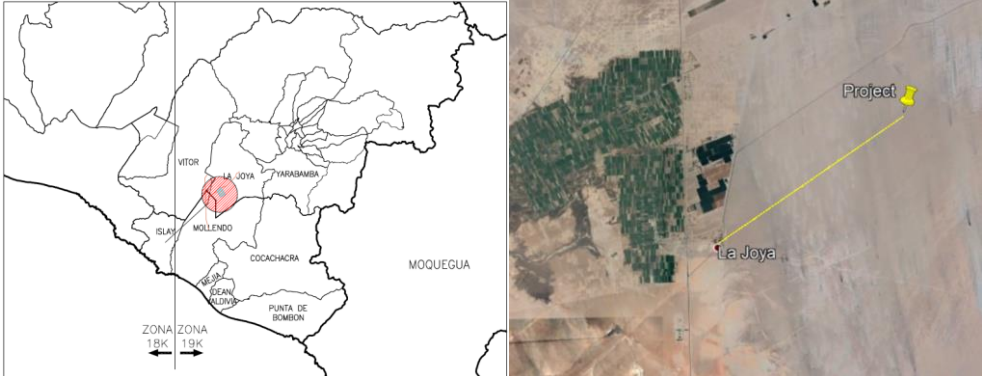
Figure 2.5 La Joya community location
Source: Google earth

2.2.2.1.3 Environmental status

Climate and meteorology

The climate is a desert (warm and dry). The average annual temperature is 19.4°C,
the average precipitation per year is 4.9 mm, and the average wind speed is 2.5 m/s. The
months with the highest amount of precipitation and the high temperatures extend from
December to March, while the months from October to January have higher values of DNI
and GHI.

Monthly	GHI (kWh/m²)	DNI (kWh/m²)	RH (%)	TEMP (°C)	WS (m/s)	PREC (mm)
January	233	217	70.2	21.2	2.8	2.1
February	192	161	72.4	21.5	2.7	1.5
March	215	201	71.1	21.3	2.6	0.8

---

[18] It is worth mentioning that the development of the proposed project was carried out during 2019
when no concessions were transposed in the polygon of the project. However, at the end of 2020 the definitive
concession of the Misti solar project was approved, which affects 35% of the project's surface, therefore it is
recommended to move the polygon to the north assuming that the terrain and radiation conditions are similar.

Monthly	GHI (kWh/m²)	DNI (kWh/m²)	RH (%)	TEMP (°C)	WS (m/s)	PREC (mm)
April	192	209	71.1	20	2.3	0.2
May	176	222	65.3	18.5	2.2	0
June	158	207	58.8	17.6	2.1	0
July	168	211	56.6	17.7	2.2	0.1
August	195	228	54.2	17.8	2.3	0
September	218	239	61.4	18.5	2.5	0
October	249	263	61.4	19.1	2.6	0
November	254	266	59.1	19.1	2.7	0
December	252	248	66.2	20	2.8	0.2
Annual	2,502	2,672	64	19.4	2.5	4.9

Table 2.3 Meteorological characteristics
Source: Bankable Data SolarGis – Private information

Protected natural areas

The area defined for the project does not pass through any natural area protected by the state, according to the National System of Natural Areas Protected by the State. Likewise, it has been concluded that protected natural areas do not overlap the area of interest. However, 45.5 km away is the protected natural area known as the Santuario Nacional Lagunas de Mejía, 47 km away is the Reserva Nacional de Salinas y Aguda Blanca, and 52.9 km away is the Parque Nacional Punta Hornillos.
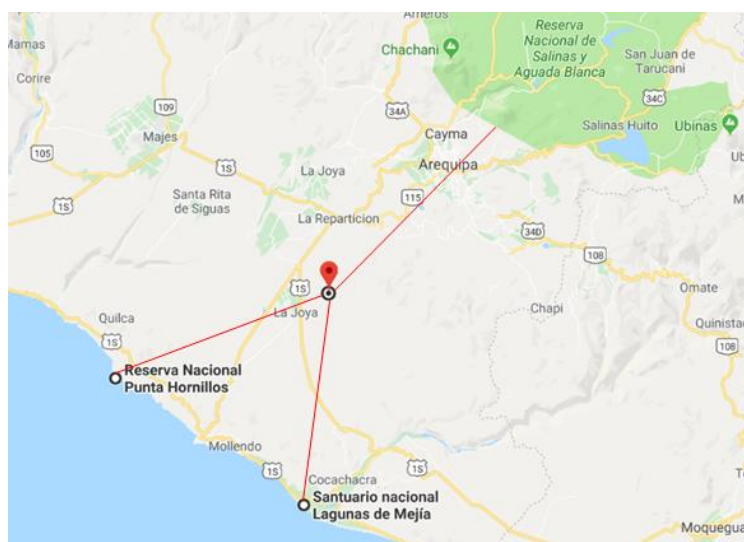
Figure 2.6 Location of protected natural areas near the project
Source: Own elaboration

Landscape

The study area is located in a desert environment, which has non-existent or very scarce vegetation, with halophytic species distributed as small green dots across a vast, monotonous, gray, and windy expanse of sand.

Figure 2.7 Detailed view of the place of study
Source: Private information

Map of life zones and vegetation cover

With consideration of the Leslie R. Holdridge system (1947) and the Ecological Map of Peru (ONERN, 1976: 41; INRENA, 1995: 33; MINAM, 2015), the project area located in the La Joya district is within a desiccated-subtropical desert life zone, characterized by broad plains and devoid of vegetation. In addition, according to the vegetation cover map of Arequipa (Regional Government of Arequipa), the project is located in the Coastal Desert and outside the coastal and Andean agriculture zones.

Capacity for major land use and current land use

According to the map of Capacity for Major Land Use (MINAGRI), the project belongs to the protected lands "X," subclass "S," which due to its severe limitations, does not allow agricultural, livestock, or forestry activities to be carried out. Currently, the lands belong to unused or unproductive areas that lack vegetation cover due to their extremely arid conditions.

Geomorphology and geological formations

For the geological description of the study area, information published in Bulletin No. 19, Quadrangle of La Joya (Sheet 34s) (Ingemmet, 1968), was collected. The stratigraphy of the study area shows quaternary deposits, represented by wind deposits[19] and alluvial deposits.[20]

Figure 2.8 View of the area of interest with presence of alluvial deposits (left) and wind deposits (right)
Source: Private information

In the study area, predominant geomorphological features corresponding to desert areas are observed, such as transverse dunes. Additionally, within the study area, two geomorphological units have been identified: alluvial plain (which represents 79% of the study area) and uadis.

---

[19] Quartz sands form dunes and pampas.
[20] Accumulation of gravel, sand, silt, and clay with subangulous to angled, heterometric, and different composition clasts.

Hydrographic basin

Based on the map of Arequipa hydrographic basins (ANA), it was determined that the project belongs to the Quilca-Vitor-Chili Basin and is located on the hydrographic unit N° 13230, which is located in an arid zone away from active surface and underground waterways.

Archaeology

Based on a visual prospecting analysis, it has been determined that the archaeological risk is low, considering the absence of surface evidence. However, in the future, it will be necessary to carry out the process to obtain a CIRA to mitigate possible risks.

2.2.2.1.4 Facilities availability

The project will be located on an open, flat site with some sand deposits on the surface. Therefore, it will not have potable water, sewerage, an electricity network, natural gas network, or rainwater channels.

Access and roads

To access the project area, there are the following options: by land on the Lima-Arequipa route, by air, and by land on the Arequipa-La Joya route. In addition, it is worth mentioning that the project is close to the Arequipa-Mollendo railway.

Electrical grid connection

The electrical substation closest to the project is the San José Substation owned by Sociedad Minera Cerro Verde. Likewise, as seen in **Figure 2.4**, near the project area there are several transmission lines: the San José-Ocoña LLTT (500 kW), the San José-Montalvo LLTT (500 kW), the San José-Puerto Bravo LLTT (500 kW), and the San José-San Luis LLTT (220 kW).

2.2.2.2 Inherent institutional features

2.2.2.2.1 Authorities

Government authorities

The project is located on land where there are no populations or settled human groups. Therefore, there will be no direct impacts to the extent that there is no population around the project. In that sense, the direct influence area would be limited to the area of the property as mentioned above. As the indirect influence area (IIAR), the populated centers of San Camilo and San Isidro are considered because they are closer to the project area, and the District of La Joya is considered because it is the geographical and political-administrative area where these population centers are located.

- **District Municipality of La Joya:** This is the most representative institution in the IIAR, which promotes the integral development of the district to improve the quality of services to the population. Its current mayor is the lawyer Gilmar Henry Luna Boyer, who is responsible for executing works, urban development planning, supervision, and addressing population needs and complaints.

- **Municipalities of the populated centers San Camilo and San Isidro:** These are the populated centers closest to the project area and are part of the IIAR. These populated centers depend on the management of the Municipality of La Joya; in addition, the mayors of the municipalities are Cirilo Lázaro Quispe, in San Isidro, and Carlos Gutiérrez Álvarez, in San Camilo.

Regulatory bodies

The main bodies whose role is to control project activities and compliance with laws, permits, and contracts are the following:

- **Ministry of Energy and Mines:** This ministry is responsible for formulating and evaluating national policies for mining and energy activities. In addition,

it promotes the development of activities in the sector that promotes private investment [105].

- ▪ **Ministry of Culture (MINCUL):** This ministry is responsible for establishing cultural promotion strategies and carrying out conservation and cultural heritage protection actions [106].

- ▪ **National Environmental Certification Service for Sustainable Investments (SENACE):** This is responsible for reviewing and approving the instruments of environmental management of public, private, or mixed capital investment projects [107].

- ▪ **Supervisory Agency for Energy and Mining Investment (Osinergmin):** This agency is responsible for regulating and supervising companies in the electricity, hydrocarbons, and mining sectors so that they comply with the legal provisions of the activities they carry out [108].

Utility system operators

- ▪ **Operations Committee of the National Interconnected System:** This defines the operating procedures and technical requirements for new projects to integrate the SEIN without impacting its current operation and reliability.

2.2.2.2.2 Law and regulation

The regulatory framework applicable to the project has been described in Section 1.2 of Chapter I.

2.2.2.2.3 Social conflicts

The main social conflicts around IIAR are characterized by the following issues:

- **Urban sprawl:** This population growth disorder has increased due to emigration to La Joya and due to the presence of land invasions, which have resulted in the construction of infrastructure without licenses.

  The invasions have caused internal disputes among 38 organizations that accuse each other of usurpation and overlap. The areas where there is a greater extent of invasions are San José, San Isidro, and San Camilo; even properties belonging to the Ministry of Agriculture have been compromised.

- **Security:** The presence of problems regarding citizen security is due to the shortage of police officers assigned in the district.

- **Water supply:** In the district of La Joya and the populated centers, there is evidence of a lack of drinking water, causing the population to use water intended for cultivation, which is not suitable for human consumption, causing the community to suffer from digestive and diarrheal diseases. Therefore, water is obtained from cisterns.

- **Domestic violence:** A study prepared by DEMUNA determined high levels of domestic violence directed toward children and other family members; therefore, the municipality works on interventions that provide a solution and impact society.

- **Informal commerce:** Street vending has grown in recent years due to constant migration to La Joya and due to the lower in labor supply.

2.2.2.2.4 Market

Supply and demand in the south of Peru

Demand in the south is continuously increasing, and the participation of free clients in demand has been rising over the years, boosted by the development of new mining projects, the expansion of existing mines, and very competitive electricity prices. At the same time, the Peruvian government is trying to reactivate the SIT GAS project, which would

allow 1,200 MW worth of existing gas turbines to operate with natural gas. Nevertheless, no new energy projects (such as efficient generation) are being developed, which in a few years will cause congestion in the central-south grid connection.

Considering a medium-term mining growth scenario and the increment of the central-south limit up to 1,650 MW (by 2022), the potential congestion might arise in 2023[21] (during the night), requiring the operation of gas turbines burning diesel (180–190 USD/MWh), because planned projects will not cover the growth in demand. In addition, in the medium term from 2024 to 2025, 100–150 MW of efficient generation will be required (see **Figure 2.9**), with consideration of the arrival of gas to the south in 2026 to relieve congestion. However, due to the uncertainty of the SIT GAS project, in case of a delay (COD in 2028), demand in the south would continue to grow and new projects would be required to improve the central-south transfer.
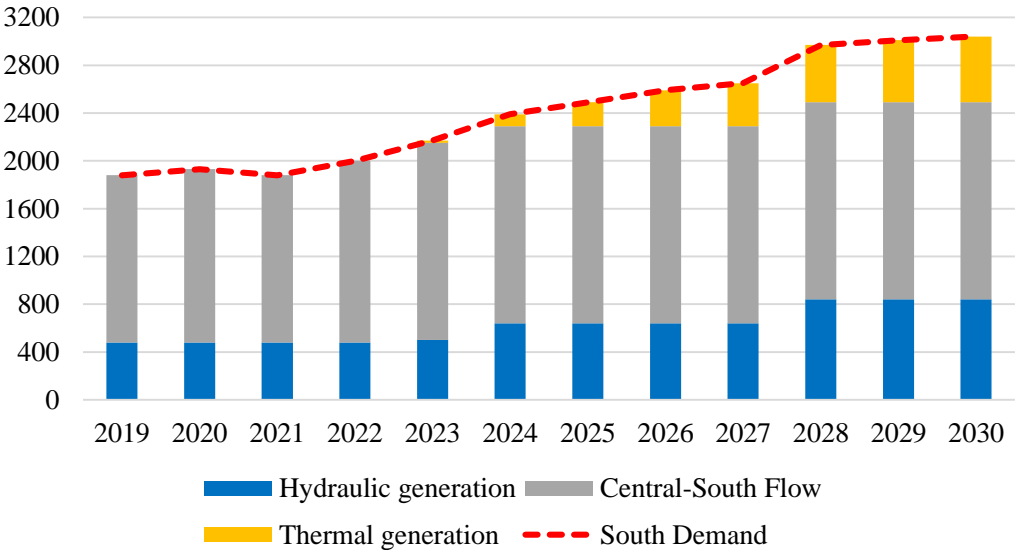
Figure 2.9 Maximum demand balance of generation/transmission/demand in the south of Peru
Source: Own elaboration [8],[7]

---

[21] The actual date for the potential congestion will depend on the growth in demand in the south.

In that context, the congestion of the transmission system to the south depends on the following:

- New mining demand (expansion or new projects), which in Peru has a load factor above 85% (see **Figure 2.10**).
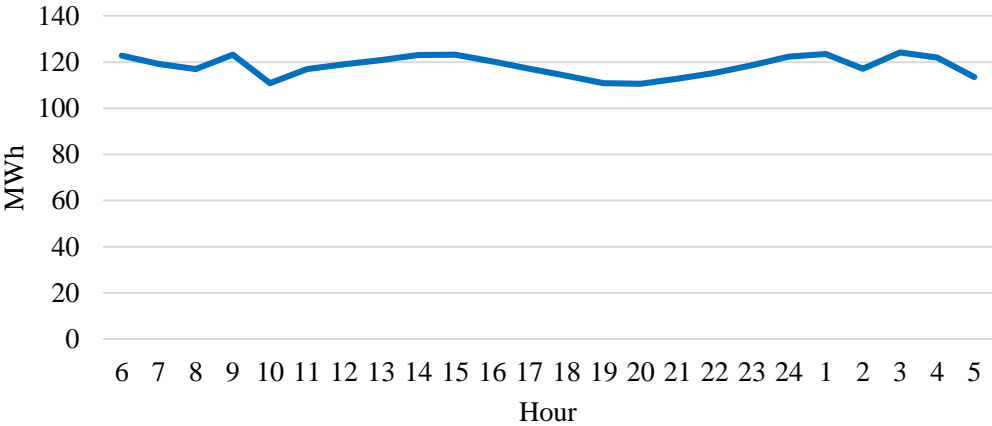
Figure 2.10 Daily demand of a mining client with a 110 MW PPA contract
Source: Private information

- Minimum planned generation projects (due to uncertainty surrounding the SIT GAS project), such as C.H. Moquegua 32 MW (COD 2021) and C.H. San Gaban 205 MW (COD 2024), and the decommissioning of ILO21 (-135 MW) coal-fired power plant.

- The COES do not have, in its actual plan, new transmission projects to improve the link between central and southern Peru.

Market prices

Due to the future context of congestion in the south, the impact of the efficient generation deficit would increase marginal costs up to 70–150 USD/MWh, requiring the projection of new projects that reduce the impact.

To better assess the impact, three cases of the evolution of the maximum marginal costs in the south were developed in a 2018–2030 horizon (see **Figure 2.11**).
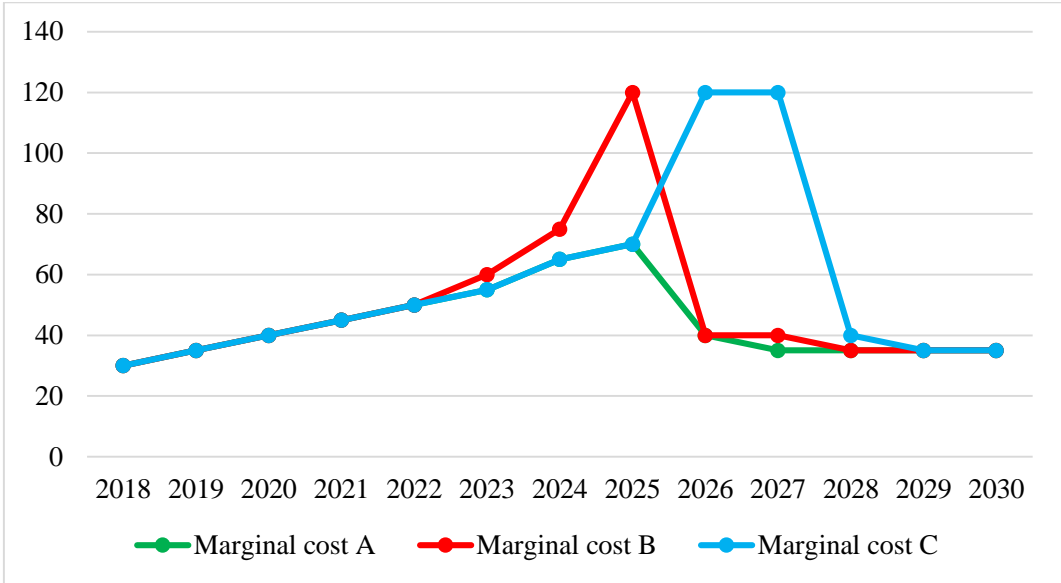
Figure 2.11 Evolution of the maximum marginal cost in the south
Source: Own elaboration [7]

- ▪ Marginal cost A: This represents a scenario without new efficient generation projects until 2028 with a maximum marginal cost of 75 USD/MWh, which considers the COD of C.H. San Gaban in 2024, SIT GAS in 2026, and C.H. Lluta and C.H. Lluclla in 2028.

- ▪ Marginal cost B: This represents a scenario without new efficient generation projects until 2028 with a maximum marginal cost of 120 USD/MWh, which considers the COD of C.H. San Gaban in 2026, SIT GAS in 2026, and C.H. Lluta and C.H. Lluclla in 2028.

- ▪ Marginal cost C: This represents a scenario without new efficient generation projects until 2028 with a maximum marginal cost of 150 USD/MWh, which considers the COD of C.H. San Gaban in 2024, SIT GAS in 2028, and C.H. Lluta and C.H. Lluclla in 2028.

On the other hand, the current PPA market has very competitive prices[22] between 24–39 USD/MWh. Due to the current generation oversupply, free clients have signed medium-term PPAs at low prices to reduce their exposure to the spot market and assure known electricity costs for their projects.

Competitors

Arequipa has opted for RES generation to take advantage of the valuable solar resource in the area and currently has three solar projects in commercial operation. One of them, C.S. Solar Distribution 20T, like the project under study, is located in La Joya-Arequipa.

On the other hand, as direct competitors, four new projects that would be connected in the S.E. San José have been considered (see **Table 2.4**), which have an environmental study, pre-operational study or Definitive and Temporary concession approved in the last year.

Solar PV project	Power (MW)	Concession		Environmental management instrument		EPO
		Type	**Status**	**Type**	**Status**	**Status**
C.S. Continua Chachani	100	Definitive	Approved	DIA	Approved	Approved
C.S. Continua Misti	300	Definitive	Approved	DIA	Approved	Approved
C.S. Continua Pichu Pichu	60	Definitive	Approved	DIA	Approved	Approved
C.S. Solar Sunny	500	Temporary	Approved	DIA	Development	Development

Table 2.4 Direct competitors
Source: Own elaboration (COES, OSINERGMIN, MINEM and SENACE)

---

[22] These depend on the characteristics of the client, such as load factor and contracted power.
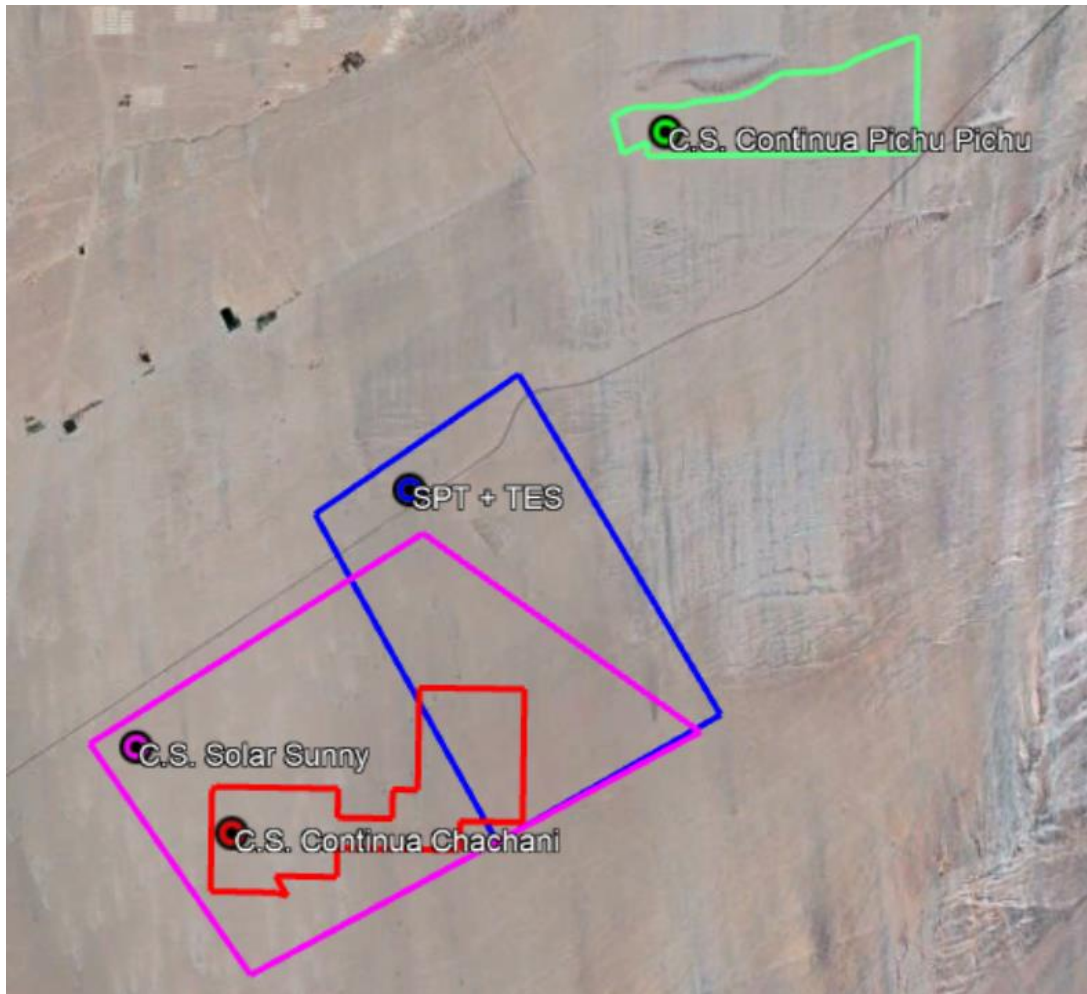
Figure 2.12. Impact of direct competitors on the project polygon
Source: Own elaboration (COES, OSINERGMIN, MINEM and SENACE)

The direct competitors that affect the study site are two projects. The impact of C.S. Solar Sunny commits 50% of the area destined to the project under study, while C.S. Continua Chachani commits only 18%. However, the only project with a definitive permit on the land is C.S. Continua Chachani, so it is suggested to redistribute the compromised area by extending the project to the northwest in a future evaluation.

2.2.2.3 Project architecture

2.2.2.3.1 Design and technology selection

To achieve an adequate design of the generation plant, four available CSP technologies have been evaluated by considering 39 parameters, resulting in SPT-TES technology as being considered the best option for the following characteristics:

- Over 30% more efficiency (PTC)

- Increased storage capacity (12–15 h)

- Flexibility in operation (demand adjustment) and maintenance (punctual)

- Lower maintenance cost by 15% (compared to PTC)

- Lower energy consumption for pumping

Likewise, to evaluate an optimal configuration of the plant that ensures firm capacity, flexibility in operation, reliability, and a competitive price, the design option of a hybrid power plant has been considered (see **Figure 2.13**), which combines the proposals mentioned above (SPT-TES) with a PV solar power plant.
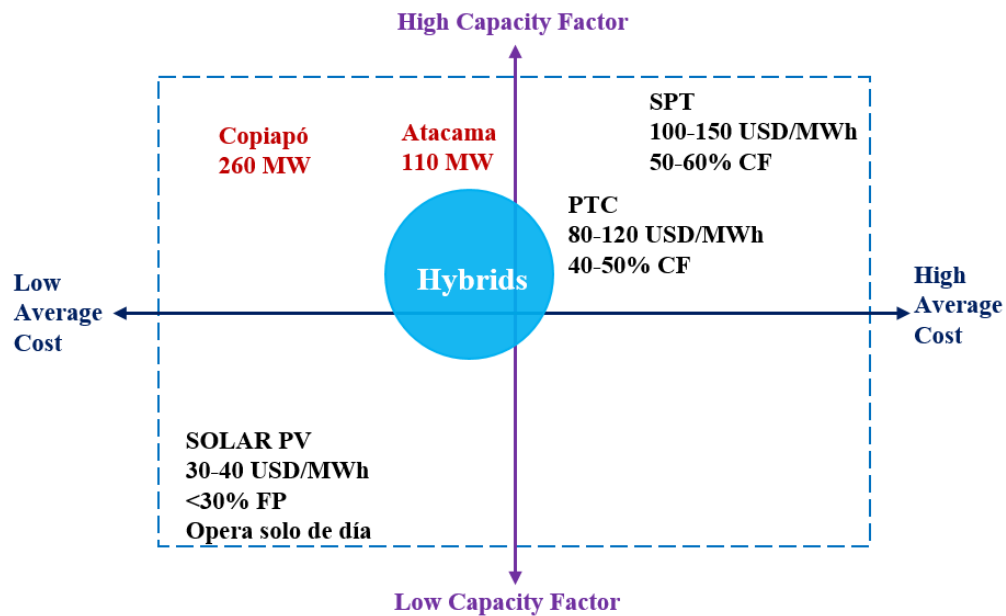
Figure 2.13 Characteristics of a concentrating solar power and photovoltaic hybrid system
Source: Own Elaboration

2.2.2.3.1.1 Layout

The proposed design for the plant is shown in **Figure 2.14**. The plant will consist of three blocks: the SPT-TES system, the power block, and PV system.
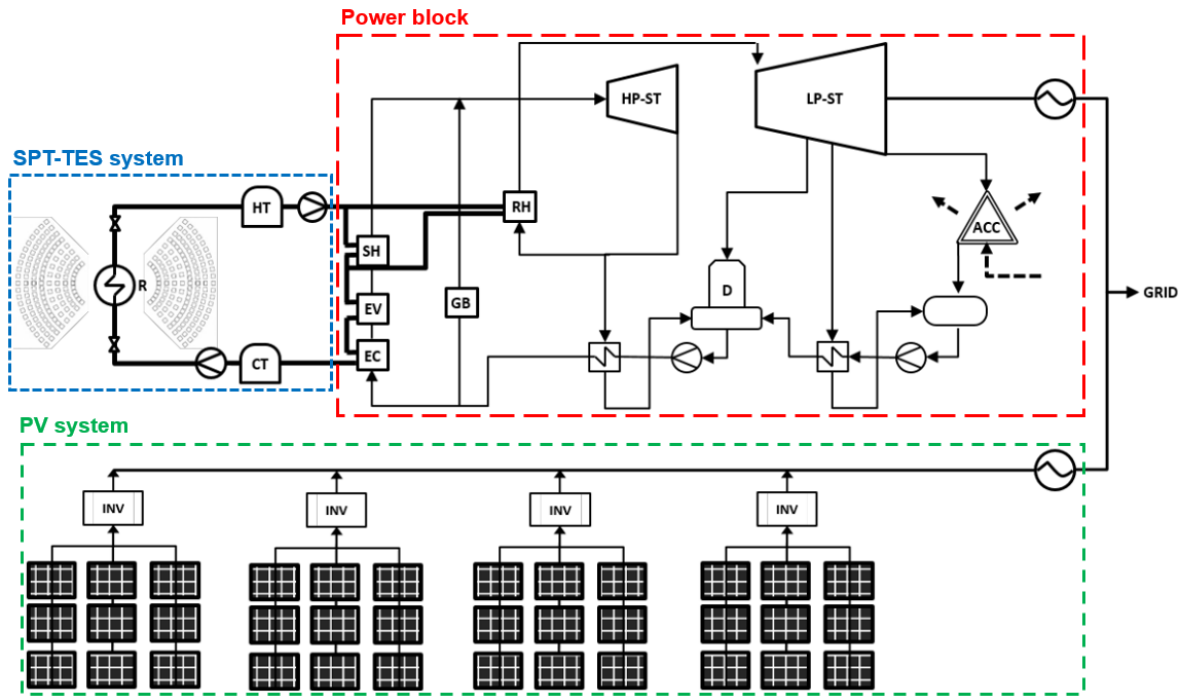
Figure 2.14 Layout of the proposed solar power tower with thermal energy storage and photovoltaic hybrid concept
Source: R. Guédez. A Techno-Economic Framework for the Analysis of Concentrating Solar Power Plants with Storage [102]

- **SPT-TES system:** This includes the heliostat field, tower and receiver, and TES tanks.

- **Power block:** This includes the main equipment of the ranking cycle such as a heat exchanger, turbine and generator, pumps, an air cooler, and a substation.

- **PV system:** This is composed of photovoltaic modules, trackers, and conversion blocks (inverters).

2.2.2.3.1.2 Components

The information presented below on the characteristics of the components and fluids of the system was collected from commercial technical data sheets of plants in development and operation, business case studies, and research papers to achieve a design with successful results.

Solar power tower-thermal energy storage system components:

Heliostats	Value	Units
Heliostats width	14.685	m
Heliostats height	12.51	m
Heliostats effective area	178.54	m^2
Ratio of reflective area to profile	97.19	%

Table 2.5 Technical characteristics of commercial heliostats
Source: Private information

Receiver	Equation/value	Units
Model	Vertical cylindrical receiver	-
Receiver thermal power	440–700	MWth
Receiver diameter	13.4–18.9	m
Exposed height	16.94–21.75	m
Receiver emissivity	94	%
Receiver thermal efficiency	89.4	%
Receiver thermal losses at design point (@900 W/m^2)	33.8	MWth
Receiver inlet/outlet temperature	300/565	°C

Table 2.6 Technical characteristics of commercial receiver
Source: Private information

Storage tank	Value	Units
Storage tank diameter (hot/cold)	40–50	m
Storage tank height (hot/cold)	10–15	m
Tank heat loss	0.3 (cold)/0.5 (hot)	MWth

Table 2.7 Technical characteristics of commercial storage tanks for thermal energy storage systems
Source: Private information

Molten salt	Value	Units
Molten salt composition	$NaNO_3$ (60%) / KNO_3 (40%)	-
Molten salt freeze protection level	260	°C
Density (@Temp °C)	$\rho(T) = 0.636 * (T) + 2090$	kg/m³
Specific heat (@Temp °C)	$Ce(T) = 0.172 * (T) + 1443.18$	J/kg.°C
Viscosity (@Temp °C)	$\mu(T) = 0.000000139 * (T)^3$ $+0.00022 * (T)^2 -0.1177 * (T) + 22.49$	mPa.s
Thermal conductivity (@Temp °C)	$k(T) = 0.00188 * (T) + 0.44732$	W/m.°C

Table 2.8 Properties and composition of commercial molten salts
Source: Private information

Power block components:

Power block	Value	Units
Steam turbine gross output nameplate	150	MWe
Max. operating pressure	140	bar
Steam admission temperature	550	°C
Steam cycle efficiency	40	%
Cooling system	Air-cooled condenser	-

Table 2.9 Technical characteristics of commercial power block for solar power tower systems
Source: Private information

Photovoltaic system components:

Photovoltaic module	Value		Units
Model	Polycrystalline		-
Cell arrangement	72 (6x12)		-
	STC	NOCT	
Rater output (Pmpp)	360	251.4	Wp
Rater voltage (Vmpp)	37.62	34.35	V
Rater current (Impp)	9.58	7.32	A
Open circuit voltage (Voc)	46.8	42.94	V
Short circuit current (Isc)	9.85	7.62	A
STC module efficiency	18.6		%
Maximum system voltage (IEC)	1,500 DC		V
Maximum series fuse rating	15		A

Table 2.10 Technical and electrical characteristics of commercial photovoltaic modules
Source: Private information

Tracker	Value
Model	Single axis
Orientation	East/west

Table 2.11 Technical characteristics of commercial trackers
Source: Private information

Inverter	Value	Units
AC output power @25°C	3550	kVA/kW
Max. AC output current @25°C	3175	A
MPPt @full power (DC)	913–1,310	V
Max. DC voltage	1,500	V
Max. DC continuous current	3,970	A
Max. DC short circuit current	6,000	A
Frequency	50/60	Hz

Table 2.12 Technical characteristics of commercial inverters
Source: Private information

2.2.2.3.1.3 Permits

The following table documents the permissions for the development stage before the Notice to Proceed:

Permits	Authority	Required for
EVAP classification	SENACE	EIA
EIA	SENACE	Generation concession, construction license, TL concession
Preoperative study	COES	Generation concession
Temporary concession	MINEM	Resource measurements and exploration
CIRA (plant)	MINCUL	Site access
CIRA (transmission Line)	MINCUL	Site access
PMA	MINCUL	Studies involving the removal of land and underground works (geological)

Table 2.13 List of main permissions for development stage before the notice to proceed
Source: Web portal of MINEM, SENACE, MINCUL, and COES

2.2.2.3.1.4 Access

From the city of Lima, there are two ways to access the project area:

- By land: The Lima–Arequipa–La Joya route takes an approximate travel time of 18 hours. The road is paved and in good condition, and the approximate distances are 1,000 km from Lima to Arequipa and 70 km from Arequipa to La Joya.

- By air: The Lima–Arequipa flight takes 1 hour and 30 minutes, and then the Arequipa–La Joya route by land is on a paved road in good condition.

2.2.2.3.1.5 Plant cleaning

For cleaning and the control of dust, a local company will be hired that supplies water every month through a tank truck for washing and accessing irrigation to avoid excessive dust removal. This contribution of water is not a park consumption.

2.2.2.3.1.6 Grid connection

The project will be connected to the existing San José Substation owned by Sociedad Minera Cerro Verde, which is located 450 m from the plant substation.

2.2.3 Results and evaluation

2.2.3.1 Development of models

2.2.3.1.1 Technical model

As a starting point for dimensioning the SPT-TES plant's main components, it is essential to define some characteristics, which are shown in the following table.

Parameter	Symbol	Value	Unit	Description
Power plant	P_e	150	MW	Range: 110–160 MW * Maximum size 160, avoid major losses
Design normal direct irradiation	$DNI_{@DIC}$	873	W/m²	Maximum DNI in December (Dec 21) * The selection of DNI@design will depend on whether the plant is oversized (Jun. 21) or if it will require storage for the months of lower production
Rankine cycle efficiency	η_{cycle}	40	%	Range: 0.35–0.55 * Values taken from commercial plants in operation
Alternator efficiency	η_{gen}	92	%	Range: 0.90–0.95 * Values taken from commercial plants in operation

Table 2.14 Assumptions for the design of the solar power tower and thermal energy storage plant
Source: Own elaboration

Likewise, as part of the analysis, it has been proposed to design two solar concentration plant arrangements that allow offering (a) a continuous operating solution (24 hours per day, seven days per week) and (b) a solution that provides energy during solar hours and covers demand during peak hours (15:00–23:00 hours).

Next, the procedure used for the sizing of the components of both SPT-TES plants is detailed.

2.2.3.1.1.1 Solar field

Usually, to size and optimize the field of heliostats, processing software is used due to their complexity. Therefore, for design purposes and in search of greater simplicity in the calculations, the procedures of two methodologies were combined.

The first methodology, proposed by Collado et al. [109], describes a quick way of determining the optimum separation radius of the tower toward the first ring and the radial increase between rings by using only two variables.

Parameter	Symbol	Equation/remark	Results	Units
Heliostat footprint	DM	$DM = DH + dsep$	19.29	m
Heliostat diagonal	DH	$DH = \sqrt[2]{hel_{height}{}^2 + hel_{width}{}^2}$	19.29	m
Additional security distance	$dsep$	Despicable value for agile calculation purposes	0	m
Number of heliostats	N_{hel}	$N_{hel} = 60$ (Assumed*) *Based on the Noor Ouarzazate III plant	60	-
Radial distance from the first ring to the tower	R_1	$R_1 = (DM * N_{hel})/2\pi$	184.22	m
Radial increment between rings	ΔR_1	$\Delta R_1 = \cos 30° * DM$	16.71	m

Note: Details of the distribution of variables in the heliostat field can be found in Figure 2.15

Table 2.15 Parameters and equations for calculating the dimensions of the first ring
Source: F. J. Collado and J. Guallar. Quick design of regular heliostat fields for commercial solar tower power plants [109]
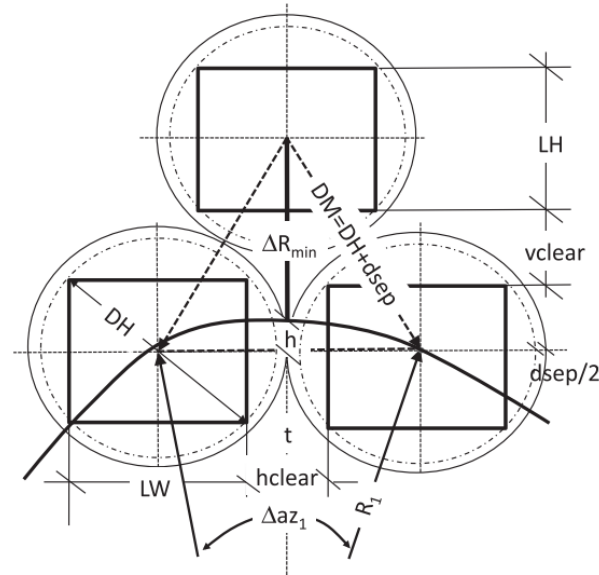
Figure 2.15 Scheme of heliostat field variables
Source: F. J. Collado and J. Guallar. Campo: Generation of regular heliostat fields [110]

Once the characteristics of the first ring have been defined, one can proceed to dimension the distribution of heliostats in the solar field by considering a vertical cylindrical receiver and using the methodology described by Joga [111].

Parameter	Symbol	Equation/remark		Units
Effective heliostat surface	A_{hel}	$A_{hel} = hel_{height} * hel_{width} * 0.9719$		m²
Ring number	i	$i = 1,2,3 \ldots.$		-
Azimuthal separation between heliostats	$\Delta L_{(i)}$	$\Delta L_{(i)} = \sqrt{A} * (1.5 + i/20)$		m
Radial separation between rings	$\Delta R_{(i)}$	$\Delta R_{(i)} = \sqrt{A} * (1.25 + i/20)$		m
Radial distance from the tower to the ring (i)	$R_{(i)}$	$R_{(i+1)} = R_{(i)} + \Delta R_{(i)}$		m
Number of heliostats per ring	$N_{hel(i)}$	$N_{hel(i)} = (2 * \pi * R_i)/(\sqrt{A} * (1.25 + i/20)$		-

Table 2.16 Parameters and equations to calculate the distribution of heliostats in the solar field
Source: H. Joga. Diseño de una planta termosolar de receptor central con sales fundidas como fluido de trabajo y sistema de almacenamiento [111]

In the case of the dimensioning of the solar field area and the total number of heliostats required to cover the thermal demand, the power block efficiencies and the optical losses of the heliostats were considered.
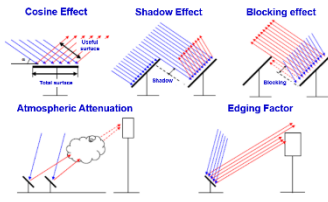
Parameter	Symbol	Equation/remark	Value	Units
Thermal power plant	P_{th}	$P_{th} = P_e * \eta_{cycle} * \eta_{gen} * SM$	398–716	MW
Cosine effect	η_{cos}		85–95	%
Shadow effect	η_{sh}		95	%
Blocking effect	η_{bl}		95–97	%
Atmospheric attenuation	η_{aa}		90	%
Edging factor	η_{edg}		86	%
Collecting surface per ring	$S_{(i)}$	$S_{(i)} = \dfrac{\left(\sqrt[2]{(H_{tower} - hel_{height})^2 + R_i^2}\right)}{1000}$		km
Atmospheric attenuation corrected	η_{aa-c}	$\eta_{aa-c} = 0.002845 * S_{(i)}^3 + 0.017 * S_{(i)}^2 + 0.1046 * S_{(i)} + 0.006789$	92–94	%
Total optical losses	η_{SF}	$\eta_{SF} = \eta_{cos} * \eta_{sh} * \eta_{bl} * \eta_{aa-c} * \eta_{edg}$	68–71	%
Solar field area	A_{SF}	$A_{SF} = (P_{th} * 10^6)/(DNI_{@DIC} * \eta_{SF})$		m²
Total number of heliostats	$N_{hel(total)}$	$N_{hel(total)} = A_{SF}/A_{hel}$		-

Table 2.17 Parameters and equations to calculate the dimensions of the solar field and the total number of heliostats
Source: H. Joga. Diseño de una planta termosolar de receptor central con sales fundidas como fluido de trabajo y sistema de almacenamiento [111] and UTEC CSP lectures

In this manner, using the procedures described above, the solar field of the plant is sized by considering solar multiples (SM) of 1 and 1.8, a parameter that is described later. The distribution of heliostats on the said field is defined in the following table.

Ring (i)	$\Delta R_{(i)}$	$\Delta L_{(i)}$	$N_{hel(i)}$	$N_{hel(total)}$	$R_{(i)}$	$S_{(i)}$
1	16.7	17.4	57.6	57.6	184.2	0.3198
2	18.0	18.0	75.1	132.7	200.9	0.3297
3	18.7	18.7	81.6	214.4	219.0	0.3410
4	19.4	19.4	88.3	302.7	237.7	0.3533
5	20.0	20.0	95.3	398.0	257.0	0.3666
6	20.7	20.7	102.4	500.4	277.1	0.3809
7	21.4	21.4	109.7	610.1	297.8	0.3962
8	22.0	22.0	117.3	727.4	319.2	0.4126
9	22.7	22.7	125.0	852.4	341.2	0.4298
10	23.4	23.4	132.9	985.3	363.9	0.4481
11	24.1	24.1	141.1	1,126.4	387.3	0.4673
12	24.7	24.7	149.4	1,275.7	411.4	0.4874
13	25.4	25.4	157.9	1,433.6	436.1	0.5084
14	26.1	26.1	166.6	1,600.3	461.5	0.5304
15	26.7	26.7	175.5	1,775.8	487.5	0.5532
16	27.4	27.4	184.6	1,960.4	514.3	0.5769
17	28.1	28.1	193.9	2,154.3	541.7	0.6014
18	28.7	28.7	203.4	2,357.6	569.7	0.6268
19	29.4	29.4	213.0	2,570.7	598.4	0.6530
20	30.1	30.1	222.8	2,793.5	627.8	0.6801
21	30.7	30.7	232.9	3,026.3	657.9	0.7079
22	31.4	31.4	243.0	3,269.4	688.6	0.7366
23	32.1	32.1	253.4	3,522.8	720.0	0.7660
24	32.7	32.7	264.0	3,786.8	752.1	0.7962
25	**33.4**	**33.4**	**274.7**	**4,061.5**	**784.8**	**0.8272**
26	34.1	34.1	285.6	4347.0	818.3	0.8590
27	34.7	34.7	296.7	4643.7	852.3	0.8915
28	35.4	35.4	307.9	4951.6	887.1	0.9248
29	36.1	36.1	319.3	5270.9	922.5	0.9588
30	36.7	36.7	330.9	5601.8	958.6	0.9936
31	37.4	37.4	342.6	5944.4	995.3	1.0291
32	38.1	38.1	354.5	6298.9	1032.7	1.0653
33	38.8	38.8	366.6	6,665.5	1,070.8	1.1022
34	**39.4**	**39.4**	**378.8**	**7,044.3**	**1,109.6**	**1.1399**

Table 2.18 Distribution of heliostats in the solar field
Source: Own elaboration

The number of rings for the continuous operation of the plant with *SM* = 1.8 is 34, and the total number of heliostats is 7,045. For the solution with operation during peak demand hours and with *SM* = 1, the number of rings is 25, and the number of heliostats is 4,061.

The detail of the heliostat field, generated with the help of SAM software for solar multiples of 1 and 1.8, can be seen in **Figure 2.16**.
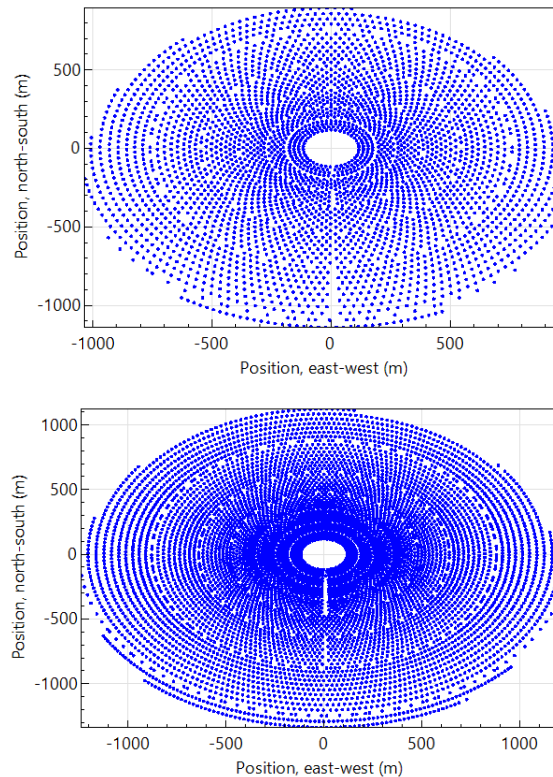
Figure 2.16 Heliostat field *SM* = 1 (up) and *SM* = 1.8 (down)
Source: Own elaboration – SAM simulation

2.2.3.1.1.2 Receiver

The design of the receiver requires in detail an independent and complex calculation methodology, since this component is custom designed and the optimal use of the solar resource will depend on the accuracy of the technology and the geometry. Given the scope of the investigation, it has been decided to use commercial data receivers that meet the needs of the thermal power plant (shown in **Table 2.6**).

Parameter	Symbol	Equation/remark	Value	Units
Receiver thermal power	$Q_{th,rec}$	$Q_{th,rec} = Pth + Q_{rad,rec}$	431–750	MW
Receiver thermal losses at design point (@900 W/m^2)	$Q_{rad,rec}$	$Q_{rad,rec}(*)$ *@DNI 900 W/m^2	33.8	MW
Receiver thermal losses (@DNI W/m^2)	$Q_{rad,rec(DNI)}$	$Q_{rad,rec(DNI)}=0.0376*(DNI)-6*10^{-14}$		MW
Mass flow rate (molten salt)	$\dot{m}_{salt}$	*SAM reference data	916–917	kg/s

Table 2.19 Parameters and equations to calculate the dimensions of the receiver
Source: Private information, UTEC CSP lectures, and SAM simulation

2.2.3.1.1.3 Solar tower

Currently, there is no reliable tower height model in the literature, because it is given as user input in all the commercial design software. Therefore, a correlation developed using state-of-the-art commercial power plant data, proposed by Stalin et al. [112], is used.

Parameter	Symbol	Equation/remark	Value	Units
Tower height	H_{tower}	$H_{tower} = 0.2552 * Q_{th,rec} + 82.60$	193–265	m
Tower height	$H_{tower(SAM)}$	SAM optimization	140–210	m

Table 2.20 Parameters and equations to calculate the dimensions of the solar tower
Source: J. Stalin and M. Jebamalai. Receiver Design Methodology for Solar Tower Power Plants [112] and SAM simulation

2.2.3.1.1.4 Energy generation

The electricity generation of the plant is calculated based on the parameters described above through the following equation:

$$E_{@h} = \left[\left(\frac{DNI_{@(h)} * N_{hel(total)} * \eta_{SF} * A_{hel}}{10^6} \right) - Q_{rad,rec@DNI(h)} \right] * \eta_{cycle} * \eta_{gen}$$

Monthly energy generation:	Yearly energy generation:
$$E_{@month} = \sum_{x=5}^{18} E_{@h} * (days_{per\,month})$$ *Units: MWh/month	$$E_{@year} = \sum_{x=1}^{12} E_{@month}$$ *Units: MWh/year

Parameter	Symbol	Equation/remark	Units
Monthly average hourly radiation	$DNI_{@(h)}$	See **Table 2.1**	W/m^2
Hourly energy generation	$E_{@h}$	See equation described above in the text	MWh
Solar hours	h_{solar}	$h_{solar} = 14\ (*)$ *Solar hours per day x= 5,6,7…18	hours
Lack of energy (SPT)	$E_{lack(SPT)}$	$E_{lack(SPT)} = P_e * 1_{hour} - E_{(Feb,h_{solar}=x)}$ $*E_{(Feb,h_{solar}=x)}$ for SM=1 (Feb - Month with lower generation)	MWh
Lack of energy (PV)	$E_{lack(PV)}$	$E_{lack(PV)} = P_e * h_{solar=7,8,16,17}$ $- E_{(Feb,h_{solar}=7,8,16,17)}$ $*E_{(Feb,h_{solar}=7,8,16,17)}$ for SM=1	MWh
Lack of energy	E_{lack}	$E_{lack} = E_{lack(SPT)} + E_{lack(PV)}$	MWh
Solar multiple	SM	$SM = \dfrac{P_e * h_{solar} + E_{lack}}{P_e * h_{solar}}$	-

Table 2.21 Parameters and equations to calculate the energy generation of the plant
Source: Own elaboration and UTEC CSP lectures

2.2.3.1.1.5 Thermal energy storage

The sizing of molten salt storage tanks was carried out based on the availability of thermal energy at the plant and the commercial properties of the salts.

Parameter	Symbol	Equation/remark	Units
Hours of thermal storage	HTS	$HTS = \dfrac{\left[P_e * h_{solar(x=12\ full\ load)} + E_{lack(PV)}\right]}{P_e}$	hours
Molten salt mass	m_{salt}	$m_{salt} = HTS * \dot{m}_{salt} * 3600$	kg
Molten salt average temperature	ΔT_{salt}	$\Delta T_{salt} = \dfrac{T_{salt(hot)} + T_{salt(cold)}}{2}$	°C
Molten salt density (@Temp °C)	ρ_{salt}	$\rho_{salt}(\Delta T_{salt}) = 0.636 * (\Delta T_{salt}) + 2090$	kg/m^3
Molten salt volume	v_{salt}	$v_{salt} = m_{salt} * \rho_{salt}(\Delta T_{salt})$	m^3

Table 2.22 Parameters and equations to calculate the HTS and the required amounts of molten salts
Source: Own elaboration and UTEC CSP lectures

2.2.3.1.2 Economical model

For the economic analysis of the proposed hybrid plants, it is necessary to define the assumptions considered for the calculation of indicators such as CAPEX, OPEX, NPV, IRR, and LCOE. For this, the costs of previous projects with similar technical characteristics have been taken into account.

General considerations:

- Plant lifetime: 30 years.

- Net power capacity: 140 MW.

- Power capacity price: 4.3 USD/kW/month.

- Annual energy generation: 1,115 GWh/year and 870 GWh/year.

- IRR range: 7–12%.

Photovoltaic solar plant considerations:

- Photovoltaic investment index[23] (CAPEX): 800 USD/kW.

- Photovoltaic OPEX index[24]: 2,000 USD/kW/year.

Solar power tower and thermal energy storage with 140 MW (9 h/15 h) plant considerations:

- Solar power tower and thermal energy storage investment index[25] (CAPEX): 6,000–3,250 USD/kW.

- Solar power tower and thermal energy storage OPEX index[26]: 100 USD/kW/year.

---

[23] Reduction by **1.5%** by 2030.

[24] Reduction by **12.5%** by 2030.

[25] Reduction by **4.3%** per year in two scenarios (high and medium cost) with consideration of 10% contingencies. **Cost reductions** are -15% for civil works (tower and solar field), -10% for erection and installation work, -40% for technology (manufacturing and volume costs), -10% for steam cycle equipment, -10% for balance of plant, -5% for TES (including erection), and -20% for sales (production and volume costs).

[26] **No cost reduction** in operation and maintenance (new technology).

Main equations:

- **CAPEX:** The component of the CAPEX comprises the investment associated with the power block, solar field (PV and SPT), storage (TES), civil works, balance of plant, and contingency:

$$CAPEX_{SPT-TES+PV} = CAPEX_{SPT-TES} + CAPEX_{PV}$$

- **OPEX:** This represents the sum of the costs associated with the plant operation and maintenance, including labor, service, and cleaning costs:

$$OPEX_{SPT-TES+PV} = OPEX_{SPT-TES} + OPEX_{PV}$$

- **LCOE:** This is calculated by summing the CAPEX in year 0 and the OPEX from the period and then by dividing the total by the generation from the period:

$$LCOE = \frac{CAPEX_{SPT-TES+PV(0)} + \sum_{t=1}^{n} \dfrac{OPEX_{SPT-TES+PV(t)}}{(1+i)^t}}{\sum_{t=1}^{n} \dfrac{Generation_{(t)}}{(1+i)^t}}$$

- **NPV:** This is used to analyze the profitability of a project and is calculated by taking the difference between the present value of cash inflows and present value of cash outflows over a period:

$$NPV = \sum_{t=1}^{n} \frac{CF_{(t)}}{(1+i)^t} - In$$

Subsequently, using an Excel model, the energy price for each hybrid plant was calculated by using different IRRs and two cost scenarios (high and medium) and by considering the annual generation, NPV, and power income.

2.2.3.2 Development of scenarios

For the development of technical-economic scenarios that allow the incorporation of a SPT-TES + PV hybrid power plant in the south of Peru (see **Table 2.23**), the following assumptions and scenarios have been taken into account:

- Projection of mining demand in the south in a medium-term scenario.

- A 2018–2030 horizon.

- Two plant arrangements: SPT-TES (9 h) + PV and SPT-TES (15 h) + PV.

- Scenarios of maximum marginal costs without new efficient generation projects until 2028:

    - **Marginal cost A:** (max. 75 USD/MWh).

        - C.H. San Gaban (COD 2024).

        - SIT GAS (COD 2026).

        - C.H. Lluta and C.H. Lluclla (COD 2028).

    - **Marginal cost B:** (max. 120 USD/MWh).

        - C.H. San Gaban (COD 2026).

        - SIT GAS (COD 2026).

        - C.H. Lluta and C.H. Lluclla (COD 2028).

    - **Marginal cost C:** (max. 150 USD/MWh).

        - C.H. San Gaban (COD 2024).

        - SIT GAS (COD 2028).

        - C.H. Lluta and C.H. Lluclla (COD 2028).

- Scenarios of projected energy price as a function of IRR by plant arrangement:

    - High energy price as a function of IRR.

    - Medium energy price as a function of IRR.

Scenario	Arrangement	Energy price (USD/MWh)		Marginal cost (USD/MWh)		
		High	Medium	A	B	C
1	SPT-TES (9 h) +PV	X		X		
			X	X		
2	SPT-TES (9 h) +PV	X			X	
			X		X	
3	SPT-TES (9 h) +PV	X				X
			X			X
4	SPT-TES (15 h) +PV	X		X		
			X	X		
5	SPT-TES (15 h) +PV	X			X	
			X		X	
6	SPT-TES (15 h) +PV	X				X
			X			X

Table 2.23 Scenario matrix
Source: Own elaboration

CHAPTER III:

RESULTS

From the technical-economic analysis, a 150 MW SPT-TES + PV installation has been modeled in the district of La Joya, using bankable data and technical and economic characteristics of commercial components. The first part of the analysis consisted of evaluating the distribution of hourly and monthly DNI, with information provided by SolarGIS, to determine the potential of the site. Then, the conditions of the location of the plant were analyzed, and it was concluded that the site has good accessibility by air and land, the connection point is close to the plant, and it has available capacity. Additionally, the area does not represent a high geological risk for the construction stage, the archaeological risk is low, the acquisition of land is accessible because the state owns it, and for the social aspect, the risk of rejection of the project is low.

As for the design of the plant, a SPT-TES + PV plant was chosen because it allows greater flexibility in its operation and at a competitive price. Then, the technical model was developed based on various methodologies found in the literature and an exhaustive review of characteristics of commercial components and case studies of plants in operation. The results of the technical model are shown in the **Table 3.1**.

Parameter	SPT –TES (9 h)	SPT –TES (15 h)
Annual energy	460 GWh	765 GWh
SM (Solar multiple)	1	1.8
# heliostat	3,926	6,976
# rings – solar field	25	34
Tower	170–90	220–250
Receiver	440 MWt	750 MWt
Salt volume	16,631 m^3	26,544 m^3
Required area	200 ha	335 ha

Table 3.1 Results of the technical model for solar power tower-thermal energy storage plant
Source: Own elaboration

The design point of the plant was 873 W/m² with a gross capacity of 150 MW and with the objective of offering a constant injection of 130–140 MW. To meet this objective and preserve the assumptions, it was determined that the system would require 9 - 15 hours of TES and consequently an increase in the solar field through the solar multiple of 1 - 1.8.

Figure 3.1 shows the average hourly production of the SPT-TES plant (9h) for an average day of each month, observing that the period from January to March shows the lowest production, while from September to December, the production reaches maximum values. The same happens in **Figure 3.2** in the SPT-TES plant with storage of 15 hours.
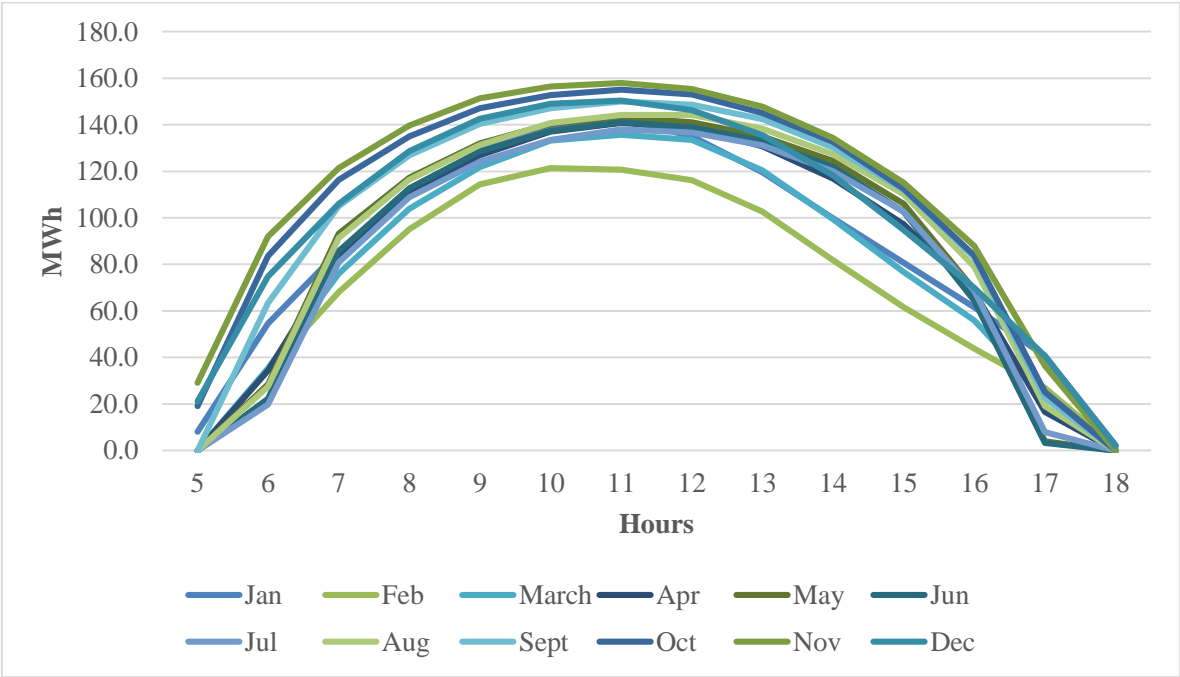
Figure 3.1 Average monthly hourly power generation of the solar power tower-thermal energy storage plant (9 h)
Source: Own elaboration
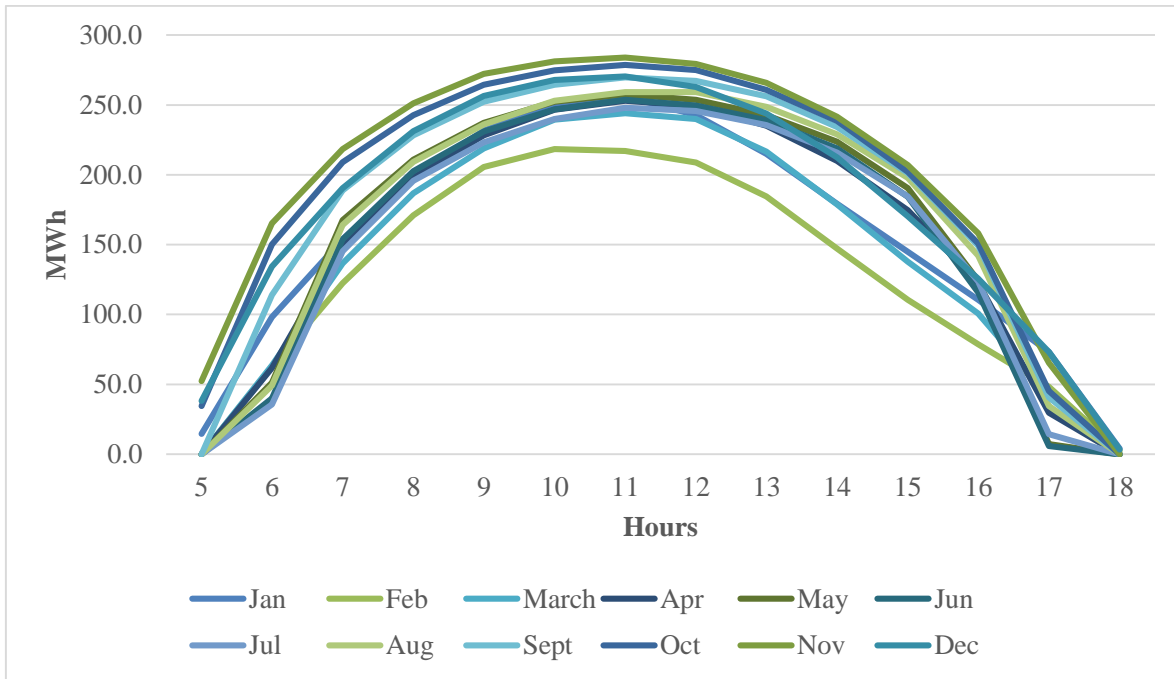
Figure 3.2 Average monthly hourly power generation of the solar power tower-thermal energy storage plant
(15 h)
Source: Own elaboration

In the case of the photovoltaic system, a 163 MW plant was designed with consideration of a GHI of 2,442 kWh/m^2 per year and an albedo of 20%, which is capable of generating 412.4 GWh per year. The main features of the system are shown below in **Table 3.2**.

Parameter	Characteristic/value
DC capacity (MWp)	163.5
Modules/inverters (#)	457,800 / 40
Annual energy (GWh)	410
Capacity factor (AC)	33.10%
Required land	310 ha

Table 3.2 Results of the technical model for photovoltaics
Source: Private information

Subsequently, by combining both plants in a hybrid SPT-TES + PV generation system, it is possible to have a load profile that provides firm power to the system and meets the objectives initially set.

In the case of both SPT-TES (9 -15h) + PV plants, it is observed that the maximum production is achieved in the month of November, while the lowest production is observed in the month of February, given the radiation conditions.

In the case of the SPT-TES (9h) + PV plant, it is observed that in February (**Figure 3.3**), it would be possible to have a constant daily energy injection and a firm power of ~ 135-138MW for 15 hours during 9:00-24:00 hours. On the other hand, in November, the month with the highest production (**Figure 3.4**), it is possible to achieve a constant daily energy injection and a steady power of ~ 140MW for 16 hours during 8:00-24:00 hours.
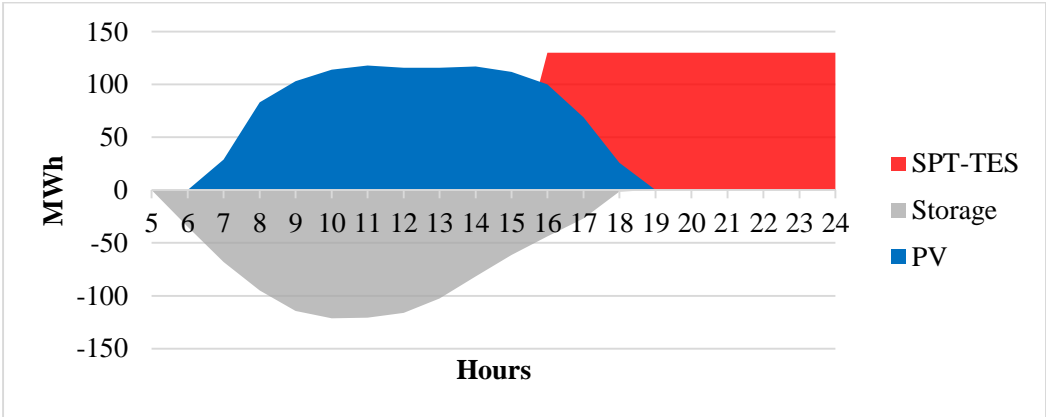
Figure 3.3 Daily power generation during February of the solar power tower-thermal energy storage plant (9 h)
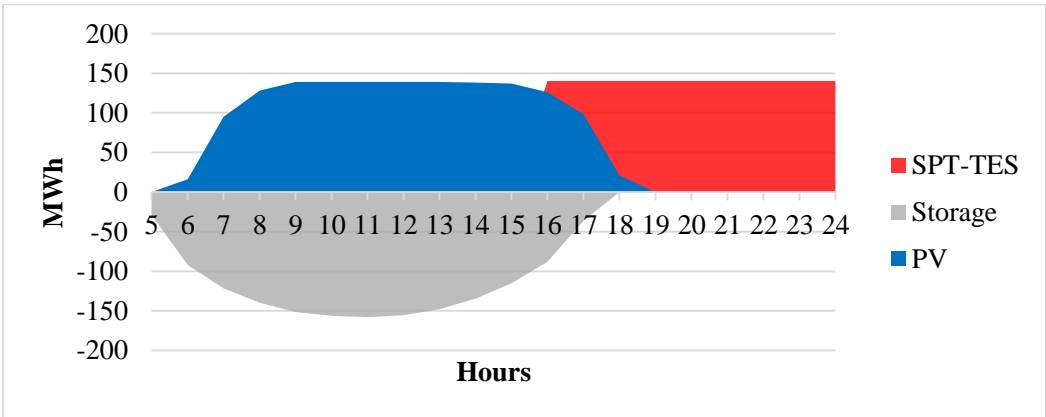
Figure 3.4 Daily power generation during November of the solar power tower-thermal energy storage plant (9 h)

It is worth mentioning that, in case of offering a 24x7 solution, energy withdrawals would be required at dawn for ~ 7-8 hours to meet customer demand.

In the case of the SPT-TES (15h) + PV plant in February (**Figure 3.5**), a constant injection of energy is achieved for 23.5 hours at ~ 135 MW. While in November (**Figure 3.6**), it is possible to maintain the constant injection of energy throughout the day (24 hours) at 140MW. This plant arrangement is ideal for a 24x7 solution.
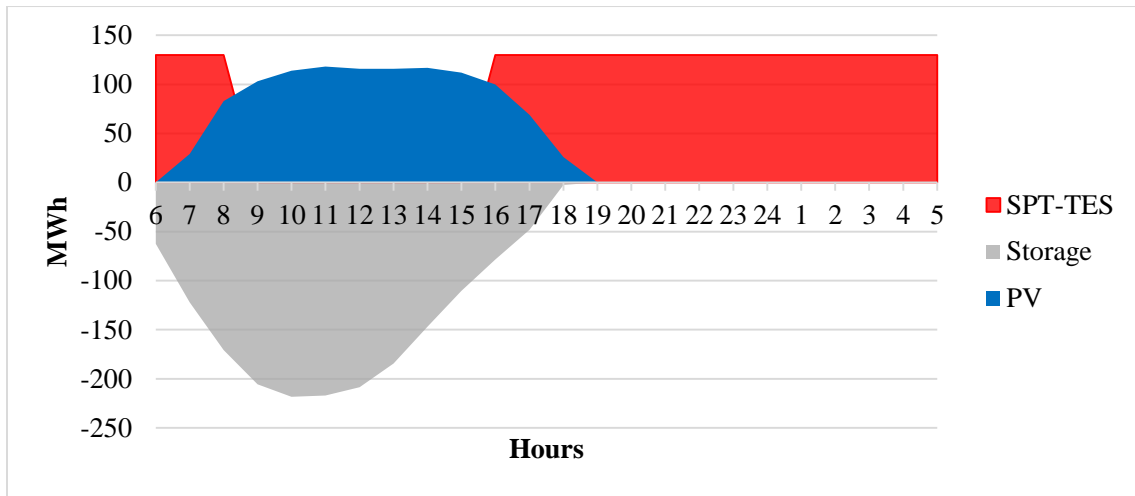
Figure 3.5 Daily power generation during February of the solar power tower-thermal energy storage plant (15 h)
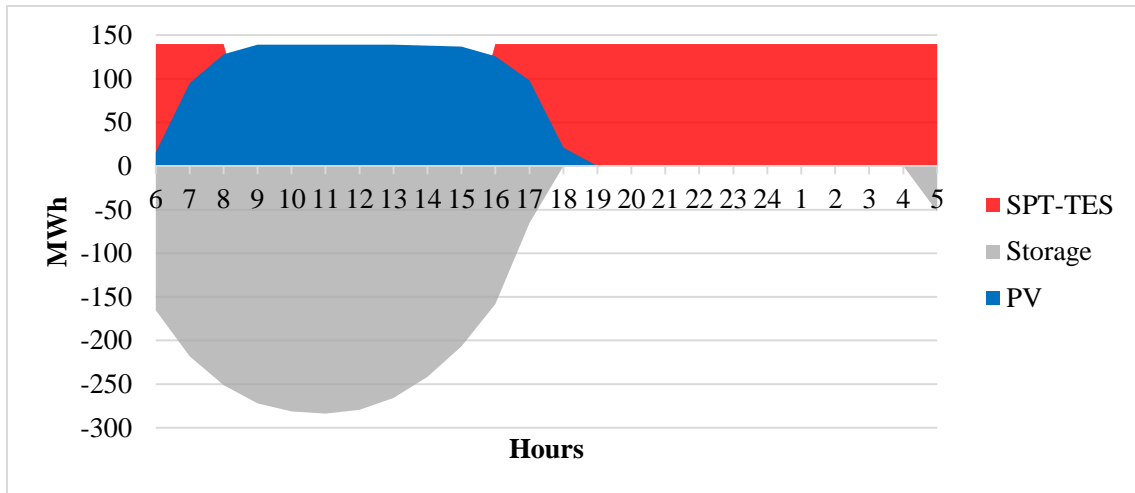
Figure 3.6 Daily power generation during November of the solar power tower-thermal energy storage plant (15 h)

3.1 Scenarios

3.1.1 Scenario 1

The most attractive offer in the first scenario is offer 1.3 (see **Table 3.3**), which proposes the incorporation of the SPT-TES (9 h) + PV plant in 2025 at 70.58 USD/MWh with an IRR of 8%.

High energy price scenario				Medium energy price scenario			
Offer	**Price (USD/MWh)**	**Year**	**IRR**	**Offer**	**Price (USD/MWh)**	**Year**	**IRR**
1.1	72.2	2025	7%	1.2	65.93	2024	7%
				1.3	70.58	2025	8%

Table 3.3 Results of Scenario 1 with the solar power tower with thermal energy storage (9 h) and photovoltaics arrangement
Source: Own elaboration

3.1.1.1 Drivers and entry mode

A new energy auction would have to be considered with the following characteristics:

- It considers new technologies capable of providing reliability (mitigating risks due to resource variability) and flexibility to the system (firm capacity requirement).

- A new energy pricing of 80–120 USD/MWh.

3.1.1.2 Risks

- Accelerated development of solar PV plants (direct competitors) and wind power plants (30–40 USD/MWh).

- Renewable energy source hydroelectric development (45–60 USD/MWh).

- Uncertainty of the conditions of the new energy auction.

3.1.2 Scenario 2

The most attractive offer in the second scenario is offer 2.4 (see **Table 3.4**), which proposes the incorporation of the SPT-TES (9 h) + PV plant in 2025 at 87.66 USD/MWh with an IRR of 10%.

However, offer 2.3 offers the lowest price of the scenarios under study, with an IRR of 8% in 2024, followed by offer 2.1 for the same year but with an IRR of 7%.

High energy price scenario				Medium energy price scenario			
Offer	Price (USD/MWh)	Year	IRR	Offer	Price (USD/MWh)	Year	IRR
2.1	75.87	2024	7%	2.3	72.85	2024	8%
2.2	99.41	2025	10%	2.4	87.66	2026	10%

Table 3.4 Results of Scenario 2 with the solar power tower with thermal energy storage (9h) and photovoltaics arrangement
Source: Own elaboration

3.1.2.1 Drivers and entry mode

A new energy auction with the same characteristics as mentioned in Scenario 1.

3.1.2.2 Risks

Scenario 2 shares the risks of Scenario 1.

3.1.3 Scenario 3

The most attractive offers in the third scenario with an IRR of 10% is offer 3.3 at 82.84 USD/MWh in 2026, offer 3.4 at 79 USD/MWh in 2027, and offer 3.2 at 89.01 USD/MWh in 2027 (see **Table 3.5**).

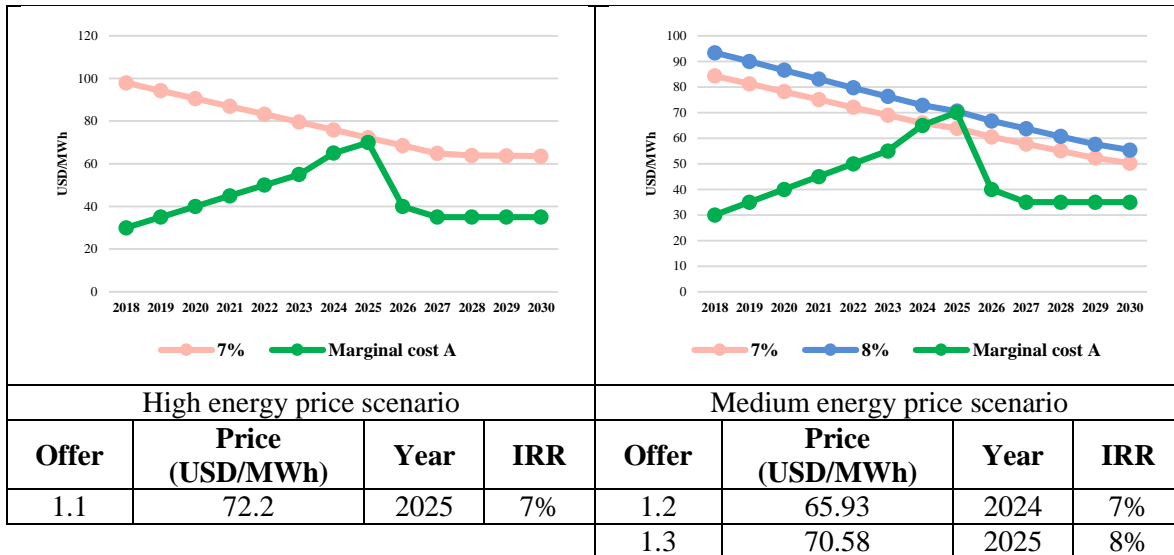| High energy price scenario				Medium energy price scenario			
Offer	**Price (USD/MWh)**	**Year**	**IRR**	**Offer**	**Price (USD/MWh)**	**Year**	**IRR**
1.1	72.2	2025	7%	1.2	65.93	2024	7%
3.1	94.21	2026	10%	1.3	70.58	2025	8%
3.2	89.01	2027	10%	3.3	82.84	2026	10%
				3.4	79	2027	10%

Table 3.5 Results of Scenario 3 with the solar power tower and thermal energy storage (9 h) with photovoltaics arrangement
Source: Own elaboration

3.1.3.1 Drivers and entry mode

A new energy auction with the same characteristics as mentioned in Scenario 1.

3.1.3.2 Risks

- Scenario 3 shares the risks of Scenario 1.

- Geothermal development[27] (69–112 USD/MWh).

- Increase of the central-south transfer limit to 1,800 MW.

- SIT GAS COD 2026.

- Approval of the hourly auction, which would grant competitive firm capacity to PV solar plants.

3.1.4 Scenario 4

The most attractive offer in the fourth scenario is offer 4.4 (see **Table 3.6**), which proposes the incorporation of the SPT-TES (15 h) + PV plant in 2025 at 65.12 USD/MWh with an IRR of 10%.

While offer 4.4 offers a highly competitive price, it is followed by offer 4.2 (at 66.04–73.38 USD/MWh in 2025) and offer 4.3 (at 61.21–67.95 USD/MWh in 2024) with an IRR range of 9–10 %.

---

[27] Start of development would be in 2020. With consideration of surface exploration activities (2 years), deep exploration (2.5 years), and engineering and construction (2 years), a possible COD would be in 2027 [118].

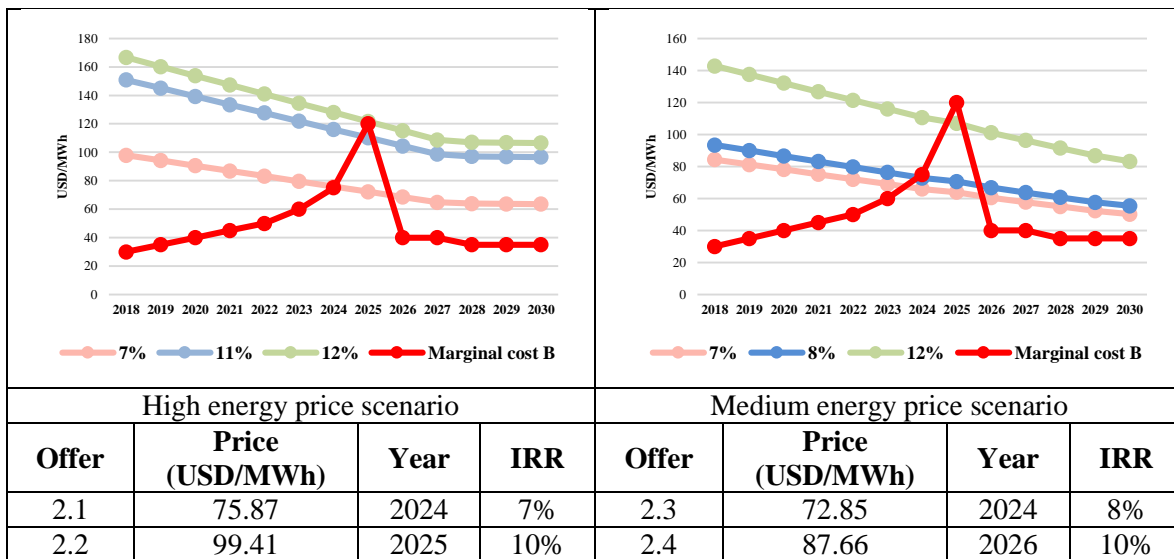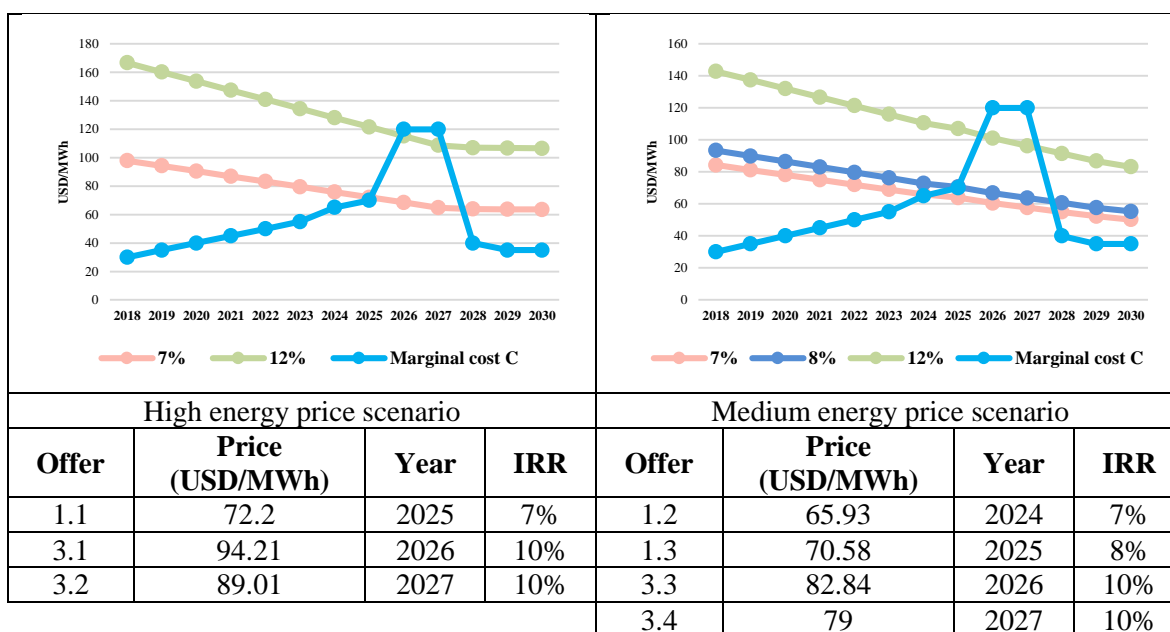| High energy price scenario				Medium energy price scenario			
Offer	**Price (USD/MWh)**	**Year**	**IRR**	**Offer**	**Price (USD/MWh)**	**Year**	**IRR**
4.1	62.61	2024	8%	4.3	61.21–67.95	2024	9–10%
4.2	66.04–73.38	2025	9–10%	4.4	65.12	2025	10%

Table 3.6 Results of Scenario 4 with the solar power tower with thermal energy storage (15 h) and photovoltaics arrangement

Source: Own elaboration

3.1.4.1 Drivers and entry mode

A new energy auction would have to be considered with the following characteristics:

- It considers new technologies capable of providing reliability (mitigating risks due to resource variability) and flexibility to the system (firm capacity requirement).

- A new energy pricing of 80–90 USD/MWh.

3.1.4.2 Risks

Scenario 4 shares the risks of Scenario 1.

3.1.5 Scenario 5

Offer 4.4 remains the most competitive for 2025, but by 2024 with an IRR of 9–10%, prices of 67.95–77.45 USD/MWh are reached through offer 5.1 and offer 5.3 (see **Table 3.7**).

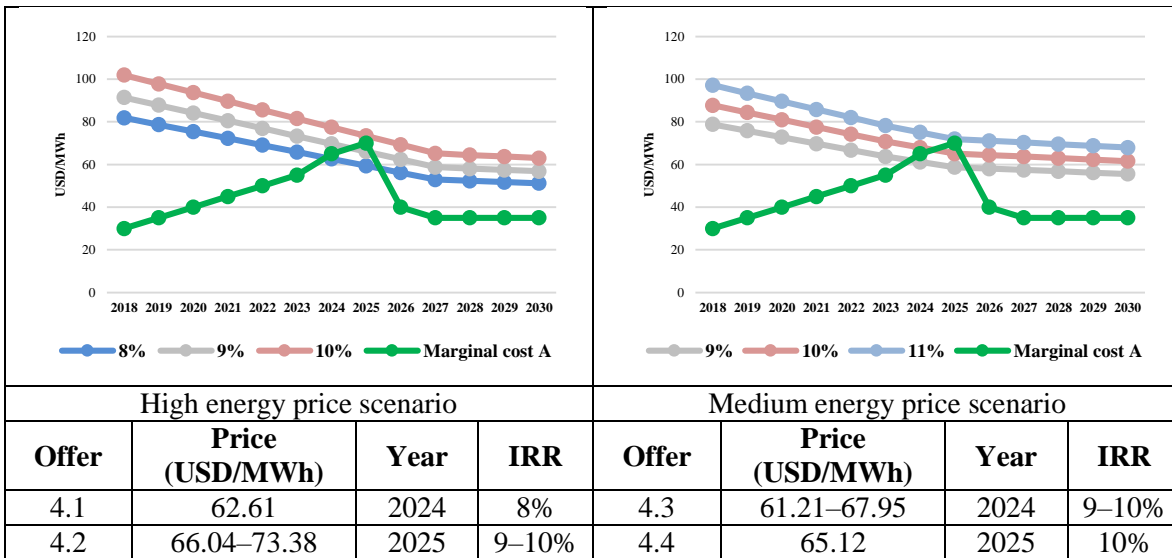| High energy price scenario				Medium energy price scenario			
Offer	**Price (USD/MWh)**	**Year**	**IRR**	**Offer**	**Price (USD/MWh)**	**Year**	**IRR**
5.1	69.66–77.45	2024	9–10%	4.4	65.12	2025	10%
5.2	73.38	2025	10%	5.3	67.95	2024	10%

Table 3.7 Results of Scenario 5 with the solar power tower and thermal energy storage (15 h) with photovoltaics arrangement
Source: Own elaboration

3.1.5.1 Drivers and entry mode

A new energy auction with the same characteristics mentioned in Scenario 4.

3.1.5.2 Risks

Scenario 5 shares the same risks as Scenario 1.

3.1.6 Scenario 6

The most competitive offers are reached in 2027 (see **Table 3.8)** with an IRR of 10% at 65.23–63.7 USD/MWh (offer 6.2 and offer 6.4), while by 2026 again with an IRR of 10%, prices of 69.3–64.41 USD/MWh are reached (offer 6.1 and offer 6.3).

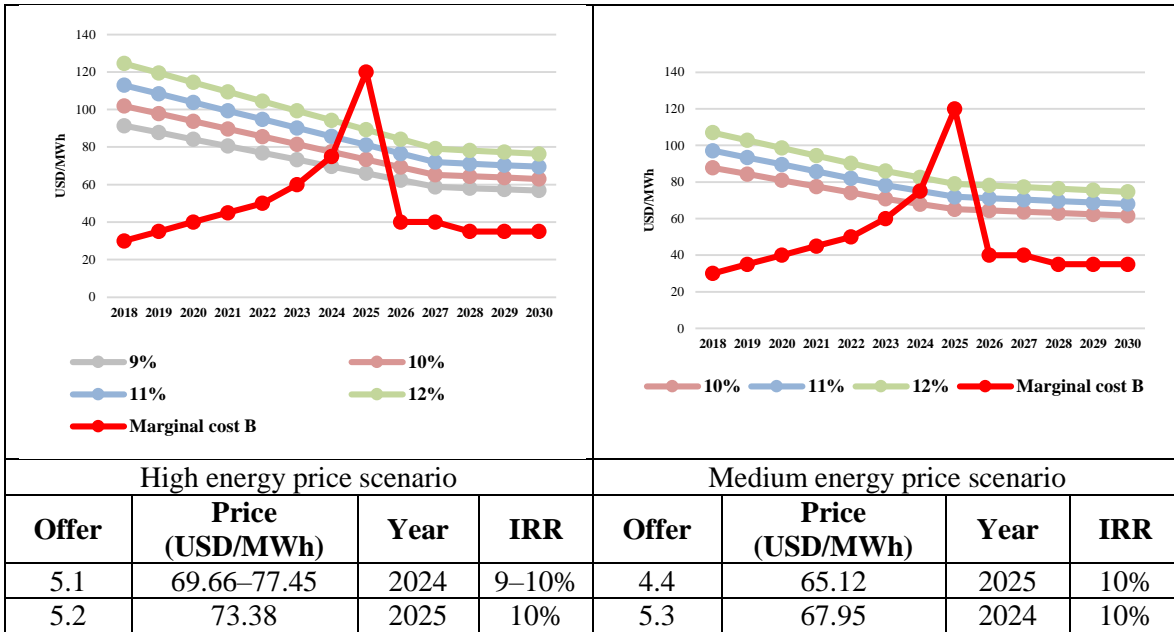| High energy price scenario				Medium energy price scenario			
Offer	**Price (USD/MWh)**	**Year**	**IRR**	**Offer**	**Price (USD/MWh)**	**Year**	**IRR**
4.1	62.61	2024	8%	4.3	61.21–67.95	2024	9–10%
4.2	66.04–73.38	2025	9–10%	4.4	65.12	2025	10%
6.1	69.3	2026	10%	6.3	64.41	2026	10%
6.2	65.23	2027	10%	6.4	63.7	2027	10%
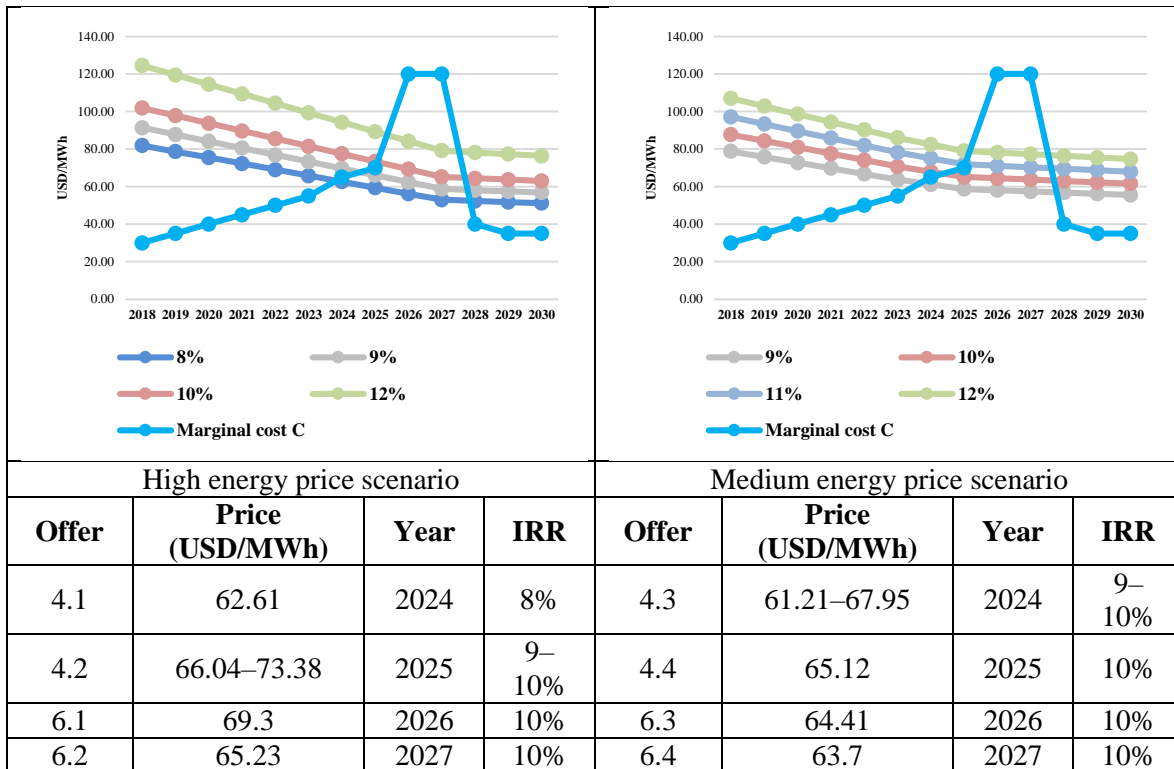
Table 3.8 Results of Scenario 6 with the solar power tower and thermal energy storage (15 h) with photovoltaics arrangement
Source: Own elaboration

3.1.6.1 Drivers and entry mode

A new energy auction shares the same characteristics as mentioned in Scenario 4, but with a modification in the energy pricing of 70–80 USD/MWh.

3.1.6.2 Risks

Scenario 6 shares the same risks as Scenario 3.

Best scenarios for the entry of a SPT-TES (9 h–15 h) + PV hybrid plant, which ensure the profitability of the project through an IRR of 10% and offers a competitive price, are shown in **Table 3.9**.

Offer	Year	Arrangement	USD/ MWh	COD SIT GAS	Energy price scenario	Marginal cost
3.4	2027	SPT-TES (9 h)+ PV	79	2028	Medium	C
4.4	2025	SPT-TES (15 h)+ PV	65.12	2026	Medium	A
6.3	2026	SPT-TES (15 h)+ PV	64.41	2028	Medium	C
6.2	2027	SPT-TES (15 h)+ PV	65.23	2028	High	C
6.4	2027	SPT-TES (15 h)+ PV	63.7	2028	Medium	C

Table 3.9 Competitive offers for the incorporation of a solar power tower and thermal energy storage with photovoltaics plant
Source: Own elaboration

It is worth mentioning that the only way to enter this technology would be through a new energy auction with revenue milestones in the period of 2024–2027. This is because it is not yet feasible to enter the market through a PPA contract as the current market conditions are not favorable (prices are below the range suitable for being offered).

CONCLUSIONS

- An adequate technology to cover the growing demand in southern Peru is the SPT because it has higher efficiency (+30%, PTC), has higher storage capacity (12–15 h), offers flexibility during its operation (adjustment to real demand), has lower maintenance costs (-15%, PTC), has lower energy consumption for auxiliary systems and pumping, and has maintenance that is sectored, allowing for uninterrupted operation for long periods, compared to other technologies.

- The most attractive configuration to reach a competitive price is the hybridization of a SPT-TES plant with a PV plant. This not only reduces generation costs but also allows flexible demand to be met and offers firm capacity to a market whose energy demands require a reliable contribution.

- The SPT-TES (9 h) + PV arrangement is not competitive against other technologies independently because the energy costs exceed the cost of a hydroelectric plant. However, it has been determined that by 2032, it will reach a competitive price of 64.4 USD/MWh (IRR: 10%, the average price of technology).

- It was validated that the design of an SPT-TES plant is technically and economically attractive when the storage characteristic is maximized, which allows for reducing the investment index for plants with higher generation capacity.

- It has been proven that the hybridization of solar concentration plants allows for reducing the investment index in areas that are in the initial phases of integrating the technology into their energy matrix.

- The SPT-TES (15 h) + PV arrangement is independently competitive compared to other technologies, reaching competitive prices of 64.41–61.58 USD/MWh (IRR: 10%, the medium and high price of the technology) by 2028.

- In case a second stage of the project is carried out, the installation of DNI measurement systems and their correct calibration is suggested to obtain real data and to adjust the solar model of the area. Additionally, it is recommended to include visibility measurements to reduce atmospheric attenuation losses.

- For future work, it is proposed to independently carry out a detailed design of the main components of the SPT-TES (15 h) arrangement such as the receiver, tower and civil works, TES system, and Rankine cycle, with the objective of optimizing the parts and achieving an annual projection of the most accurate and realistic energy generation.

- It is suggested to perform an independent design of the solar field to optimize the distribution of heliostats and to select the best arrangement.

- The development of a detailed economic model for the evaluation of new scenarios (new market conditions) is considered for future work.

- In case the development is continued, it will be necessary to carry out a corresponding environmental study to evaluate the impacts and to propose mitigation measures, in addition to a study of archaeological remains that validates the surface survey.

- The reduction in technology costs will depend on the development of local labor capacity for the construction of this type of infrastructure, the development of industry for the national production of molten salts for CSP systems, and the opening of commercial technology points in Peru, in addition to the development of national industry for the manufacture of components with greater demand and complexity (such as heliostats and the receiver).

REFERENCES

[1]   IRENA, "Global Energy Transformation: A Roadmap to 2050," Abu Dhabi, 2019.

[2]   REN 21, "Renewables 2018 - Global Status Report," Paris, 2018.

[3]   F. Ísimodes, "Avances y retos del sector energético: Competitividad y Sostenibilidad," Lima, 2018.

[4]   GTM-NDC, "Grupo de Trabajo Multisectorial de naturaleza temporal encargado de generar información técnica para orientar la implementación de las Contribuciones Nacionalmente Determinadas," LIMA, 2018.

[5]   Equilibrium, "Análisis del Sector Eléctrico Peruano: Generación," Lima, 2018.

[6]   DGPSM, "Cartera de Proyectos de Construcción de Mina 2018," Lima, 2018.

[7]   COES-SINAC, "Evaluación de la necesidad de generación eficiente en el SEIN y prospectiva del suministro eléctrico del sur en el corto, mediano y largo plazo," Lima, 2019.

[8]   COES-SINAC, "Informe de Diagnóstico de las Condiciones Operativas del SEIN, Período 2021-2030," Lima, 2019.

[9]   P. del Río, C. Peñasco, and P. Mir-Artigues, "An overview of drivers and barriers to concentrated solar power in the European Union," *Renew. Sustain. Energy Rev.*, vol. 81, pp. 1019–1029, Jan. 2018.

[10]   IEA, "Global Energy & CO2 Status Report 2018," Paris, 2019.

[11]   IRENA, "Renewable capacity highlights," Abu Dhabi, 2019.

[12]   IEA, "Renewable Power - Tracking Clean Energy Progress," *International Energy Agency*, 2018. [Online]. Available: https://www.iea.org/tcep/power/renewables/. [Accessed: 07-May-2019].

[13]   COES-SINAC, "Estadistica anual 2020," Lima, 2020.

[14]   M. Horn, "El estado actual del uso de la energía solar en el Perú," *Perú económico*,

vol. 29, no. 11, pp. 10–11, 2006.

[15]   Grupo Rural PUCP, "El desarrollo de la energía solar en el Perú," *Grupo de apoyo al Sector Rural*, 2017. [Online]. Available: http://gruporural.pucp.edu.pe/nota/el-desarrollo-de-la-energia-solar-en-el-peru/. [Accessed: 14-May-2019].

[16]   OMP, "Termas Solares," *OMP & Servicios y Contratistas Generales S.A.C.*, 2019. [Online]. Available: http://ompsac.com/termas-solares/. [Accessed: 07-May-2019].

[17]   Solstac-Lima, "Terma Solstac," *Solstac-Lima*, 2019. [Online]. Available: http://solstac-lima.com/wp/?page_id=20. [Accessed: 07-May-2019].

[18]   Eco Perú, "Termas Solares," *Eco Perú*, 2019. [Online]. Available: http://www.eco-peru.com/termas_solares.html. [Accessed: 07-May-2019].

[19]   GeoEnergía, "Termas solares para uso familiar, hoteles, colegios o industrial," *GeoEnergía Perú*, 2019. [Online]. Available: http://geoenergiaperu.com/termas-solares/. [Accessed: 07-May-2019].

[20]   Aquatherm, "Terma Solar Doméstica," *AQUATERMICA*, 2019. [Online]. Available: http://www.aquatermica.com/reportes.php?cat=112. [Accessed: 07-May-2019].

[21]   Energynet, "Entrevista con Fernando Gonzalez, CEO de Cerro Dominador," in *Planta termosolar concentrada y fotovoltaica de Chile*, 2019, pp. 1–2.

[22]   L. Terrazos, "Viabilidad técnica y económica para la construcción de una central termosolar en la región Puno," Universidad Nacional de Ingeniería, 2014.

[23]   F. P. Ruiz, "Concentrating solar power potential of Peru," Aalborg University, 2019.

[24]   I. Rodríguez, N. Caldés, A. Garrido, C. De La Rúa, and Y. Lechón, "Socioeconomic, Environmental, and Social Impacts of a Concentrated Solar Power Energy Project in Northern Chile," in *Mediterranean Green Buildings & Renewable Energy*, 2017, pp. 865–883.

[25]   A. Aly, A. Bernardos, C. M. Fernandez-Peruchena, S. S. Jensen, and A. B. Pedersen, "Is Concentrated Solar Power (CSP) a feasible option for Sub-Saharan Africa?: Investigating the techno-economic feasibility of CSP in Tanzania," *Renew. Energy*,

vol. 135, pp. 1224–1240, May 2019.

[26] T. Bouhal *et al.*, "Technical feasibility of a sustainable Concentrated Solar Power in Morocco through an energy analysis," *Renew. Sustain. Energy Rev.*, vol. 81, pp. 1087–1095, Jan. 2018.

[27] R. Mena, R. Escobar, Á. Lorca, M. Negrete-Pincetic, and D. Olivares, "The impact of concentrated solar power in electric power systems: A Chilean case study," *Appl. Energy*, vol. 235, pp. 258–283, Feb. 2019.

[28] MINEM, DGRE, GEF, and Banco-Mundial, "Atlas del potencial hidroeléctrico del Perú," Lima, 2011.

[29] Osinergmin, "Proyectos Generación," *Osinergmin*, 2018. [Online]. Available: http://www.osinergmin.gob.pe/empresas/electricidad/proyectos/generacion#. [Accessed: 11-Sep-2019].

[30] Osinergmin, "Centrales de generación eléctrica - En operación," Lima, 2018.

[31] Solargis, ESMAP, and World Bank Group, "Solar resource maps of Peru," *World Bank Group*, 2017. [Online]. Available: https://solargis.com/maps-and-gis-data/download/peru. [Accessed: 11-Sep-2019].

[32] MINEM, Vortex, and Barlovento, "Atlas Eólico del Perú," Lima, 2016.

[33] El Peruano, "Aporte de la minería al PBI," *El Peruano*, Lima, 19-Apr-2018.

[34] BCRP, "Memoria 2018 Banco Central de Reserva Del Perú," Lima, 2018.

[35] MINCETUR, "Reporte mensual de Comercio," Lima, 2018.

[36] SNMPE, "Los Minerales," *SNMPE*, 2018. [Online]. Available: https://www.snmpe.org.pe/mineria/publicaciones-del-sector-minero/los-minerales.html. [Accessed: 12-Sep-2019].

[37] Ingemmet, "Estimación del potencial minero métalico del Perú y su contribución económica al estado, acumulado al 2050," Lima, 2018.

[38] L. Espinoza, "Porque es importante desarrollar el Gas Natural en el Sur del País,"

Lima, 2019.

[39]   MINEM, "Principales indicadores de sector eléctrico a nivel nacional - Enero 2019,"
         Lima, 2019.

[40]   MINEM, "Balance Nacional de Energía 2019," Lima, 2019.

[41]   Andina, "Sistema Integrado de Transporte de Gas en reemplazo de Gasoducto del
         Sur será cofinanciado," *Andina*, Lima, 24-Jan-2019.

[42]   Energiminas, "Proyecto SIT Gas recorrerá el mismo trazo que tuvo el gasoducto
         sur," *Energiminas*, Lima, 27-Jun-2019.

[43]   Ammonit, "Solar Measurement for Solar site assessment," *Ammonit*. [Online].
         Available: https://www.ammonit.com/en/wind-solar-
         messsysteme/solarmesssysteme. [Accessed: 10-Jun-2019].

[44]   Department of Energy and Mineral Engineering, "CSP site selection and feasibility
         analysis," *PennState*. [Online]. Available: https://www.e-
         education.psu.edu/eme812/node/699. [Accessed: 10-Jun-2019].

[45]   Asian Development Bank, *Development of solar and wind power : in Karnataka and
         Tamil Nadu.* Mandaluyong: ADB, 2013.

[46]   K. Lovegrove and W. Stein, *Concentrating Solar Power Technology : Principles,
         Developments and Applications*, 1st ed. Cambridge: Woodhead Publishing, 2012.

[47]   M. Šúri and T. Cebecauer, "Requirements and standards for bankable DNI data
         products in CSP projects," Spain, 2011.

[48]   M. Chaanaoui, S. Vaudreuil, and T. Bounahmidi, "Benchmark of Concentrating
         Solar Power plants: historical, current and future technical and economic
         development," *Procedia Comput. Sci.*, vol. 83, pp. 782–789, 2016.

[49]   S. Kuravi, J. Trahan, D. Y. Goswami, M. M. Rahman, and E. K. Stefanakos,
         "Thermal energy storage technologies and systems for concentrating solar power
         plants," *Prog. Energy Combust. Sci.*, vol. 39, no. 4, pp. 285–319, 2013.

[50] X. Xu, K. Vignarooban, B. Xu, K. Hsu, and A. M. Kannan, "Prospects and problems of concentrating solar power technologies for power generation in the desert regions," *Renew. Sustain. Energy Rev.*, vol. 53, pp. 1106–1131, Jan. 2016.

[51] F. Trieb and H. Müller-Steinhagen, "Concentrating solar power," Stuttgart, 2004.

[52] NREL, "Concentrating Solar Power Projects," *NREL*, 2017. [Online]. Available: https://solarpaces.nrel.gov/. [Accessed: 10-Jun-2019].

[53] M. T. Islam, N. Huda, A. B. Abdullah, and R. Saidur, "A comprehensive review of state-of-the-art concentrating solar power (CSP) technologies: Current status and research trends," *Renew. Sustain. Energy Rev.*, vol. 91, pp. 987–1018, Aug. 2018.

[54] W. Johwa, "SA's KaXu Solar One plant wins UN climate change award," *Bizcommunity*, 2017. [Online]. Available: https://www.bizcommunity.com/Article/196/701/170244.html. [Accessed: 10-May-2019].

[55] SolarPACES, "How CSP Works: Tower, Trough, Fresnel or Dish," *SolarPACES*, 2018. [Online]. Available: https://www.solarpaces.org/how-csp-works/. [Accessed: 10-Jun-2019].

[56] A. Kumarankandath, "Reliance commissions 100 MW solar power plant in Rajasthan," *DownToEarth*, 2015. [Online]. Available: https://www.downtoearth.org.in/news/reliance-commissions-100-mw-solar-power-plant-in-rajasthan-47336. [Accessed: 28-May-2019].

[57] NREL, "Concentrating Solar Power Basics," *NREL*. [Online]. Available: https://www.nrel.gov/research/re-csp.html. [Accessed: 10-Jun-2019].

[58] Abengoa, "Atacama-1," 2014.

[59] United Sun Systems International Ltd, "Maricopa Dish-Stirling plant," *Wikimedia*, 2015. [Online]. Available: https://commons.wikimedia.org/wiki/File:Maricopa_Dish-Stirling_plant_01.jpg. [Accessed: 10-May-2019].

[60] T. Overton, "Crescent Dunes: 24 Hours on the Sun," *POWER*, 2016. [Online]. Available: https://www.powermag.com/crescent-dunes-24-hours-on-the-sun/. [Accessed: 10-May-2019].

[61] R. Musi *et al.*, "Techno-economic analysis of concentrated solar power plants in terms of levelized cost of electricity," in *AIP Conference Proceedings*, 2017, p. 13.

[62] Y. Sun, *Advances in power and energy engineering*, 1st ed. Suzhou: CRC Press, 2016.

[63] R. Zhai, Y. Chen, H. Liu, H. Wu, and Y. Yang, "Optimal Design Method of a Hybrid CSP-PV Plant Based on Genetic Algorithm Considering the Operation Strategy," *Int. J. Photoenergy*, vol. 2018, pp. 1–15, Nov. 2018.

[64] M. Petrollese and D. Cocco, "Optimal design of a hybrid CSP-PV plant for achieving the full dispatchability of solar energy power plants," *Sol. Energy*, vol. 137, pp. 477–489, 2016.

[65] C. Parrado, A. Girard, F. Simon, and E. Fuentealba, "2050 LCOE (Levelized Cost of Energy) projection for a hybrid PV (photovoltaic)-CSP (concentrated solar power) plant in the Atacama Desert, Chile," *Energy*, vol. 94, pp. 422–430, Jan. 2016.

[66] N. R. Avezova, A. E. Khaitmukhamedov, A. Y. Usmanov, and B. B. Boliyev, "Solar thermal power plants in the world: The experience of development and operation," *Appl. Sol. Energy*, vol. 53, no. 1, pp. 72–77, 2017.

[67] A. Zurita *et al.*, "Techno-economic evaluation of a hybrid CSP + PV plant integrated with thermal energy storage and a large-scale battery energy storage system for base generation," *Sol. Energy*, vol. 173, pp. 1262–1277, Oct. 2018.

[68] B. Anderson, "A Case Study for the MENA Region," Dubai, 2017.

[69] Arquitectura en acero, "Complejo Solar Atacama 1," *Arquitectura en acero*. [Online]. Available: http://www.arquitecturaenacero.org/uso-y-aplicaciones-del-acero/soluciones-constructivas/complejo-solar-atacama-1. [Accessed: 10-Jun-2019].

[70] Bloomberg, "Elefante blanco solar de Chile podría emerger del desierto - El

Mostrador," *El Mostrador*, 2017. [Online]. Available:
https://www.elmostrador.cl/mercados/2017/01/27/elefante-blanco-solar-de-chile-podria-emerger-del-desierto/. [Accessed: 10-Jun-2019].

[71]   BNamericas, "¿Es competitiva la concentración solar de potencia en Chile?,"
BNamericas, 2017. [Online]. Available:
https://www.bnamericas.com/es/reportajes/energiaelectrica/es-competitiva-la-concentracion-solar-de-potencia-en-chile. [Accessed: 10-Jun-2019].

[72]   A. Boretti, S. Castelletto, and S. Al-Zubaidy, "Concentrating solar power tower
technology: present status and outlook," *Nonlinear Eng.*, vol. 8, no. 1, pp. 10–31,
2019.

[73]   Business Wire, "SolarReserve Receives Environmental Approval for 390 Megawatt
Solar Thermal Facility with Storage in Chile," *Business Wire*, 2017. [Online].
Available:
https://www.businesswire.com/news/home/20170719005167/en/SolarReserve-Receives-Environmental-Approval-390-Megawatt-Solar. [Accessed: 10-Jun-2019].

[74]   B. Gallego, "How to achieve US$63/MWh in a CSP tower project with storage,"
2018.

[75]   GE Renewable Energy, "Ashalim Power Station, Israel," Baden, 2016.

[76]   HeliosCSP, "Infinia begins commissioning 1.5 MW dish Stirling solar Concentrating
Solar Power plant in Utah," *HeliosCSP*, 2013. [Online]. Available:
http://helioscsp.com/infinia-begins-commissioning-1-5-mw-dish-stirling-solar-concentrating-solar-power-plant-in-utah/. [Accessed: 10-Jun-2019].

[77]   Lazard, "Levelized Cost of Energy Analysis V. 12.0," 2018.

[78]   J. A. Lobo, "Jornada Internacional Implementación del Acuerdo de Paris -
Universidad Nacional de La Plata, Argentina," 2016.

[79]   J. Ponce de Leon, "Dubai pushes solar power cost to world's lowest as largest
single-site solar park set to rise," *Gulf News*, 2018. [Online]. Available:

https://gulfnews.com/uae/environment/dubai-pushes-solar-power-cost-to-worlds-lowest-as-largest-single-site-solar-park-set-to-rise-1.2191086. [Accessed: 10-Jun-2019].

[80]   Reve, "Alstom obtains financing for Israeli concentrated solar power (CSP) plant," *Reve*, 2014. [Online]. Available: https://www.evwind.es/2014/07/16/alstom-obtains-financing-for-israeli-concentrated-solar-power-csp-plant/46479. [Accessed: 10-Jun-2019].

[81]   Reve, "Cornerstone Laid At Ashalim, Concentrated Solar Power (CSP), Plant In Israel," *Reve*, 2015. [Online]. Available: https://www.evwind.es/2015/06/15/cornerstone-laid-at-ashalim-concentrated-solar-power-csp-plant-in-israel/52747. [Accessed: 10-Jun-2019].

[82]   P. Sánchez, "$758 million financing for the first PV-CSP plant in Latin America," *Pv Magazine International*, 2018. [Online]. Available: https://www.pv-magazine.com/2018/05/22/758-million-financing-for-the-first-pv-csp-plant-in-latin-america/. [Accessed: 10-Jun-2019].

[83]   SmartGrid Spain, "SolarReserve recibe aprobación medioambiental para una planta de 390 Mw. con almacenamiento en Chile," *SmartGrid Spain*, 2017. [Online]. Available: http://smartgridspain.org/web/blog/2017/07/20/solarreserve-recibe-aprobacion-medioambiental-una-planta-390-mw-almacenamiento-chile/. [Accessed: 10-Jun-2019].

[84]   SolarPACES, "Israel CSP Potencial," *SolarPACES*, 2017. [Online]. Available: https://www.solarpaces.org/csp-technologies/csp-potential-solar-thermal-energy-by-member-nation/israel/. [Accessed: 10-Jun-2019].

[85]   SolarReserve, "Likana," *SolarReserve*, 2018. [Online]. Available: https://www.solarreserve.com/es/proyectos-globales/csp/likana/. [Accessed: 10-Jun-2019].

[86]   SunShot, "CSP Apollo Solar Receiver with Supercritical Carbon Dioxide," *Brayton Energy*, 2016. [Online]. Available: https://www.braytonenergy.net/our-projects/csp-

apollo/. [Accessed: 20-Jun-2019].

[87] D. Tapia, "Copiapó Solar: proyecto clave de SolarReserve en Chile," *Nueva Minería & Energía*, 2017. [Online]. Available: http://www.nuevamineria.com/revista/copiapo-solar-proyecto-ficha-clave-de-solarreserve-en-chile/. [Accessed: 10-Jun-2019].

[88] P. Tisheva, "Chile's Cerro Dominador CSP project secures USD-758m financing," *Renewables Now*, 2018. [Online]. Available: https://renewablesnow.com/news/chiles-cerro-dominador-csp-project-secures-usd-758m-financing-613267/. [Accessed: 10-Jun-2019].

[89] U.S. Department of Energy, "Crescent Dunes," *Energy.Gov*. [Online]. Available: https://www.energy.gov/lpo/crescent-dunes. [Accessed: 10-Jun-2019].

[90] World Bank Group, "Atacama 1 Solar Power Project," *World Bank roup*, 2014. [Online]. Available: https://ppi.worldbank.org/snapshots/project/Atacama-1-Solar-Power-Project-8185. [Accessed: 10-Jun-2019].

[91] S. Kraemer, "Shouhang and EDF to Test s-CO2 Cycle in Concentrated Solar Power," *SolarPACES*, 2019. [Online]. Available: https://www.solarpaces.org/shouhang-and-edf-first-to-test-s-co2-cycle-in-concentrated-solar-power/. [Accessed: 10-Jun-2019].

[92] Brayton Energy, "SolarCAT Solar Compressed Air Turbine," *Brayton Energy*. [Online]. Available: https://www.braytonenergy.net/our-projects/solarcat/. [Accessed: 10-Jun-2019].

[93] F. Dominio, "Techno-Economic Analysis of Hybrid PV-CSP Power Plants Advantages and disadvantages of intermediate and peak load operation," KTH Royal Institute of Technology, 2017.

[94] R. Buck and P. Schwarzbözl, "Solar Tower Systems," in *Comprehensive Energy Systems*, Elsevier, 2018, pp. 692–732.

[95] K. Vignarooban, X. Xu, A. Arvay, K. Hsu, and A. M. Kannan, "Heat transfer fluids

for concentrating solar power systems – A review," *Appl. Energy*, vol. 146, pp. 383–396, May 2015.

[96]   T. L. Liu, W. R. Liu, and X. H. Xu, "Properties and heat transfer coefficients of four molten-salt high temperature heat transfer fluid candidates for concentrating solar power plants," *IOP Conf. Ser. Earth Environ. Sci.*, vol. 93, pp. 1–7, 2017.

[97]   X. Zhuang *et al.*, "LCOE Analysis of Tower Concentrating Solar Power Plants Using Different Molten-Salts for Thermal Energy Storage in China," *Energies*, vol. 12, no. 7, pp. 1–14, Apr. 2019.

[98]   V. Khokhlov, I. Korzun, V. Dokutovich, and E. Filatov, "Heat capacity and thermal conductivity of molten ternary lithium, sodium, potassium, and zirconium fluorides mixtures," *J. Nucl. Mater.*, vol. 410, no. 1–3, pp. 32–38, Mar. 2011.

[99]   X.-H. An, J.-H. Cheng, H.-Q. Yin, L.-D. Xie, and P. Zhang, "Thermal conductivity of high temperature fluoride molten salt determined by laser flash technique," *Int. J. Heat Mass Transf.*, vol. 90, pp. 872–877, Nov. 2015.

[100]   M. Salanne, C. Simon, P. Turq, and P. A. Madden, "Heat-transport properties of molten fluorides: Determination from first-principles," *J. Fluor. Chem.*, vol. 130, no. 1, pp. 38–44, Jan. 2009.

[101]   M. Mehos *et al.*, "Concentrating Solar Power Gen3 Demonstration Roadmap," 2017.

[102]   R. Guédez, "A Techno-Economic Framework for the Analysis of Concentrating Solar Power Plants with Storage," KTH Royal Institute of Technology, 2016.

[103]   TSK-Flagsol, "Developing a 24-hour Renewable Energy System, CSP-PV-Hybrid Power Plant," Dubai, 2018.

[104]   C. A. Cornejo Gómez, "Methodology for the development of hydroelectric power plants," MIT Libraries, 2016.

[105]   MINEM, "Ministerio de Energía y Minas - ¿Qué hacemos?," *Plataforma digital única del Estado Peruano*, 2018. [Online]. Available: https://www.gob.pe/738-ministerio-de-energia-y-minas-que-hacemos. [Accessed: 05-Oct-2019].

[106] MINCUL, "Ministerio de Cultura - ¿Qué hacemos?," *Plataforma digital única del Estado Peruano*, 2019. [Online]. Available: https://www.gob.pe/666-ministerio-de-cultura-que-hacemos. [Accessed: 05-Oct-2019].

[107] SENACE, "Sobre el Senace," *SENACE*, 2018. [Online]. Available: https://www.senace.gob.pe/nosotros/sobre-senace/. [Accessed: 05-Oct-2019].

[108] Osinergmin, "¿Qué es Osinergmin?," *Osinergmin*, 2018. [Online]. Available: https://www.osinergmin.gob.pe/seccion/institucional/acerca_osinergmin/quienes_somos. [Accessed: 05-Oct-2019].

[109] F. J. Collado and J. Guallar, "Quick design of regular heliostat fields for commercial solar tower power plants," *Energy*, pp. 115–125, Jul. 2019.

[110] F. J. Collado and J. Guallar, "Campo: Generation of regular heliostat fields," *Renew. Energy*, vol. 46, pp. 49–59, Oct. 2012.

[111] H. Joga, "Diseño de una planta termosolar de receptor central con sales fundidas como fluido de trabajo y sistema de almacenamiento," Universidad Carlos III de Madrid, 2012.

[112] J. Stalin and M. Jebamalai, "Receiver Design Methodology for Solar Tower Power Plants," KTH Royal Institute of Technology, 2016.

[113] M. Pulgar-Vidal, "El Acuerdo de París: El largo proceso hacia el éxito - Rol, retos y oportunidades para el Perú," Lima, 2016.

[114] United Nations, "Sustainable Development Goal 7," *Sustainable Development Goals Knowledge Platform*, 2018. [Online]. Available: https://sustainabledevelopment.un.org/sdg7. [Accessed: 10-May-2019].

[115] Electricidad, "Los cinco proyectos CSP en carpeta después de Cerro Dominador," *La revista energética de Chile*, Chile, Apr-2019.

[116] D. Lessard, V. Sakhrani, and R. Miller, "House of Project Complexity-understanding complexity in large infrastructure projects," *Eng. Proj. Organ. J.*, vol. 4, no. 4, pp. 170–192, 2014.

[117] INCOSE, *Systems engineering handbook : a guide for system life cycle processes and activities*, 4th ed. San Diego: Wiley, 2015.

[118] S. Bruni, "La Energía Geotérmica," 2018.